

DISPERSION MODELING AND ANALYSIS OF ACCIDENTAL RELEASE OF CHLORINE: CASE STUDIES OF THREE SELECTED LOCATIONS IN NIGERIA

Okwuba, M. J.¹ and Williams, A. O. F.²

^{1,2}Department of chemical and Petroleum Engineering, University of Lagos,
Lagos, Nigeria

*Email: afwilliams@unilag.edu.ng.

ABSTRACT

Chlorine is a toxic chemical that is nonetheless commonly employed for many industrial applications such as disinfection of water in potable water treatment plants. Accidental release of chlorine at such a facility can lead to serious environmental pollution with high adverse health consequence for both personnel and residents close to the facility. Two reported accidental releases of chlorine at water treatment plants were at the Cross River Water Board Plant and the Lamingo Water Treatment Plant which occurred in 2007 and 2015, respectively, and resulted in multiple fatalities and several hospitalizations. This paper, therefore, presents the dispersion modeling of these two cases together with a third one based on hypothetical release scenarios in order to determine the potential consequences of the releases. The modeling was carried out using the Areal Location of Hazardous Atmosphere (ALOHA) software developed and made freely available by the United State Environmental Protection Agency (US EPA). The Google Earth mapping software, which is also freely available, was employed to graphically display the results of the dispersion modeling from the ALOHA software so that it is easy to identify the areas that could be impacted by the releases. The results showed three threat zones (red, orange and yellow) for all the hypothetical release cases of the three locations. The results also show that the potential for much higher multiple fatalities and hospitalizations exist for the third location. Thus, every effort must be made by implementing measures to prevent the accidental release of chlorine, as well as adequate/robust emergency response plans for mitigation and recovery in the event of a release. The dispersion modeling results are useful for planning emergency response and evacuation/escape routes.

Keywords: Dispersion modeling, Chlorine, Toxicity, ALOHA software, Google Earth, Threat zones, emergency response planning.

1. INTRODUCTION

From the start of the industrial revolution till date, the world has continued to experience major accidents with numerous fatalities, economic losses, destruction of raw materials, finished products, and industrial equipment as well as damage to the environment. The ability to predict the occurrence of these accidents will help to prevent or mitigate the consequences of such events. Chlorine is a strong oxidizing agent and is highly toxic (Ilic et al, 2018). The airborne migration or movement of chlorine gas, as well as any other toxic material from the accident site to other locations, is described by dispersion modeling (Paul et al, 2014). Bosanquet and Pearson (1936) derived the early air pollutant plume dispersion equations. However, they did not assume Gaussian distribution for pollutants dispersion. Sutton (1947) derived plume dispersion equation for pollutants and made use of the assumption of Gaussian distribution for the vertical and crosswind dispersion of the

pollutant. Afterward, the Gaussian dispersion model has been modified by many researchers and computer programs have been developed making use of this model for calculating the dispersions of the pollutants (Paul et al, 2014). Eidsvik (1980) proposed heavy gas dispersion model for released gases that are heavier than air. It was observed that the initial behavior of a heavy gas will be different from a neutrally buoyant gas. Initially a heavy gas will sink owing to the fact that it is heavier than the surrounding air. As the gas cloud moves downwind, it becomes diluted and its density reduces and it begins to behave like a neutrally buoyant gas. The results of dispersion modeling are applicable in determining the consequences of accidental releases of hazardous or toxic materials e.g., location of impacted areas, ambient concentrations. The sources of chlorine gas release could range from industrial to community to household and warfare environments. Children could be exposed to chlorine gas release through accidental releases of

chlorine vapor at swimming pools, improper mixing of hypochlorite bleach with acidic cleaning agents, mixing of ammonia and hypochlorite bleach (forming chloramine gas), school chemistry experiments, and industrial or chemical transportation accidents (GuKloglyu et al, 2002). Although Sonibare and Adeniran (2019) state that accidental release of chlorine is uncommon, there have, nonetheless been a number of serious accidental release of chlorine incidents in Nigeria and elsewhere. Two cases of serious accidental release of chlorine gas in Nigeria were the Lamingo water treatment plant in Jos (Marie-Therese, 2015) and Cross River State water board water treatment plant (The new humanitarian, 2007), both of which resulted in multiple fatalities and hospitalization of several people. The expansive use of chlorine which is a hazardous/toxic chemical and the related potential risk requires the development of practical and well-tested models for estimating vulnerable zones in relation to their accidental release in the atmosphere. As a result, a number of studies on the dispersion modeling of chlorine have appeared in the literature (Tseng et al, 2012; Setareshenas et al, 2014; Hosseini, 2016; Ilić et al, 2018; Al-Sarawi, 2018; Law and Gimbin, 2020 and Jayakumar et al, 2021).

The purpose of this paper is to carry out dispersion modeling and analysis of the accidental release of chlorine at three locations in Nigeria in order to determine the potential consequences. These are (i) the Lamingo water treatment plant in Jos, (ii) the Cross River State Water Board water treatment plant, and (iii) XYZ Chemical Ltd at Oshodi-Apapa Express Way, Lagos. A number of hypothetical release scenarios are considered and presented. The dispersion modeling analyses are done using the Areal Location of Hazardous Atmospheres (ALOHA) software. The attraction of the use of the ALOHA software is that it is a free and open-source software that is very easy to use. In general, carrying out this kind of analysis is important for consequence analysis and risk assessment. If such analysis had been done, it could have served as a useful guide to create rescue plans, emergency responses, and neighborhood warnings to ensure the safety of all the people in the areas of the Lamingo and Cross River State water treatment plants where there was accidental release of chlorine. Although there has been no reported accidental release of chlorine for the third location considered, the results of the modeling and analysis presented suggest potentially high consequence in the event of an occurrence. This should elicit the implementation of robust preventive measures to

safeguard against accidental release, and in the event of a release, the deployment of the necessary emergency response and rescue plans to mitigate the potential impact.

2. MATERIALS AND METHODS

2.1 About the ALOHA Software

ALOHA has been successful in the calculation of the concentration of the released chlorine out of the wide varieties of available software. It is a program designed to model chemical releases for emergency responders and planners (Paul et al, 2014). ALOHA is applicable in the modeling of many release scenarios: toxic gas clouds, Boiling Liquid Expanding Vapor Explosions (BLEVE), jet fires, vapor cloud explosions, and pool fires. Depending on the release scenario, ALOHA evaluates the corresponding type of hazard (Paul et al, 2014). ALOHA displays its estimate as a threat zone, which is an area where hazards (such as toxicity, flammability, thermal radiation, or damaging over-pressure) exceed a user-specified level of concern. It is also possible to generate a variety of scenario-specific outputs, including threat zone plots, threats at specific locations, and source strength graphs (Paul et al, 2014).

The model predicts the concentration of the chemical in the atmosphere and the plume boundaries, it then shares the resulting threat zone simultaneously with MARPLOT. Threat zone shows the area where the ground level concentration exceeds the range entered as the level of concern. MARPLOT is a mapping application that can be used together with ALOHA to provide a visual of the extent of the plume using a variety of base maps (Bhattacharya et al, 2015).

ALOHA contains very powerful integral databases. It consists of data files with physical, chemical, and toxicological properties for hundreds of pure chemicals and some common chemical solutions. Usually, every chemical data file contains chemical names, CAS registry numbers, molecular weight, and toxicological data. These are the minimum data required for the Direct Source option and the Gaussian dispersion model in ALOHA. Data are available for the following properties: critical temperature, critical pressure, critical volume, freezing point, normal boiling point, vapor pressure, liquid density, gas density, heat of vaporization, heat of combustion, liquid heat capacity, and vapor heat capacity (Bhattacharya et al, 2015).

2.2 Selection of Toxic Level of Concern

Toxic Levels of Concern (LOCs) are used in assessing the toxicity threat of a discharged chemical. A toxic

LOC indicates the threshold concentration of exposure to a chemical that is extremely dangerous to human health if inhaled for a specific period. Generally, the lower the toxic LOC value for a substance, the more toxic the substance is by inhalation (Paul et al, 2014). In the course of this research work, Acute Exposure Guideline Levels (AEGLs) concentrations are used to define the toxic zones. AEGLs are the best public exposure LOCs available to date and all three tiers (AEGL-1, AEGL-2, and AEGL-3) are developed for 5 exposure periods: 10 minutes, 30 minutes, 60 minutes, 4 hours and 8 hours (Paul et al, 2014). Other types of public exposure guidelines are Emergency Response Planning Guidelines (ERPGs) and Temporary Emergency Exposure Limits (TEELs) but these are not considered here. AEGL-1 is the airborne concentration (expressed as ppm or mg/m³) of a substance above which it is predicted that the general population could be subjected to a slight discomfort and irritation. However, the effects are not too severe as they are not disabling and are transient and reversible upon cessation of exposure. AEGL-2 is the airborne concentration (expressed as ppm or mg/m³) of a substance above which it is predicted that the general population could experience irreversible or other serious, long-lasting adverse health effects. AEGL-3 is the airborne concentration (expressed as ppm or mg/m³) of a substance above such level it is predicted that the entire people dwelling in such environment could experience life-threatening health effects or death (Paul, et al., 2014).

Table 1: AEGLs for Chlorine Exposure in ppm (Paul et al., 2014)

Exposure Time	Toxic level		
	AEGL-3	AEGL-2	AEGL-1
10 min.	50	2.8	0.5
30 min.	28	2.8	0.5
60 min.	20	2.0	0.5
4 hours	10	1.0	0.5
8 hours	7.1	0.71	0.5

2.3. Description of Study Areas

1. Lamingo Water Treatment Plant- Jos, Plateau State: a major chlorine accidental release occurred on a Saturday morning on July 25, 2015, in Jos in Nigeria. This accident was as a result of gas leakage from the Lamingo water treatment plant which left eight people dead and over 100 others hospitalized (Marie-Therese, 2015). Jos is the capital of Plateau state located near the center of Nigeria and is the largest area of over 1000m. It has a population of

about 900,000 inhabitants based on the 2006 census (Official Gazette, 2006). It has an average altitude of 1280m. Jos is a semi-temperate climate with temperatures ranging from 18°C to 25°C. Lamingo water treatment plant in Jos of Plateau state is located on the latitude 9⁰55N and 8⁰55E, having an elevation of 1227m above ground level (Google Earth).

2. Cross River State Water Board Plant: Another case is a chlorine accidental release that occurred on July 5, 2007, in Cross River State. The accident occurred as a result of chlorine gas leakage in the water treatment plant leading to three fatalities and several hospitalized. Cross River is a state in South-South Nigeria, bordering Cameroon to the east. It is a coastal state located in the Niger Delta region and occupies 20,156 square kilometers (Nwabueze, 1982). It has a total area rank of 20,156 km² and a population of 3,737,517 (Official Gazette, 2006). The climate within Cross River State is tropical-humid with wet and dry seasons, with average temperatures ranging between 15°C to 30°C, and the annual rainfall between 1300 – 3000mm (Cross River State Government, 2004). Cross River Water Board Water Treatment Plant is located on the latitude 5⁰49”N and 8⁰20”E with an elevation of 54m above ground level (Google Earth).
3. XYZ Chemical Limited Lagos State: Lagos State is a state located in the southwestern geopolitical zone of Nigeria. The smallest in area of Nigeria's 36 states, with a population of over 15 million, Lagos State is arguably the most economically important state of the country, the nation's largest urban area. It has an Area of 2,500/km² (Ngex, 2013). XYZ Chemical Limited, whose actual name has been replaced for anonymity, is located on the latitude 6⁰31”N and 3⁰ 20” E with an elevation of 35m above ground level (Google Earth).

2.4 Compilation of the Required Data for the Modeling/Analysis Using the ALOHA Software

Appendix A shows the compiled data for the study areas described above required for the dispersion modeling using the ALOHA software (Version 5.4.7). As indicated, some of the data (such as the chemical data) are available in the ALOHA software, while others have to be provided by the user for entry into the software. Two release scenarios were considered for each of the study areas as follows:

1. Lamingo Water Treatment Plant Jos Plateau State:
 - (a) It was reported that the chlorine tank was relatively empty, therefore 90.7 kg was assumed for

the chlorine contained in tank before the release. This amount of chlorine is assumed to be contained in a 1.829 m long and 0.609 m wide tank. Ajijah (2015) reported that there were eight fatalities with 101 people hospitalized. Thus, it is most probable that the fatalities resulted from people closest to the point of the release, which suggests that the threat zone with the highest chlorine concentration didn't spread too far from the source. Consequently, a small leakage width of 0.018 m was assumed to simulate the suspected reduced rate of dispersion based on the reported consequence. (b) A mass of 1179.34 kg was assumed for the chlorine contained in tank before the release. This amount of chlorine is assumed to be contained in a 1.829 m long and 1.219 m wide tank. In this case, the leakage width is assumed to be 0.076 m to simulate the case of large quantity of chlorine released into the environment.

2. Cross River State Water Board Plant: (a) According to the reported information (The New Humanitarian, 2007), there were three fatalities, while several others were hospitalized from the accidental release of chlorine at this facility. An opening diameter of 0.127 meters was assumed for the leakage hole from the chlorine storage tank, which resulted to a total release of 58.513 kg for gaseous chlorine and 57.606 kg for liquid chlorine. Any increase in the leakage diameter will result to a larger volume of chlorine release which will be too much to have caused the little impact reported. (b) A larger tank size of 2.134 m tall was assumed as this will cause a reduced volume of chlorine in the tank compared to a tank of 1.219 m tall containing the same quantity of chlorine. For a 2.134 m tall tank, the volume of the tank was given by ALOHA to be 3.153 m³, while the mass of gaseous chlorine in the tank was 69.853 kg and liquid chlorine was 80.739 kg
3. XYZ Chemical Limited Lagos State: The company in question is involved in the sales of chlorine chemical, as such there is a high probability of chlorine leakage. On this note, the company was chosen as a case study for pre-incident scenario analysis. Since the company is into sales of chlorine chemical, there is every tendency that the chemicals are stored in several tanks of different sizes in the company environment. Therefore, a big tank of 2.134 m was assumed as the height of leaked tank. (a) A maximum value was assumed for mass of gaseous chlorine in tank as 55.338 kg, as based on ALOHA, any value much higher than this, the chemical will seize to exist as gas but liquid. (b)

A minimum value was assumed for mass of gaseous chlorine in tank as 8.165 kg, as based on ALOHA, any value much lesser than this, the chemical will not be released out through the orifice. (c) The average values for mass of gaseous and liquid chlorine in tank was taken as the average of both maximum and minimum assumed values.

2.5 The ALOHA Modeling Procedure

The ALOHA software used for this modeling is the ALOHA 5.4.7 version. The modeling procedure is as follows:

1. Start the software.
2. Choose the location to be modeled.
3. Specify the types of building surrounding the point of chemical release.
4. Specify the exact date and time of the accident.
5. Select the type of chemical involved (in this study, chlorine is the chemical involved).
6. Input the weather information at the time of chemical release.
7. Specify the source of discharge (i.e., tank, pipeline, etc.).
8. Input the mass of tank or pipeline as the case may be.
9. Specify the length and width of the leakage (hole) through which the chemical escapes.
10. Specify the distance of the leakage (hole) from the bottom of the tank.
11. Choose a level of concern (for this study, AEGL-1, AEGL-2, and AEGL-3 were used).
12. Obtain the threat zone in graph format.
13. Obtain the released chlorine gas concentration at specific distances away from the point of release.
14. Save the information as a Keyhole Markup Language (KML) file.

Keyhole Markup Language is a notation for expressing geographic annotation and visualization within 2-Dimensional and 3-Dimensional maps and earth browser such as Google Earth (Wikipedia, 2021).

The Google Earth Mapping Procedure is as follows:

- i. Start the software.
- ii. Import KML file into Google earth.
- iii. Zoom out to get wider coverage of the threat zone.
- iv. Navigate around the threat zone to get a clearer view.

3. RESULTS AND DISCUSSION

The results of the ALOHA dispersion modeling for the three locations are presented and discussed here.

3.1 Lamingo Water Treatment Plant- Jos, Plateau State

Table 2 presents the summary of the threat zone estimates for the two scenarios (a and b) considered. The corresponding graphic representations are shown in Figure 1.

Table 2: Threat Zone Estimates by the ALOHA Software for Scenarios (a and b) - Lamingo Water Treatment Plant, Jos

Threat Zone	Parameters (Scenario a)	Parameters (Scenario b)
Model run	Heavy gas	Heavy gas
Red	504.749 m (20 ppm = AEGL-3 [60 min])	2574.95 meters (20 ppm = AEGL-3 [60 min])
Orange	1472.184 m (2 ppm = AEGL-2 [60 min])	5954.57 meters (2 ppm = AEGL-2 [60 min])
Yellow	2574.95 m (0.5 ppm = AEGL-1 [60 min])	9656.06 meters (0.5 ppm = AEGL-1 [60 min])

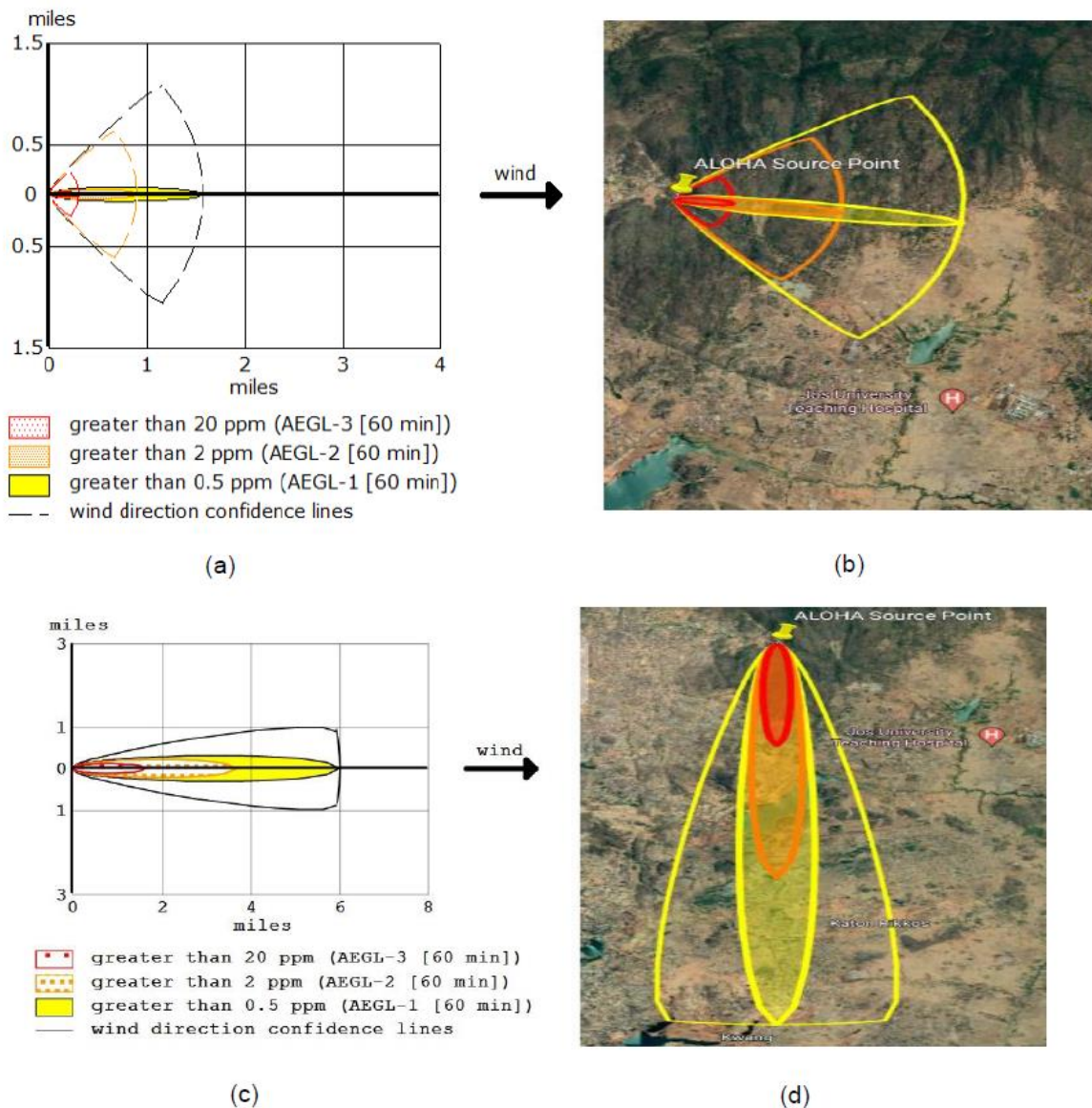
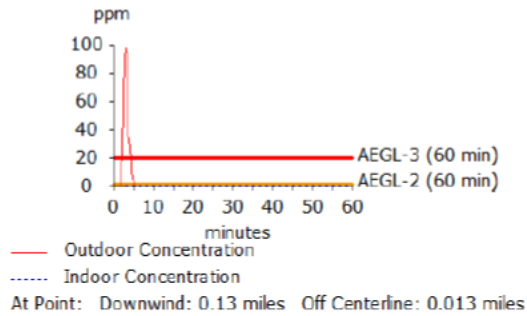


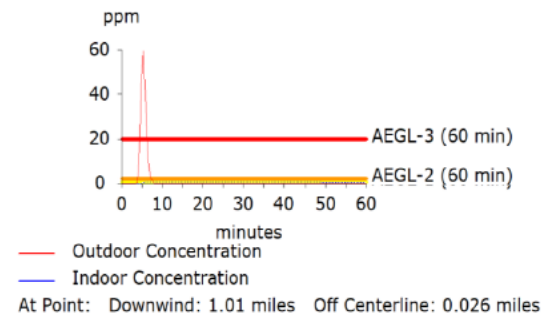
Figure 1: ALOHA generated threat zones and the corresponding Google Earth map representation for the Lamingo Water Treatment Plant, Jos. a, b: Scenario (a); c, d: Scenario (b).

From Table 2 and Figure 1 (a, c), it can be seen that for Scenario (a), the chlorine dispersion was modeled for a maximum distance of 2574.95 m from the point of release. This is the yellow (AEGL-1) threat zone which could result in slight breathing discomfort to anyone in the area. On the other hand, the orange threat zone

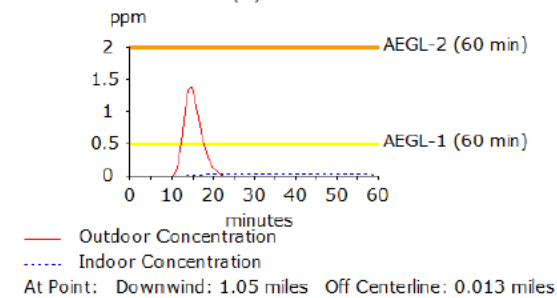
(AEGL-2) can be seen to cover an estimated distance of 1472.18 m from the point of release. Anyone in this zone may experience serious long-lasting health impact. The red threat zone (AEGL-3) is estimated to cover about 504.75 m from the point of release. In this zone, the impact could be fatality or very serious health impact for anyone found here for an extended period of time.



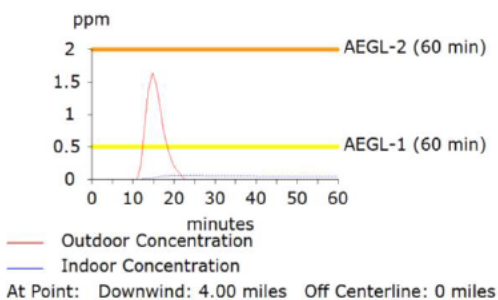
(a)



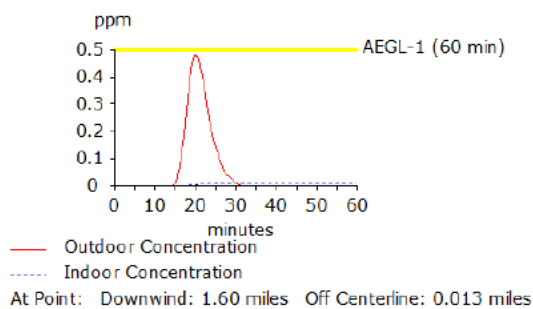
(d)



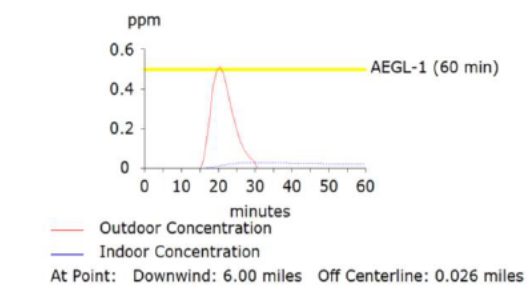
(b)



(e)



(c)



(f)

Figure 2: Transient chlorine concentration at different distances from the source point for the Lamingo Water Treatment Plant, Jos (a) 209.215 m, (b) 1689.811 m, (c) 2574.95 m for Scenario (a), (d) 1609.34 m, (e) 6437.38 m, and (f) 9656.06 m for Scenario (b)

For Scenario (b), it can be seen from Table 2 and Figure 1 (b, d) that the corresponding red, orange and yellow threat zones were estimated to be 2574.95 m, 5954.57 m, and 9656.06 m with potentially similar health impacts as for Scenario (a). The threat zones for this

scenario are seen to cover much longer distances compared to the corresponding ones for Scenario (a).

This is not surprising since Table A1.4 shows that the Scenario (b) is a case where more chlorine was released (1139.1 kg) compared with only 15.74 kg released for

Scenario (a), notwithstanding that the release durations were 60 s for the former and 180 s for the latter. This is attributable, largely, to the differences in the size of the chlorine tanks together with the opening width from which the chlorine leaked. The table shows that the maximum average release rate was 0.192 kg/s for the Scenario (a), while for Scenario (b), it was 19.01 kg/s.

Figure 2 shows the concentration transient at the indicated points with the three threat zones based on the AEGL (60 min). For the Scenario (a), it can be seen that even at a distance of about 209 m downwind of the release point, the ALOHA software estimated that the outdoor concentration exceeded the AEGL-3 (60 min) for a duration of about 7-8 min (Figure 2a). Although the scale of the plot does not make this clear in Figure 2a, the AEGL-2 (60 min) is also exceeded at this distance. On the other hand, at about the 1689.8 m downwind of the release point, only the AEGL-1 (60 min) is exceeded by the outdoor concentration for a duration of about 10 – 12 mins. Similar trend is seen for the Scenario (b) although at much higher distances as

shown in Figures 2e and 2f. The practical implications of the concentration variation, as to be expected, is that as one moves downwind of the release point, the health impact of the toxic effect of the chlorine reduces. For the previously indicated duration, Figures 2(a) and 2(d) show that the outdoor chlorine concentrations far exceed even the AEGL-3 (10 min) and AEGL-3 (30 min) presented in Table 1, suggesting that the potential for fatality of persons in this red threat zone is indeed very high. As previously reported, there were eight fatalities for the accidental chlorine release at the Lamingo Water Treatment Plant, Jos. Even for the much smaller quantity of the hypothetical release of chlorine for Scenario (a), the ALOHA results is able to identify the red threat zone with high fatality potential.

3.2 Cross River State Water Board Plant

Table 3 presents the summary of the threat zone estimates for the two scenarios (a and b) considered. The corresponding graphic representations are shown in Figure 3.

Table 3: Threat Zone Estimates by the ALOHA Software for Scenarios (a and b) - Cross River State Water Board Plant

Threat Zone	Parameters (a)	Parameters (b)
Model run	Heavy gas	Heavy gas
Red	482.803 m (20 ppm = AEGL-3 [60 min])	693.627 m (20 ppm = AEGL-3 [60 min])
Orange	2027.773 m (2 ppm = AEGL-2 [60 min])	2092.15 m (2 ppm = AEGL-2 [60 min])
Yellow	3637.117 m (0.5 ppm = AEGL-1 [60 min])	3572.744 m (0.5 ppm = AEGL-1 [60 min])

The major distinguishing factor in the two Scenarios considered here was that the chlorine in the tank was assumed to be in the gaseous state for Scenario (a), and in the liquid phase for Scenario (b). Also, the initial quantity of chlorine in the tank is about 10 kg more for Scenario (b) than for Scenario (a).

From Table 3 and Figure 3, it can be seen that except for the red threat zones determined to be about 482.8 m and 693.6 m respectively for the Scenarios (a) and (b), the other threat zones (i.e. orange and yellow) were determined to be relatively close for the two Scenarios. Similar comments made earlier in regard to the health impact of the threat zones also apply for this case. Table A.2.4 shows that more chlorine (58.513 kg) was released under the gaseous chlorine case compared with only 57.606 kg released for the liquid chlorine case, notwithstanding that there was a higher amount of liquid chlorine in the tank prior to the release.

Figure 4 (a, b, d, e) shows the concentration transient at the indicated points with only two threat zones. Unlike the case shown in Figure 2, it can be seen that the outdoor concentrations only exceeded the AEGL-2 (60 min) and AEGL-1 (60min) at large distances (804.672 m and 1609.34 m) downwind of the release points for Scenario (a), and 804.672 m and 1609.34 m) for Scenario (b), respectively. Since the duration of the concentration transient is very short, it can be inferred that the health impact on any one in this threat zones will not be significant. Although not shown, at closer distances to the release point, there is still a red threat zone where the concentration transients exceeded the AEGL-3 (10 min), AEGL-3 (30 min) and AEGL-3 (60 min). This red threat zone also has high potential for fatality which aligns with the reported two fatalities reported for this case.

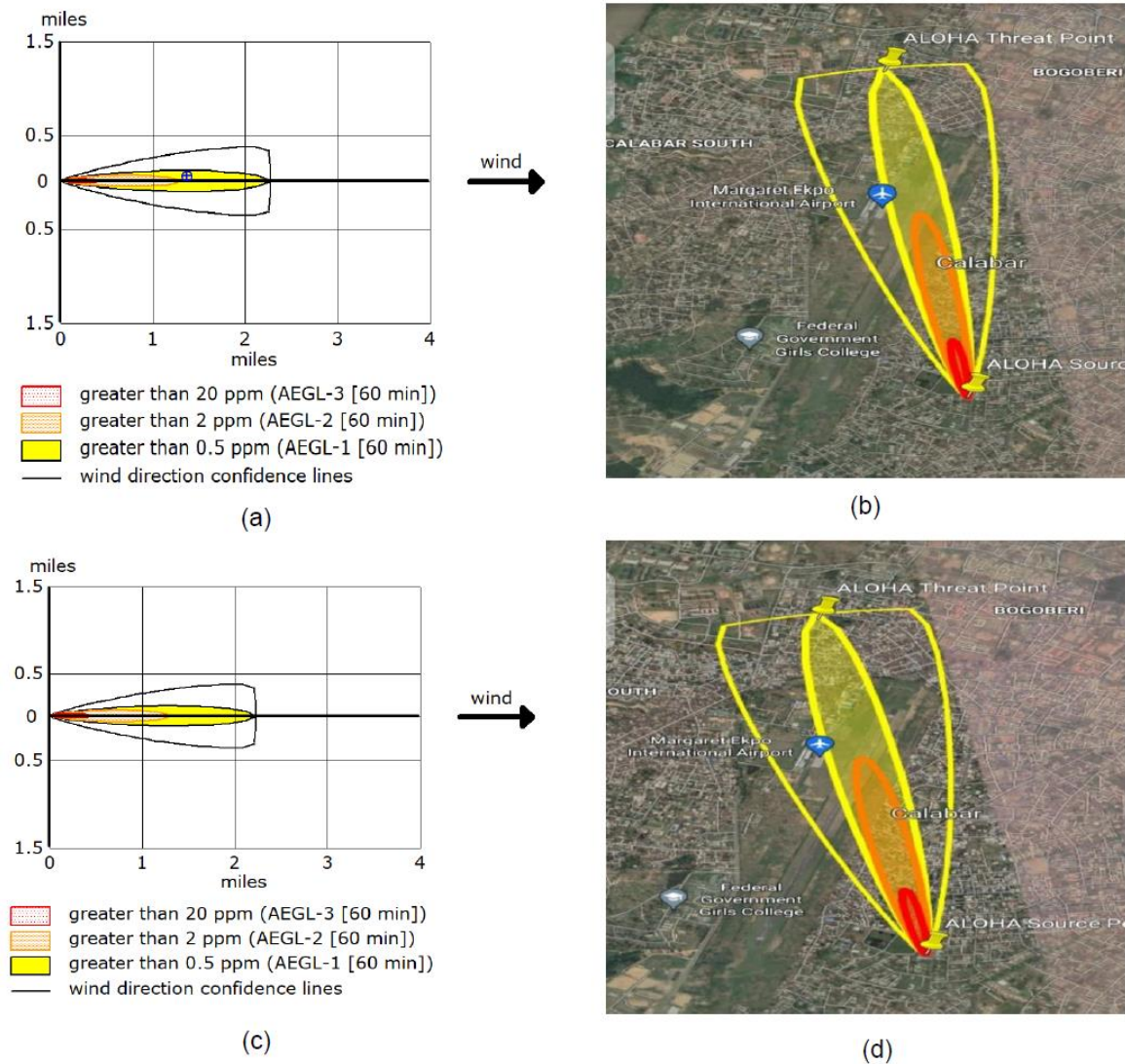


Figure 3: ALOHA generated threat zones and the corresponding Google Earth map representation for the Cross River State Water Board Plant. a, b: Scenario (a); c, d: Scenario (b).

3.3 XYZ Chemical Limited, Lagos State

Table 4 presents the summary of the threat zone estimates for the two scenarios (a and b) considered. The corresponding graphic representations are shown in Figure 5.

Table 4: Threat Zone Estimates by the ALOHA Software for Scenarios (a and b)- XYZ Chemical Ltd, Lagos

Threat Zone	Parameter (a)	Parameter (b)
Model run	Heavy gas	Heavy gas
Red	2253.08 m (20 ppm = AEGL-3 [60 min])	579.364 m (20 ppm = AEGL-3 [60 min])
Orange	5632.7 m (2 ppm = AEGL-2 [60 min])	1931.21 m (2 ppm = AEGL-2 [60 min])
Yellow	9173.26 m (0.5 ppm = AEGL-2 [60 min])	3379.62 m (0.5 ppm = AEGL-2 [60 min])

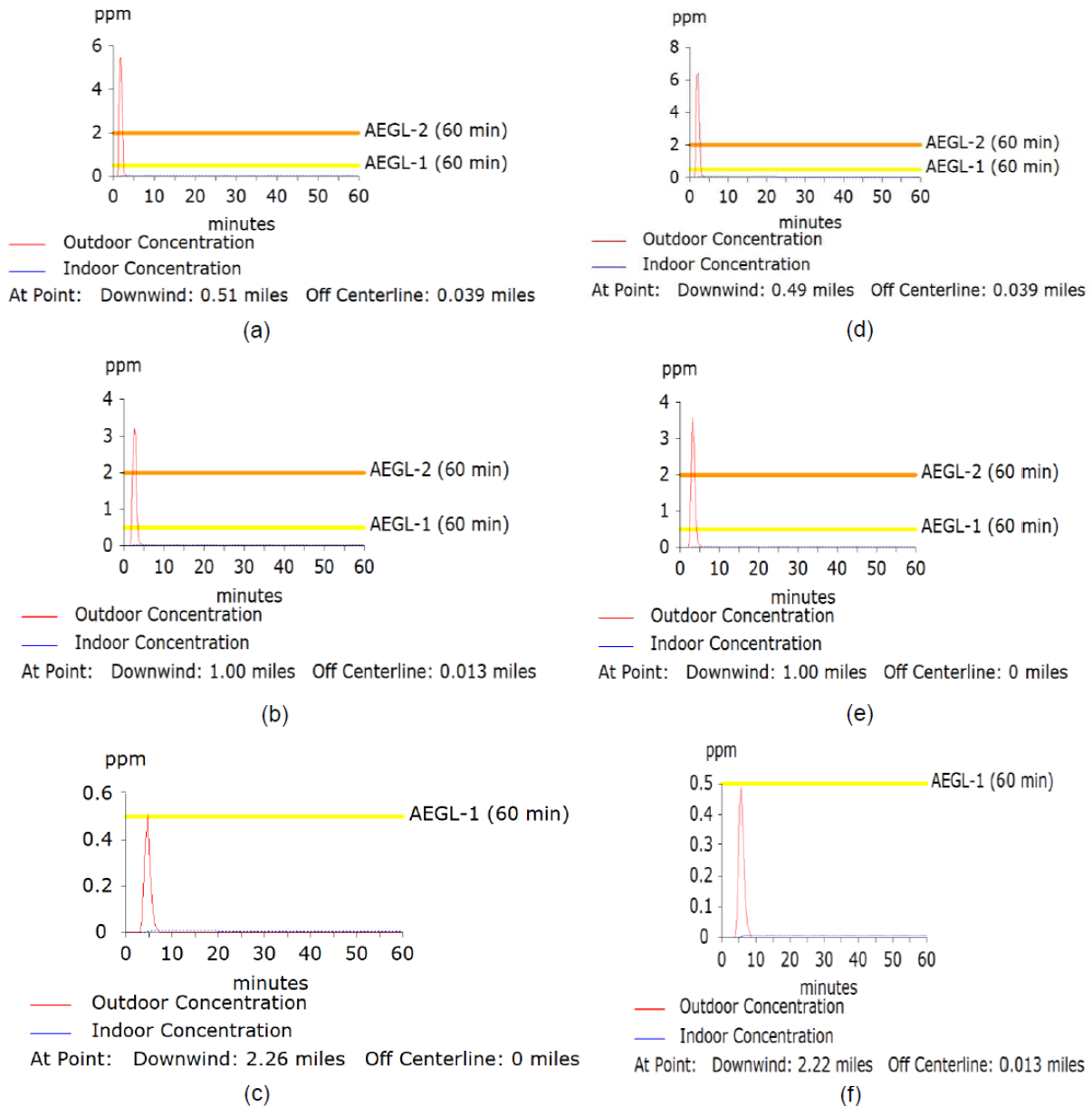


Figure 4: Transient chlorine concentration at different distances from the source point for the Cross River State Water Board Plant. (a) 804.672 m, (b) 1609.34 m, (c) 3637.117 m for Scenario (a), (d) 804.672 m, (e) 1609.34 m, and (f) 3540.56 m for Scenario (b)

The major distinguishing factor in the two Scenarios considered here was that the modeling assumed a maximum and minimum value for the mass of chlorine gas in the tank where the accidental release occurred to simulate the likely accidental releases.

As in the two previous cases above, it can be seen that the red, orange and yellow threat zones were also generated for the two Scenarios considered. For Scenario (a), the red threat zone was estimated to cover about 2253 m from the release point, while the orange and yellow threat zones were estimated to cover 5632.7 m and 9173.3 m, respectively. On the other hand, for

Scenario (b), the red, orange and yellow threat zones were estimated to be 579.4 m, 1931.2 m and 3379.6 m, respectively. As to be expected, the estimated threat zones for Scenario (b) are smaller than those for Scenario (a) due to the smaller amount of chlorine released. Nonetheless, the striking observation to be made about the outcome of the modeling for the two Scenarios considered is that it is a heavily populated area as can be inferred from the Google map representation of the threat zones. Consequently, the potential for high number of fatalities is great for the red threat zones.

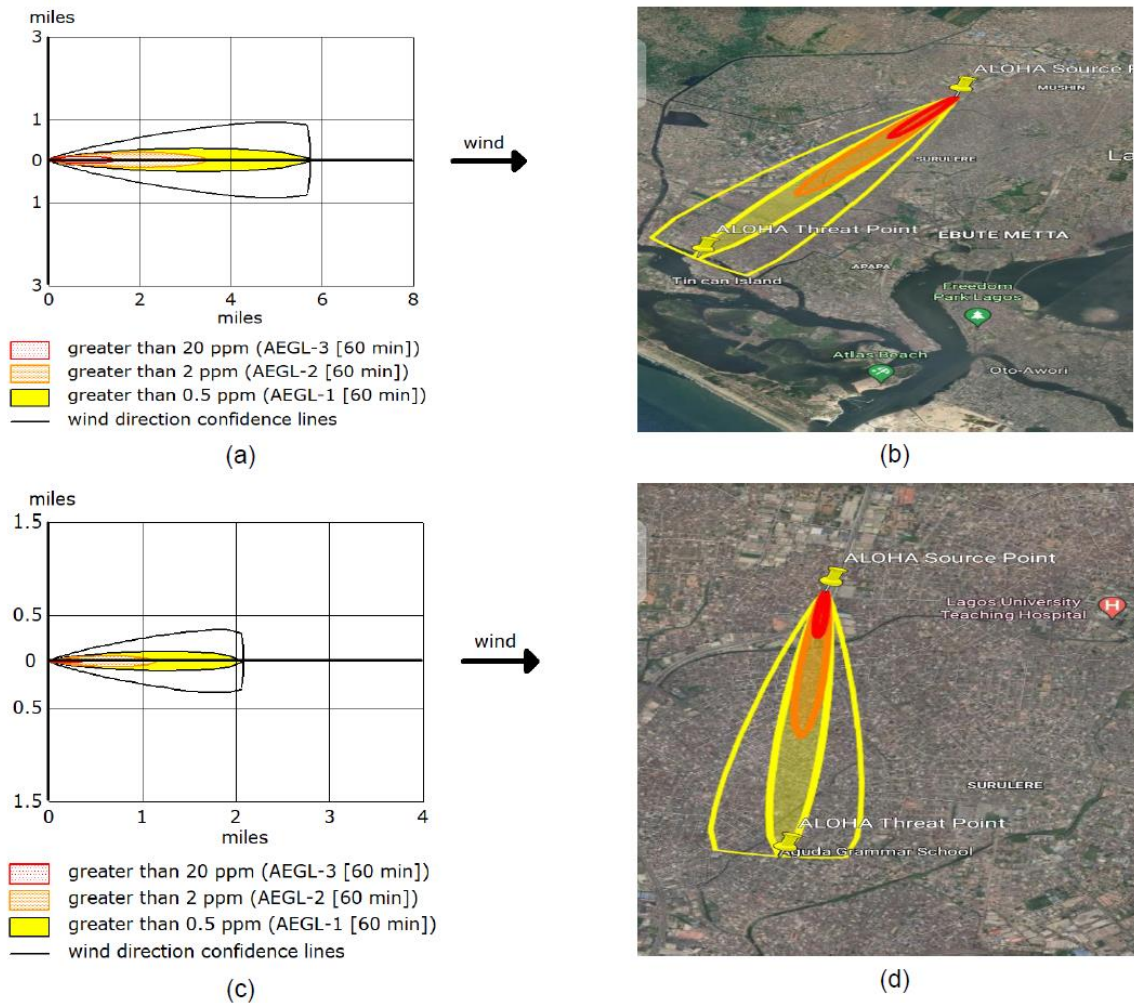


Figure 5: ALOHA generated threat zones and the corresponding Google Earth map representation of the threat zones. a, b: Scenario (a); c, d: Scenario (b).

Figure 6 shows the concentration transient at some selected points within the threat zones. It can be seen (Figure 6a) that even at about 1609.34 m downwind of the release point, the outdoor concentration exceeded the AEGL-3 (60 min) for a duration of about 2 to 3 min for Scenario (a). This plot also indicates that the AEGL-2 (60 min) is exceeded although the scale of the plot makes it impossible to show this. As to be expected, at closer distances to the release point, the AEGL-3 (10 min), AEGL-3 (30 min) and AEGL-3 (60 min) will all be exceeded to varying degrees and imply a zone with potentially high fatality. At a distance of about 4828 m downwind of the release point, both the AEGL-2 (60

min) and AEGL-1 (60 min) were exceeded for a duration of about 5 min. However, at a distance of about 9173.3 m downwind of the release point, the AEGL-1 (60 min) is not exceeded. On the other hand, for Scenario (b), Figure 6(d) shows that at a distance of about 804.7 m downwind of the release point, the AEGL-3 (60 min) is not exceeded but the AEGL-2 (60 min) and AEGL-1 (60 min) were exceeded for about 2 mins. Figure 6 (e) shows that about 1609.3 m downwind of the release point, both the AEGL-2 (60 min) and AEGL-1 (60 min) were exceeded for a duration of about 2 min. At a distance of about 3379.6 m downwind of the release point, Figure 6 (f) shows that the AEGL-1 (60 min) is not exceeded.

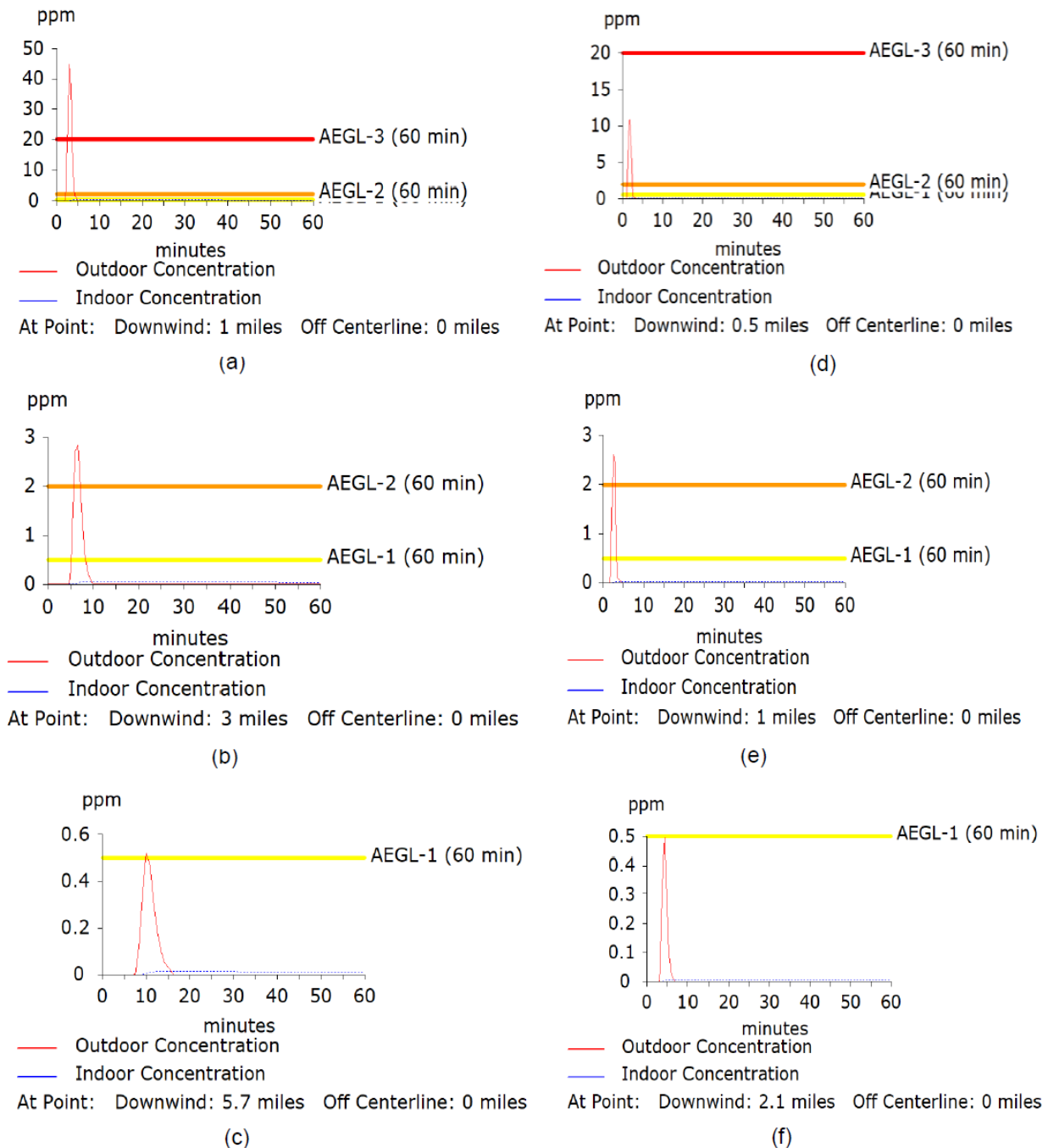


Figure 6 Transient chlorine concentration at different distances from the source point (a) 1609.34 m, (b) 4828.03 m, (c) 9173.26 m for Scenario (a), (d) 804.672 m, (e) 1609.34 m, and (f) 3379.62 m for Scenario (b)

It is to be noted that both outdoor and indoor concentration transients are plotted in Figures 2, 4 and 6. In all the cases, the indoor concentration profiles are very small (and therefore not visible on the displayed plots) compared with the outdoor concentrations. Thus, apart from getting potential victims upwind or crosswind of a release or out of the threat zones in order to reduce potential health impact, another risk mitigation measure

appears to be to get people indoors with doors and windows closed.

The foregoing results from the ALOHA software were based on a number of assumptions and hypothetical release scenarios in order to produce the dispersion modeling threat zones and hence the Google Earth maps. Even for the two reported cases of accidental release of chlorine that resulted in multiple fatalities, the absence of a documented investigation report with the necessary

technical details made it impossible to study the actual dispersion modeling of the releases. Nonetheless, the assumptions and hypothetical approach adopted helped to achieve the main purpose, which was to see how the accidental release of chlorine will impact the three locations considered. In the situation of actual accidental release scenarios, the analyst would have to make efforts to quickly obtain the relevant data for input into the ALOHA software in order to generate the threat zones. The results obtained can depend on many of the ALOHA inputs, but key amongst these, include the quantity of chlorine initially in the tank that leaked, the size/type of leakage that occurred, wind speed and direction, and whether the chlorine leaked as a liquid or as a gas, duration of the leak, etc. The dispersion modeling results are useful for risk assessment of facilities handling chlorine and for emergency response personnel in planning evacuation and mitigation measures in the event of the accidental release of chlorine. It should be noted that because the impact of a release incident may occur as soon as the release event itself, there may not be enough time for emergency response. Thus in practice, much attention is paid to efforts to prevent the release incident using such methods as inherently safer designs, engineering barriers and operational procedures/management, mitigation and emergency response in the event of a release. A general presentation of these methods can be found in Crowe and Louvar (2011). Based on the results of ALOHA dispersion modeling, Law and Gimbum (2020) and Jayakumar et al (2021) have recently presented emergency response plans for the hypothetical release of chlorine for an industrial complex and a sewage treatment plant, respectively. These studies demonstrate the importance and benefit of the kind of modeling and analysis carried out in this paper as a desirable basis for the development of emergency response plans for accidental release of chlorine.

4. CONCLUSIONS

This paper has presented the dispersion modeling of the accidental releases of chlorine at three locations in Nigeria based on hypothetical release scenarios using the ALOHA software and the Google Earth mapping software. The purpose was to determine the potential consequence of the accidental releases of chlorine at these locations which can then form the basis of risk assessment, emergency response and evacuation plans. Two of the locations had previously experienced accidental releases of chlorine with resultant multiple fatalities and several hospitalizations. The dispersion modeling results were presented graphically showing the

three threat zones of red, orange and yellow for all the three locations and the two scenarios considered for each. These were examined with respect to AEGL-3 value limits and time duration of concentration transients at a particular point in the threat zones. It was then possible to infer threat zones with potential fatality on people who may be exposed in the zones. For the Lamingo Water Treatment Plant, the red threat zones were determined to be about 505 m and 2575 m for the two release scenarios considered, while for the Cross River Water Board, these were about 482 m and 693 m, respectively. On the other hand, the red threat zones for the XYZ Chemical Ltd were about 2253 m and 579 m for the two release scenarios. It was inferred that the third location has the potential for much higher multiple fatalities and hospitalization. Consequently, serious efforts must be made by implementing measures to prevent the accidental release of chlorine at this location, together with putting in place a robust emergency response for mitigation/recovery. Methods that are usually employed in practice to do this were briefly highlighted.

The availability of the free and open source ALOHA software and the free Google Earth Pro mapping software should make it possible to readily carry out risk assessment of accidental releases of chlorine and other toxic chemicals as well as use in emergency planning and response.

5. REFERENCES

- Ajijah, A. (2015). Chemical explosion kills 8, injures 101 in Jos. Available at: <https://www.premiumtimesng.com/regional/north-central/187233-chemical-explosion-kills-8-injures-101-in-jos.html>
- Al-Sarawi, N. M. (2018). Evaluation of Accidental Atmospheric Releases of Chlorine and Butane from a Mobile Source Using ALOHA and MARPLOT. *American Journal of Environmental Protection*, 6(6), pp.144 - 155.
- Bosanquet, C. H. & Pearson, J. L. (1936). The Spread of Smoke and Gases from Chimneys. *Transactions of the Faraday Society*, 32, pp. 1249-1263. DOI: [10.1039/tf9363201249](https://doi.org/10.1039/tf9363201249)
- Eidsvik, K. J. (1980). A model for heavy gas dispersion in the atmosphere. *Atmospheric Environment* (1967), 14(7), 769-777. [https://doi.org/10.1016/0004-6981\(80\)90132-8](https://doi.org/10.1016/0004-6981(80)90132-8).
- GuKlogylyu, C., Kara, I. H. & Erten, P. G. (2002). Acute Accidental Exposure to Chlorine Gas in

- the Southeast of Turkey: A Study of 106 Cases. *Environmental Research*, Volume 88, pp. 89-93. DOI:10.1006/enrs.2001.4324.
- Crowe D. A. & Louvar, J. F. (2011). *Chemical Process Safety: Fundamentals with Applications* 3rd Edition., PTR Prentice Hall, Engelwood Cliffs, New Jersey.
- Hosseini, S. H. (2016). Assessment and modeling of chlorine release in urban region: A case study in water supply of Eyvan city, Iran. *Journal of Basic Research in Medical Sciences*. Volume 3, Issue 3, pp. 7 – 14. Ilic, P., Ilic, S. & Bjelic, L. S. (2018). Hazard Modelling of Accidental Release Chlorine Gas Using Modern Tool-Aloha Software. Original scientific paper, 9(1-2), pp. 38-45. DOI:10.7251/QOL1801038I.
- Jayakumar, C. Isac, S., & Prasad, D. R. (2021). Emergency Response Plan for Methane and Chlorine with Dispersion Modeling using CAMEO. *International Journal of Occupational Safety and Ergonomics*, 1-9. Doi.org/10.1080/10803548.2021
- Law, W. P. & Gimbut, J. (2020). Modeling the effect of hypothetical chlorine leakage from Malay-Sino Chemical Industries using ALOHA software and development of an emergency evacuation route around Teluk Kalong industrial area. In *IOP Conference Series: Materials Science and Engineering*, Vol. 736, No. 7, p. 072015. DOI:10.1088/1757-899X/736/7/072015. IOP Publishing.
- Marie-Therese, N. (2015). Death in chlorine cylinder: How gas leakage at water treatment plant wreaked havoc in Jos. [Online] Available at: <https://www.google.com/amp/s/www.vanguardngr.com/2015/07/death-in-chlorine-cylinder-how-gas-leakage-at-water-treatment-plant-wreaked-havoc-in-jos/> [Accessed 13 March 2020].
- Paul, R., Mondal, A. & Shoukat Choudhury, M. A. A. (2014). Dispersion Modeling of Accidental Release of Chlorine Gas. In *Proceedings of the International Conference on Chemical Engineering Dhaka, Bangladesh*, pp. 213-217. DOI:10.1088/1757-899X/736/7/072015
- Setareshenas, N., Khalilipour, M. M., Shahraki, F. & Mansouri, M. (2014). Consequence Modeling of Chlorine Release from Water Treatment Plant. *American Chemical Science Journal*. 2014; 4 (1): 102. doi: 10.9734.ACSJ/2014/5961.
- Sonibare, O. O. and Adeniran, J. A. (2019). Exposure assessment and environmental consequence evaluation of accidental chlorine release in an industrial area. *International Journal of Environmental Studies*, 76(3), pp.396-411.
- Sutton, O. G. (1947). The theoretical distribution of airborne pollution from factory chimneys. *Quarterly Journal of the Royal Meteorological Society*, 73(317-318), 426-436. Doi:10.1002/qj.49707331715.
- The New Humanitarian, (2007). chlorine gas from water plant kills three in the southeast, cross river: the new humanitarian. Available at: <https://www.thenewhumanitarian.org/report/73168/nigeria-chlorine-gas-water-plant-kills-three-southeast>.
- Tseng, J. M., Su, T. S. & Kuo, C. Y. (2012). Consequence evaluation of toxic chemical releases by ALOHA. *Procedia Engineering*, 45, 384-389. DOI: 10.1016/j.proeng.2012.08.175

Appendix A

A.1 CASE 1 RELEASE: Lamingo Water Treatment Plant Jos Plateau State

Table A.1. 1: Site data (Google map, Ajijah, 2015).

SITE DATA	PARAMETERS (a)	PARAMETERS (b)
Location	Lamingo water treatment plant, Lamingo road, Jos, Plateau state, Nigeria.	Same
Building air exchanges per hour	0.28 (Sheltered Single Storied)	0.50 (enclosed office)
Date/Time of accident	July 25 th , 2015, 04.00 AM.	July 25 th , 2015, 05:45 AM.

Table A.1. 2: Chemical data (ALOHA Software).

CHEMICAL DATA	PARAMETERS (a)	PARAMETERS (b)
Chemical name	Chlorine	Same
CAS Number	7782-50-5	Same
Molecular weight	70.91 g/mol	Same
AEGL-1 (60 min)	0.5 ppm	Same
AEGL-2 (60 min)	2 ppm	Same
AEGL-3 (60 min)	20 ppm	Same
IDLH	10 ppm	Same
Ambient boiling point	-37.28 ⁰ C	Same
Vapor pressure at ambient temperature	Greater than 1 atm	Same
Ambient saturation concentration	1,000,000 ppm or 100%	Same

Table A.1. 3: Atmospheric data (Weather spark, 2016).

ATMOSPHERIC DATA	PARAMETERS (a)	PARAMETERS (b)
Wind	2.058 m/s from 270 ⁰ true at 10m	6.173 m/s from 360 ⁰ true at 10 m
Ground roughness	Open country	Same
Cloud cover	8 tenths	10 tenths
Air temperature	17.22 ⁰ C	Same
Stability class	E	D
Relative humidity	75%	Same
Inversion height	No inversion height	Same

Table A.1. 4: Source strength (Aqua Services, Marie Therese)

SOURCE STRENGTH	PARAMETERS (a)	PARAMETERS (b)
Leak description	Nonflammable chemical leaks from valve in horizontal cylindrical tank, escaping as a gas.	Nonflammable chemical leaks from hole in vertical cylindrical tank, escaping as a mixture of gas and aerosol (two phase flow).
Tank diameter	0.61 m	1.219 m
Tank length	1.829 m	1.829 m
Tank volume	0.641 cu. m	2.564 cu. m
Phase of chemical in tank	Liquid	Liquid
Chemical mass in tank	90.718 kg	1179.1 kg
Circular opening diameter	0.018 m	0.254 m
Distance of opening from tank bottom	0.505 m	0.127 m
Release duration	180 s	60 s
Maximum average sustained release rate	0.192 kg/s	19.005 kg/s
Total amount released	15.74 kg	1139.878 kg
Internal temperature	17.22 ⁰ C (63 ⁰ F)	21.111 ⁰ C (70 ⁰ F)
Volume of chemical in tank	11% of total tank volume	38% of total tank volume
Opening width	0.018 m	0.076 m
Opening length		0.254 m

A.2 CASE 2 RELEASE: Cross River State Water Board Water Treatment Plant**Table A.2. 1: Site data (Google map).**

SITE DATA	PARAMETERS (a)	PARAMETERS (b)
Location	Cross River Water Board Water	Same

	Treatment Plant, Cross River state, Nigeria.	
Building air exchanges per hour	0.50 (enclosed office)	Same
Date/Time of accident	July 5th, 2007, 10:50 AM	Same

Table A.2. 2: Chemical data (ALOHA Software): Same as Table A.1.2 but Ambient boiling point = -34.17°C

Table A.2. 3: Atmospheric data (Weather spark, 2016).

ATMOSPHERIC DATA	PARAMETERS (a)	PARAMETERS (b)
Wind	6.706 m/s from 360° true at 3 meters	Same
Ground roughness	Open country	Same
Cloud cover	10 tenths	Same
Air temperature	26.11°C	Same
Stability class	D	Same
Relative humidity	74%	Same
Inversion height	No inversion height	Same

Table A.2. 4: Source strength (Aqua Services, Marie Therese)

SOURCE STRENGTH	PARAMETERS (a)	PARAMETERS (b)
Leak description	Chlorine gas leaks from hole in horizontal cylindrical tank.	Nonflammable chemical leaks from hole in horizontal cylindrical tank. Chemical escaped as a two-phase mixture of gas and aerosol
Tank diameter	1.372 m	Same
Tank length	2.134 m	Same
Tank volume	3.787 cu.m	Same
Phase of chemical in tank	Gas	Liquid
Chemical mass in tank	69.853 kg	80.739 kg
Circular opening diameter	0.127 m	Same
Distance of opening from tank bottom		0.0762 m
Release duration	60 s	60 s
Maximum average sustained release rate	0.975 kg/s	0.962 kg/ss
Total amount released	58.513 kg	57.606 kg
Internal temperature	26.11°C	Same
Internal pressure	7 atm	

A.3 CASE 3 RELEASE: XYZ Chemical Limited Lagos State

Table A.3.1: Site data (Google map).

SITE DATA	PARAMETERS (a)	PARAMETERS (b)
Location	XYZ Chemicals Ltd, Oshodi/Apapa Expressway, Lagos state, Nigeria.	Same
Building air exchanges per hour	0.50 (enclosed office)	Same
Date/Time of accident	October 7th, 2021, 6.40 AM.	Same

Table A.3.2: Chemical data (ALOHA Software): Same as Table A.1.2 but Ambient boiling point = -34.11°C

Table A.3.3: Atmospheric data (Weather spark, 2016).

ATMOSPHERIC DATA	PARAMETERS (a)	PARAMETERS (b)
Wind	7.717 m/s from 360 ⁰ true at 3 meters	Same
Ground roughness	Open country	Same
Cloud cover	10 tenths	Same
Air temperature	23.89 ⁰ C	Same
Stability class	D	Same
Relative humidity	70%	Same
Inversion height	No inversion height	Same

Table A.3.4: Source strength (Aqua Services, Marie Therese)

SOURCE STRENGTH	PARAMETERS (a)	PARAMETERS (b)
Leak description	Chlorine gas leaks from hole in horizontal cylindrical tank.	Same
Tank diameter	1.219 m	Same
Tank length	2.134 m	Same
Tank volume	2.9911 cu. m	Same
Phase of chemical in tank	Liquid	Gas
Chemical mass in tank	907.185 kg	55.338 kg
Opening width	0.076 m	Same
Opening length	0.178 m	Same
Opening from tank bottom	0.152 m	
Release duration	60 s	Same
Maximum average sustained release rate	13.925 kg/s	0.776 kg/s
Total amount released	834.61 kg	46.72 kg
Internal temperature	23.89 ⁰ C	Same

INVESTIGATING THE EFFECTS OF SHEA NUT PROCESSING CONDITIONS ON THE YIELD AND QUALITY OF TRADITIONALLY PRODUCED SHEA BUTTER

Saba, A. M.¹, Baba, A. H.¹, Mohammed, I. Y.¹ and AbdulQadir, M.³

¹Department of Chemical Engineering, The Federal Polytechnic P. M. B. 65 Bida

²Department of Chemical Engineering, Abubakar Tafawa Balewa University, P. M. B 0248, Bauchi

³Science Department, Government Girls' Science College P.M.B 41 Bida

Corresponding authors E-mail: sabaam2006@gmail.com, aliyuharunababa2003@gmail.com

ABSTRACT

Agricultural diversification has been identified as part of measures for minimising global yearning for developing opportunities for sustainable production systems. Processing of Shea nut into Shea butter is mostly carried out by women in Nigeria using traditional methods. This approach is currently not well-standardized and has significant impact on the yield and product quality. Robust investigations of process variables are needed to identify the most important process parameter(s) that would guarantee high yield and good quality Shea butter. In this study, effects of Shea kernel roasting temperature (30, 90 and 150 °C), roasting time (10, 35 and 60 minutes), Shea paste kneading speed (100, 200 and 300 rpm), and time lag between Shea kernel milling and Shea paste kneading (5, 15 and 25 minutes) on the yield and quality of Shea butter produced through traditional extraction method were evaluated. At 30 °C roasting temperature, 31.68 wt % Shea butter was recorded, which increased to 36.4 wt % when the roasting temperature was raised to 150 °C. Free fatty acid content increased significantly from 1.28 to 2.1 % while the peroxide value was maximum at 100 °C (2.1 meq/kg). Longer roasting time and time lag between milling and kneading also led to high free fatty acid and peroxide contents. This study indicates that the roasting temperature, roasting time and time lag between milling and kneading represent the most significant parameters for high yield and good quality Shea butter production via traditional extraction method.

Keywords: Shea kernel; free fatty acid; kneading speed; Shea butter quality.

1.0. INTRODUCTION

Agricultural diversification has been identified as part of measures for minimising global yearning for developing opportunities for sustainable production systems (Mohammed et al., 2017). Shea butter is one of these numerous vegetable oils and it's a fatty extract obtained from the kernels of Shea fruit. It is also a mixture of fatty acids usually Oleic, Stearic, Palmitic, Linoleic and Arachidic Acids with Oleic and Stearic acids predominating and together constituting about 85 % of the fatty acid content of Shea butter (Coulibaly et al., 2009; Julius et al., 2013). The presence of these fatty acids in Shea butter varies in proportion depending on the source of the Shea nuts. The nut is obtained from Shea tree which is a native of Africa and it is either called *Vitellariaparadoxa* or *Butyrospermum parkii* in West Africa or "*nilotica*" in East Africa. Examples of countries where Shea trees are found include Senegal, Mali, Ivory Coast, Burkina Faso, Togo, Ghana, Benin, Niger, Nigeria, Cameroon and further east in Uganda, Sudan and Ethiopia (Walter et al., 2003). The tree bears

fruit up to 4 cm in diameter and contains a nut. It grows wild up to 9-12 m in height and begins to bear fruits after approximately 15–20 yrs. The tree gets matured at about 45 years and continues to bear fruits for about 200 years (Alander, 2004).

Nigeria is well endowed with this tree accounting for about 50-60 % of West African Shea tree population. In Nigeria, these trees are concentrated in states of Niger, Kwara, Nassarawa, Kogi, FCT and Plateau. It is also found in some parts of Zamfara, Adamawa, Edo, Yobe, Plateau, Kaduna, Kebbi, Bauchi and Oyo (National Shear Products Association of Nigeria (NASPAN), 2018).

Statistics has shown that 40–50 % of these Shea trees are found in Niger state. The tree starts flowering and fruiting in January and harvest begins between May to June through to August. After the harvest, the pulp is removed and the nuts are dried followed by the removal

of the shell. The Shea kernels is then processed for Shea butter via three methods namely: solvent extraction, mechanical expression and traditional method. The solvent extraction method is an expensive and a high-tech process of Shea butter extraction involving the use of organic solvents such as straight chain hydrocarbons, alcohols, chlorinated hydrocarbons and ketones to recover the oil from the kernels. The Shea butter from this method is highly refined and hence contains little or no bio-active components. The mechanical expression method involves the use of expellers or hydraulic press which exerts high pressure on the heated kernels to express the Shea oil. The Shea oil obtained from this method has high FFA and requires refining before use (Julius *et al.*, 2013). Lovett (2004) stated that traditional methods of Shea butter extraction is the most preferred method because of its retention of bio-active components.

It involves the use local material like fire wood, pots, pestle and mortar, milling machine and plastic vats. The product from this method of extraction if controlled gives a grade of Shea butter referred to as unrefined with high bio-actives (Triterpines alcohol, vitamin E, phytosterols and catehins) greater than 5 %. This characteristic is more desirable in both cosmetics and pharmaceutical industries and attracts more premiums (William and Isemde, 2015) and is rarely obtained among Shea butter producing countries including Nigeria (Lovett, 2013). Consequently, robust investigations of the traditional extraction method are needed to identify the most important process parameter(s) that would guarantee high yield and good quality Shea butter. The object of this study is to investigate the impact of Shea kernel roasting temperature, roasting time, Shea paste kneading speed, and time lag between Shea kernel milling and Shea paste kneading on the yield and quality of Shea butter produced through traditional extraction method. Attempts made by several researchers to improve the yield and quality of traditional method of processed Shea butter laid emphasis only on the extraction methods without considering the quality of the kernels (Didia *et al.*, 2018; Obibuzor *et al.*, 2014; Julius *et al.*, 2013; Munir *et al.*, 2012; Okullo *et al.*, 2010; Chukwu and Adgidzi 2008). Yonas *et al.* (2016); Aculey *et al.* (2012) and Alonge and Olaniyan (2007) however opined that the properties of shea butter is fundamentally influenced by the quality of the Shea kernel which is dependent on its origin, genetic variation, pre-treatments, processing factors and methods of

extraction. The results of these researches only gave a minimal improvement on the physicochemical properties of the Shea butter without improving the quality of Shea butter.

2.0. MATERIALS AND METHODS

2.1. Materials

The following materials were used for the research: Shear nuts; wooden pestle and mortar; 1.5 kilowatt milling machine; water bath; 0.25 N NaOH; Pottasium Iodine; Sodium Thiosulphate; Hydrochloric acid; Variable mixer; Starch solution; Phenolphthalein; Glacial acetic acid; Chloroform; Reflux condenser; Whatman filter paper; Refractometer; Meter Telodo Balance; Alcoholic Pottasium Hydroxide; Reflux air condenser; Petroleum ether; Etc.

2.2. Methods

Freshly de-pulped Shea nut were collected from Sonmajigi (N09° 11' 56"; E05° 35' 45") in Lavun local government, Pati- Ndeji (N09° 23' 38"; E06° 36' 25") in Gbako local Government, and Chengudu (N09° 07' 40"; E05° 32' 34") in Edati local government, all in Niger State, Nigeria. The nuts were assessed as received, mixed, and sorted but the sprouted ones were discarded. 4 kg of Shea nuts were processed at earlier determined optimum conditions of 4.0 day conditioning period, 120 minutes boiling duration, and 86 °C drying temperature (Saba, 2019). These nuts were crushed using wooden pestle and mortar. 2 kg of the crushed kernels were then processed by roasting the kernels in a laboratory oven at temperatures of 30, 90 and 150 °C for 10, 35, and 60 minutes. The warm crushed kernels were then milled using 1.5 kilowatt Atlas milling machine. Samples were taken from the milled kernels in paste form after cooling for 5, 15, 25 hour. Kneading was performed at 100, 200, 300 rpm using a laboratory variable mixer and subsequently used to produce Shea butter. The Shea butter obtained was characterized for both physical and chemical properties. The experiment was repeated in triplicates and mean values reported. The Shea butter produced was characterized according to African Organisation for Standardization (ARSO) (2017), methods

2.2.1. Determination of Oil Yield (Y_0)

A sample of the Shea butter produced was weighed on a weighing balance and the weight recorded as W_u . The weighed Shear butter was then pressed in a pressing

machine and the weight recorded until a constant weight was achieved. This constant weight was recorded as W_e . The Oil yield was calculated using equation (1):

$$Y_0 = (W_u - W_e) / W_u \times 100 \quad (1)$$

Where:

Y_0 = percentage oil yield; W_u = weight of sample before pressing (g), W_e = weight of sample after pressing (g).

2.2.2. Determination of Free Fatty Acid (FFA)

The FFA content of the Shea butter was determined using American Oil Chemists Society (AOCS) (1994) method. 7 g of the Shea butter was measured and poured into a 250 mL flask and 50 mL neutralized alcohol added. The mixture was titrated with 0.25 N NaOH with vigorous shaking until permanent faint pink colour appeared and was maintained for a period of 60 seconds. The volume (mL) of 0.25 N NaOH used in the titration was used to calculate the percentage FFAs present in the oil which was calculated using equation (2).

$$FFA = \{(V - B) \times N_f \times 28.2\} / W \quad (2)$$

Where:

FFA = free fatty acid (%), V = Volume of NaOH ethanolic solution used for titration (mL), B = Volume of NaOH ethanolic solution used for blank, W = weight of oil sample (g).

2.2.3. Determination of Peroxide Value (PV)

Peroxide value was determined following International Organisation for Standardization (ISO) (2005). 2 gram of Shea butter sample was weighed and transferred into a clean tube immersed in boiling water. 1 g of potassium iodine powder was added to the oil samples and 20 cm³ of the solvent mixture (glacial acetic acid and chloroform in the ratio 2:1). Then the boiling tube was placed in different boiling water bath so that the liquid mixture boils for 30 seconds. The mixtures were allowed to boil vigorously for not more than 30 seconds; the contents after boiling were quickly transferred into a flask containing 20 cm³ of 5 % potassium iodine solution. The tube was washed out twice with 25 cm³ of water. The resulting mixtures were then titrated with 0.002 M sodium thiosulphate using fresh 1 % starch solution. A blank titration was also carried out at the same time. The analysis was performed in triplicate. The peroxide value in milliequivalent per 100 g (Meq/100 g) was determined for each sample using equation (3).

$$PV = (T \times M \times 1000) / W \quad (3)$$

Where:

T = Titre value of Na₂SO₃ (cm³), M = Molarity of Na₂SO₃(M) and W = weight of Oil sample (g)

2.2.4. Determination of Refractive Index (RI)

The Refractive Index (RI) analysis was carried out following Association of Official Analytical Chemists (AOAC) (2000) method. 2 g of Shea butter sample was melted into liquid and filtered through 11 cm whatman filter paper to remove impurities and traces of moisture. Few drops of the dried Shea butter sample were then placed on the prism. The prism was closed and allowed to stand for 2 minutes. The temperature of the refractometer was adjusted to 40 °C and the light passing through was sufficient to obtain the most distinct reading possible. The refractive index was then read.

2.2.5. Determination of saponification Value (SV)

Determination of saponification value (SM) followed ISO 3657: 2005 method. 2g of Shea butter was weighed into a clean dried 250 mL conical flask and 25 mL of alcoholic potassium hydroxide (K(OH)₄) was added. A reflux condenser was attached and the flask was heated for an hour with frequent shaken. 1 mL of 1 % phenolphthalein indicator was added and the hot excess alkali was titrated with 0.5 M hydrochloric acid (HCl) until it reached the end point where it turns to colourless. A blank titration was carried out at the same time and under the same condition. The saponification value was calculated using equation (4).

$$SV = \{(a - b) \times 0.0205\} / W \quad (4)$$

Where: a, b = constants and W = weight of oil sample (g).

2.2.6. Determination of Unsaponifiable fraction (UF)

The unsaponifiable fraction (UF) of Shea butter was determined using AOAC (2000) method. 5 g of Shea butter was accurately weighed using metler Toledo balance and mixed in a 250 mL of conical flask. 50 mL of alcoholic potassium hydroxide was added to the mixed Shea butter. The mixture was then boiled under reflux air condenser until saponification was completed. The saponified mixture was transferred while warm to a separating funnel. The mixture was washed with ethyl alcohol and then with cold water, ensuring that a total of 50 mL of water was used to rinse the flask. 50 mL of petroleum ether was added to mixture and shook vigorously until the layers separate. The lower layer was transferred into another separating funnel and the ether

extraction was repeated thrice using 50 mL portion of petroleum ether. The combined ether extract was first washed thrice with 25 mL of distilled water to ensure the ether extract was free of alkali. The ether solution was transferred to 250 mL beaker and the separator was rinsed with ether. The rinsings were added to the main solution. The bulk solution was evaporated to about 5 mL and quantitatively transferred using several portion of ether to 50 mL. The ether was then completely evaporated by boiling at 100 °C for 30 minutes and 2-3 mL of acetone was added while heating on a water bath until a constant weight was obtained. The residue was dissolved in 50 mL of warm ethanol which has been neutralised to phenolphthalein end point. The dissolved residue was titrated with 0.02 N NaOH. The unsaponifiable fraction was calculated using equation (5)

$$UF = 100(A - B)/0.282 \times V \times N \quad (5)$$

Where:

A = weight of the residue in (g), B = weight of the FFA in the extract (g), W = weight of the sample (g), V = volume of standard NaOH solution (mL) and N = Normality of standard NaOH solution

3.0. RESULTS AND DISCUSSION

3.1. Effect of Roasting Temperature (RT) on the Yield and Quality of Shea Butter

Yield and quality of the Shea butter produced through the traditional extraction method were analysed and results shown in Table 1.

Table 1: Effect of Roasting Temperature on the yield and quality of Shea butter produced at Rt:10 min, Ksp; 200 rpm and TLBMK;15 h

RT (°C)	Yield (%)	SV mg KOH/g	UF (%)	FFA (%)	PV meq/kg	RI
30	31.7	186.2	12.0	1.28	1.68	1.44
90	35.6	186.2	10.2	1.47	2.10	1.52
150	36.4	190.2	10.0	2.10	1.82	1.47

Table 1 shows the effect of RT on the yield and quality of Shea butter as indicated by FFA, PV, RI, SM and UF. At (30 °C, RT) and constant roasting time of 10 minutes, kneading speed (K_{sp}) of 200 rpm and Time Lag Between Milling and Kneading (TLBMK) of 15 hour, the Shea butter yield was 31.68 wt %, which increased to 35.6 wt % and subsequently to 36.4 wt % as the temperature increased from 30 °C through 90 °C to 150 °C. This shows that when the value of RT tripled the initial, the

corresponding Shea butter yield increased by about 12 %. On the other hand, when the temperature was further increased to 150 °C, only additional 0.8 % increase in the yield was recorded. Recent study has shown that RT of around 171 °C is enough to produce optimum oil yield (Honfo *et al.*, 2017). The result of this investigation revealed that about 30 w % oil yields was recorded at the said temperature. This value is only comparable to the yield reported herein at room temperature, suggesting high RT of the kernel above 90 °C may not have substantial impact on the Shea butter yield. This observation is in good agreement with the report of Olaniyan and Oje (2011). The authors stated that an optimum heating temperature of 82 °C would produce about 35 wt % Shea butter. On the contrary, according to Obeng *et al.* (2010), oil extraction using roasted kernels produced lower yield of Shea butter compared to those obtained with raw kernels. These divergence views about the roasting temperature of the kernel suggest that a comprehensive process optimisation be carried out couple with other variables to ascertain the optimum working condition. Table 1 further shows impact of RT on FFA, PV, RI, UF and SM. Increasing RT from 30°C to 150 °C resulted in significant increase in the FFA while other parameters were less affected. At 30 °C RT, the value of FFA recorded was 1.28 %, which increased by 15 % and 64 % at 90 and 150 °C respectively. This trend may be due to presence of moisture in the Shea butter, which may have resulted in hydrolysis since higher temperatures generally increase the rate of hydrolysis reaction. According to Honfo *et al.* (2017) high moisture content in kernel promote hydrolysis reaction that subsequently result in the increase in FFA value. Therefore, the high FFA value recorded in this study could be linked to the pre-processing conditions of the kernel prior to the Shea butter production stage.

3.2. Effect of Roasting Time (Rt) on Yield and Quality of Shea Butter

Effect of Roasting time on the yield and quality of Shea butter produced at constant Roasting Temperature of 30 °C, K_{sp} of 200 rpm and TLBMK of 15 hour is presented in Table 2.

Table 2: Effect of Roasting time on the yield and quality of Shea butter produced at RT:30 °C, Ksp; 200 rpm and TLBMK;14h

Rt (min)	Yield (%)	SV mg KOH/g	UF (%)	FFA (%)	PV meq/kg	RI
5	31.7	186.2	11.9	1.44	1.68	1.44
35	34.2	182.2	11.8	2.54	1.68	1.45
60	31.6	180.2	12.2	1.78	1.64	1.45

The results show that FFA is significantly affected by the RT while the PV, RI, UF and SM remained relatively constant at 1.64 meq/kg, 1.45 %, 12.2 % and 180-186 mg KOH/g respectively. This result indicates that after pre-processing of the kernel and allowing it to stay at room temperature for up to 35 minutes, builds up the FFA value to a maximum of 2.54 %. Beyond 35 minutes, the FFA value reduced to 1.78 % at 60 minutes, which is equivalent to about 39 % improvement on the initial FFA value. This observation is similar to the effect of RT on FFA reported by Honfo *et al.* (2017). They recorded increase in the FFA value with increasing roasting time. This trend suggests that a shorter RT would generally result in lower FFA value in the butter in addition to other economic advantage such as cost reduction in terms of energy usage.

3.3. Effect of Kneading Speed (Ksp) on the Yield and Quality of Shea Butter

Effect of kneading speed on the yield and quality of Shea butter produced at constant roasting temperature of 30 °C, Rt = 35 min and TLBMK of 14 hour is presented in Table 3.

Effect of K_{sp} on the yield and quality of Shea butter produced at constant RT of 30 °C, Rt of 35 minutes and TLBMK of 14 hours is presented on Table 3.

Table 3: Effect of Kneading speed on the yield and quality of Shea butter produced at RT:30 °C, Rt =35 min and TLBMK;14h

K_{sp} (rpm)	Yield (%)	SV mg KOH/g	UF (%)	FFA (%)	PV meq/kg	RI
100	31.6	187.2	12.0	1.84	1.72	1.44
200	34.2	182.2	11.8	2.54	1.68	1.45
300	38.7	190.6	12.8	2.02	1.64	1.45

The result shows that FFA is increased by 38 % as the K_{sp} increased from 100 to 200 rpm and further increase of K_{sp} to 300 rpm caused a reduction of 20 %, this also cause a corresponding increase in yield as the kneading increases while the PV, RI, UF and SM remained relatively constant at 1.68 meq/kg, 1.446 %, 11.8 % and 182.20 mg KOH/g respectively. Beyond 200 rpm, the FFA value reduced to 2.02 %, which is equivalent to about 10 % higher than the initial FFA value. This observation is similar to the effect of RT on FFA reported by Honfo *et al.* (2017). They recorded increase in the FFA value with increasing roasting time. This

trend suggests that a longer K_{sp} would generally result in lower FFA value in the butter.

3.4. Effects time lag between milling of kernel and kneading of Shea paste on yield and quality of Shea butter

Effect of time lag between milling of kernel and kneading of Shea paste on the yield and quality of Shea butter produced at constant roasting temperature of 30 °C, Rt = 35 min and TLBMK of 14 hour is presented in Table 4.

Table 4: Effect of time lag between milling of kernel and kneading of Shea paste on the yield and quality of Shea butter produced at RT:30 °C, Rt = 60 min and K_{sp} = 200 rpm

TLBMK (h)	Yield (%)	SV mg KOH/g	UF (%)	FFA (%)	PV meq/kg	RI
5	31.0	178.8	12.4	1.60	1.48	1.45
15	31.6	180.4	12.2	1.78	1.64	1.45
25	32.2	188.2	11.8	2.44	2.04	1.45

The time lag between milling and kneading shows significant effect on the FFA and PV with RT of 30 °C, K_{sp} of 200 rpm and Rt of 60minutes as shown in Table 4. At 5 hour TLBMK, the FFA value recorded was 1.6 %, which almost doubled when the TLBMK increased by 5-fold. The corresponding PV increased from 1.48 to 2.04 meq/kg. Similarly, with increase in the TLBMK from 5 to 25 hours, the SM value increased from 178.8 to 188.2 mg KOH/g, which correspond to 5 % increase. The implication of higher SM means that more consumption of alkali before saponification reaction is completed. This high caustic consumption may lead to high cost of saponification but has the corresponding advantage of high yield of soap as a result of high Total Fatty Matter (TFM) in the Shea butter.

4.0. CONCLUSION

This study evaluates the effect of Shea butter process variables such as kernel roasting temperature, roasting time, Shea paste kneading speed, and time lag between Shea kernel milling and Shea paste kneading on the yield and quality of Shea butter produced through traditional extraction method. The result showed that roasting temperature, roasting time and time lag between milling and kneading individually represent significant parameters for high yield and good quality Shea butter.

These variables need to be further optimised collectively in order to establish optimum condition for good quality Shea butter.

ACKNOWLEDGEMENTS

The authors are grateful to TETFund for providing grant for funding the research and also the management of Federal Polytechnic, Bida for providing enabling environment.

REFERENCES

- Aculey, P.C.; Lowor, S. T.; Kumi, W. O. and Assuah, M. K. (2012). The Effect of Traditional Primary Processing of the Shea Fruit on the Kernel Butter Yield and Quality. *American Journal of Food Technology*. 7 (2), 73-81.
- Alander, J (2004). Shea butter- a Multi Functional Ingredient for Food and Cosmetics. *Lipid Technology*, 16, 202-205.
- AOAC (2000) Official methods of analysis of the Association of official Analytical Chemists', Washington DC.
- AOCS (1994) Official methods of recommended practices of the AOCS, Champaign, III, American Oil Chemist's Society ARSO, (2017). A
- ARSO, (2017). African Organization for Standardization; Building capacity to help Africa trade better, <https://www.tralac.org/news/article/11646-activities-of-the-african-organisation-for-standardisation-arsorelated-to-the-work-of-the-wto-tbt-committee.html>
- Chukwu, O. and Adgidzi, P.P. (2008). Evaluation of Some Physico-Chemical Properties of Shea-Butter (*Butyrospermum Paradoxum*) Related to its Value for Food and Industrial Utilisation. *Int. J. Postharvest Technology and Innovation*, 1(3), 1-7
- Coulibaly, Y., Ouédraogo, S., Niculescu, N. (2009). Experimental Study of Shea Butter Extraction Efficiency Using a Centrifugal Process. *Asian Research Publishing Network (ARPN)*, 4(6), 14-19.
- Didia, B.; Zakpaa, H. D.; Mills-Robertson, F. C. and Abdul-Mumeen, I. (2018). Enzyme-assisted Traditional Extraction of shea butter using different Levels of Pre-treated Shea Kernels. *Journal of Agricultural Biotechnology and Sustainable Development*. 10(1), 1-10
- Honfo, F.G., Linnemann, A.R., Guo, M., Akissoe, N., Soumanou, M.M., and Boekel, M.A.J.S. (2017). Influence of roasting of Shea kernels on their fat content and some quality characteristics of Shea butter. *Journal of Food Studies*, 6(1), 66-80.
- ISO 3960 (2005). International Organization for Standardization. Animal and Vegetable fats and oils –Determination of Peroxide Value. pp. 1-6
- Julius, K.I., Lilly, N., and Ayangealumun, I. (2013). Effects of Extraction Methods on the Yield and Quality Characteristics of Oils from Shea nut. *Journal of Food Resource Science*, 2(1), 1-12.
- Lovett, P. (2013). Quality @ Quantity @ Price: A Report Submitted to USAID, (Ed.) USAID, Shea Abuja, Nigeria: Global Shea Alliance., pp. 1-20.
- Lovett, P. (2004). The Shea Butter Value Chain., United States Agency for International Development (USAID).
- Mohammed, I.Y., Abakr, Y.A., Hui, J.N.X., Alaba, P.A., Morris, K.I., Ibrahim, M.D. (2017). Recovery of clean energy precursors from Bambara groundnut waste via pyrolysis: Kinetics, products distribution and optimisation using response surface methodology. *Journal of Cleaner Production*, 164, 1430-1445.
- National Shear Products Association Nigeria (NASPAN). (2018). Road Map Document.
- Obeng, G.Y., Adjaloo, M.K., Donkor, P. (2010). Effect of temperature, moisture content, particle size and roasting on Shea butter extraction efficiency. *International journal of food engineering*, 6(2).
- Obibuzor, J. U., Omamor, I., Omoriyekemwen, V., Okogbenin, A., & Okunwaye, T. (2014). A Two Year Seasonal Survey of the Quality of Shea butter Produced in Niger State, Nigeria. *African Journal of Food Science*, 8(2), 64-74.
- Okullo, J. B. L., Omujal, F. Agea, J. G., Vuzi, P. C., Namutebi, A., Okello, J. B. A. & Nyazi, S. A. (2010). Physico-chemical characteristics of Shea butter (*Vitellaria paradoxa* CF Gaertn.) oil from the Shea district of Uganda. *Africa Journal of Food Agriculture Nutrition and Development*. 10, 2070-2084.
- Peers, K. (1977). The Non Glyceride Saponifiables of shea butter . *Journal of Science Food Agric*, 1000-1009.
- Olaniyan, A.M., Oje, K. (2011). Development of model equations for selecting optimum parameters for

- dry process of Shea butter extraction. *Journal of Cereal and Oil Seed*, 2(4), 47-56.
- Saba, A. M. (2019). Upgrade and optimization of a typical traditional shea butter extraction process. PhD Thesis, Federal University of Technology, Minna, Nigeria.
- Walter, S., Cole, D., Kathe, W., Loveth, P., Paz Soldam, M.(2003). Impact of certification on the sustainable use of NWFP: Lessons learnt from three case studies. *International Conference on Rural Livelihoods, Forest and Biodiversity*, Bonn, Germany.
- William, E., Isemeye, J. (2015). Issues in the Shea butter value chain at the UNIDO workshop for stakeholders in the Shea butter value chain held in Minna, Nigeria.
- Yonas, A. G., Shimel, A., & Sisay, E. A. (2016). Optimisation of shea butter quality using screw impeller extraction. *Food science and nutrition*. 2, 840-846

PREDICTION OF HIGHER HEATING VALUE OF BIOMASS BASED ON ULTIMATE AND PROXIMATE ANALYSES

Osuolale, F. N.¹, Olateju, I. I.², Oke E. O.³, Alade A. O.¹, Agarry S. E.¹, Alagbe S. O.¹, Ogunleye O. O.¹ and *Agbede, O. O.¹

¹Department of Chemical Engineering, Ladoke Akintola University of Technology, Ogbomosho, Oyo State, Nigeria

²Department of Chemical Engineering, Afe Babalola University, Ado-Ekiti, Nigeria

³Department of Chemical Engineering, Michael Okpara University of Agriculture, Umudike, Abia State, Nigeria

*Correspondence: ooagbede@lautech.edu.ng; Tel.: +234-806-550-2864

ABSTRACT

High heating value (HHV) of biomass is important for the design and operation of biomass based energy conversion processes. Experimental determination of this property is always time consuming and expensive. This paper compares existing empirical correlations based on proximate and ultimate analysis of biomass for the determination of the HHV. The correlations were validated from experimental data for twelve biomass that are typical to Nigeria. The correlation based on proximate analysis with the least error is $HHV = (354FC + 170.8VM)/1000$ having a mean absolute error of prediction in the range 0.12 to 5.71 and average absolute error of 0.07 to 24%. The Average absolute error of the correlation $HHV = 0.3897C + 0.2976$ from ultimate analysis ranges from 0.09 to 28.9% and the Mean absolute error ranges from 0.015 to 4.71. The predictions from the correlations are not showing good agreement with the experimental data. Ultimately, three correlations were developed in this study. The correlation based on ultimate analysis gave mean absolute prediction error of 0.11 to 2.45 and average absolute error of 0.6 to 16%. The correlation based on a combination of ultimate and proximate analysis gave mean absolute prediction error of 0.08 to 2.05 and average absolute error of 1-12%. The developed correlations are seen to be more accurate in predicting the HHV values.

Keywords: Biomass, High Heating Value, Proximate analysis, Ultimate Analysis,

1.0 INTRODUCTION

Biomass is a renewable and sustainable source of energy. It includes every type of carbonaceous materials except fossil fuels. It is widely available, cheap and easy to access (Klass, 1998). Biofuels and biohydrogen can be sustainably produced using thermochemical and biological means from agricultural wastes, domestic wastes and commercial wastes (Sharma et al., 2020). The drawback in utilizing these wastes lies in insufficient knowledge of their inherent energy since it has been established that biomass varies in composition depending on the type, locality and climatic conditions of where it grow (Hill et al., 2006).

The heating value of biomass can be reported in terms of lower or higher heating value. The higher heating value (HHV) gives the energy content of biomass (Puig-Arnavat et al., 2010, Parikh et al., 2007). HHV can be used to estimate the devolatilization product compositions when modeling and simulating biomass conversion technology (Wen et al., 2017). It is the most important parameter to evaluate the fuel quality of

biomass (Ozyuguran et al., 2018) and the design and operation of biomass fueled reactors (Khodaei, 2015). HHV should be known to determine the conversion efficiency (Mckendry, 2002) and optimization of some biomass conversion process (Prins et al., 2007).

HHV is determined experimentally using bomb calorimeter. The use of bomb calorimeter might not always be accessible or conducive for researchers especially in the developing world. Consequently, researchers with ultimate and proximate analysis results of biomass can use the resulting data to determine the heating value using established correlations. There have been many presented correlations for HHV in literatures from proximate and ultimate analyses and increasingly researchers are shifting to renewable energy especially from biomass (Yin, 2011). This work attempts to present correlations that predict accurately the HHV of biomass that are typical to Nigeria. These correlations are faster, affordable and particularly useful for researchers without access to experimental HHV determination equipment.

2.0 METHODOLOGY

Samples of 12 different biomass were prepared according to ISO 14780:2017 standard. The preparation procedures include drying, size reduction and screening. The samples are: Coconut husk, Maize shell, Coconut shell, Groundnut shell, Corn cob, Palm kernel, Saw dust, Walnut shell, Bagasse, Rice Husk, Mango Pod and Cashew shell.

2.1 Proximate Analysis

The Proximate analysis was used to determine the characteristics of the biomass. This include the moisture content (MC), Volatile Matter (VM), Ash Content (A) and Fixed Carbon content.

Moisture Content was determined according to ASTM D 3173-03. One gram of the sample was measured into a crucible and placed in an oven at 105 °C for an hour. It was removed and placed in a desiccator to cool to a room temperature, after which the weight lost was measured and recorded according to the formula below

$$MCW = \frac{W_2 - W_3}{W_2 - W_1} \times 100\% \quad 1$$

$$MCD = \frac{W_2 - W_3}{W_3 - W_1} \times 100\% \quad 2$$

Where MCW is the moisture content based on wet weight basis, MCD is the moisture content based on dry weight basis, W_1 is the weight of crucible, (g) W_2 is the weight of crucible + weight of sample before heating, (g), W_3 is the weight of crucible + weight of sample after heating, (g)

Volatile Matter: One gram of sample was measured into a crucible and covered; the covered crucible was placed into a high temperature furnace which has already been preheated to 900 °C (ISO 562-2010). The sample was then heated for exactly seven minutes and removed from the furnace. It was allowed to cool for about one minute in the laboratory, and then place it in the desiccator until it has cooled to room temperature. The sample was removed, weigh and recorded according to the following formula;

$$\%VM = \left(\frac{\text{Initial weight} - \text{Final weight}}{\text{Initial weight} - M} \times 100\% \right) \quad 3$$

M = % moisture content

Ash is defined as the weight of the residue remaining after complete burning of 1g of the biomass at 750 °C for one hour. It was removed and place in a desiccator to cool to a room temperature, after which the weight lost was measured and recorded. The sample was returned back to the furnace for 20minutes interval until a constant weight is obtained (ASTM D 3174-04). The calculation was done according to equation 4;

$$Ash = \frac{\text{Initial weight} - \text{Final weight}}{\text{Initial weight}} \times 100\% \quad 4$$

Fixed Carbon was determined according to (ASTM Standard D 3172-89). The content of fixed carbon is determined by subtracting the sum of Ash %, Volatile Matter and % Moisture Content from total of 100 % composition.

$$FC = 100 - (\% Ash + \% VM + MC) \quad 5$$

2.2 Ultimate Analysis

This analysis is important for determining the elemental composition (C, N, H, S, O etc.) of the biomass fuels and is also useful for calculating their heating value

Determination of carbon and hydrogen contents

Carbon and hydrogen contents of the samples was determined simultaneously by Liebig – Pregl method (Mazor, 1983). One gram of each sample was placed in a quartz test tube and burned off through the absorbents magnesium percolate to absorb water and sodium hydroxide to absorb carbon dioxide. The amounts of water and carbon dioxide was determined from the difference between the two weighing, one before the other after the absorption of water and carbon dioxide. The percentage of Carbon (%C) and hydrogen (%H) were evaluated thus:

$$\%C = \frac{a(0.2727)}{\text{weight of the sample}} \times 100 \quad 6$$

$$\%H = \frac{b(0.2727)}{\text{weight of the sample}} \times 100 \quad 7$$

Where: a - quantity of CO₂, b - quantity of H₂O

Determination of nitrogen contents: Nitrogen content of biomass feedstock was determined by Dumas – Pregl method (Patterson, 1973). 0.2g of each sample was mixed with powder of copper oxide in the ignition tube. Air was displaced from the tube by passing it through a stream of CO₂ until minute bubble appeared in the Nitrogen flow meter filled with about 50% solution of

potassium hydrogen. The weighed sample was burned off at between 700°C and 750°C in a gas burner and later burned in an atmosphere of CO₂ with the gas cylinder shut off. After ignition, the combustion product was displaced with carbon dioxide into the nitrogen flow meter. The percentage of Nitrogen (%N) content was determined by the equation 8:

$$\% N = \frac{V(1.097)}{\text{weight of the sample}} \times 100 \quad 8$$

Where: V - volume of Nitrogen in the Nitrogen flow meter and 1.097 is the mass of 1 ml of Nitrogen in the test tube.

Determination of sulphur content : 1g of each sample was wrapped in a filter paper free from ash and it was secured in the platinum wire seal into a glass rod held fast to the stopper of a flask filled with Oxygen. The weighed sample was ignited in filter and inserted in the flask immediately, and the flask was plugged with the stopper. The product was absorbed with a mixture of water and Hydrogen peroxide to oxidize the combustion product immediately. The combustion product was titrated with a solution of Barium percolate in the

presence of the indicator Toron with a pH value of 4.5. The percentage of sulfur was calculated using equation 9:

$$\% S = \frac{(T \times V)}{\text{weight of the sample}} \times 100 \quad 9$$

Where: T - titre of Ba (CO₄)² solution , V - volume of Ba (CO₄)² solution

Determination of oxygen content: The percentage oxygen content was determined by the differences as given in equation 10.

$$\% \text{Oxygen} = 100 - (C + H + N + S) \quad 10$$

Where: C -% carbon content , H -% hydrogen content , N -% nitrogen content S -% sulphur content

2.3 Existing correlations for determining HHV from ultimate and proximate analysis

Table 1 provides recent and established correlations for predicting HHV of biomass. The correlations are derived from both ultimate and proximate analysis.

Table 1: Some existing correlations based on proximate and ultimate analyses
Correlations Based on Proximate analysis

S/N	High heating value (kJ/Kg)	References
1	$HHV = -10.8141 + 0.3133(VM + FC)$	Jimenez and Gonzales (1991)
2	$HHV = (354FC + 170.8VM)/1000$	Cordero <i>et. al.</i> , (2001)
3	$HHV = (35430 - 183.5VM - 354.3Ash)/1000$	Cordero <i>et. al.</i> , (2001)
4	$HHV = 19.914 - 0.2324 Ash$	Sheng and Azevedo (2005)
5	$HHV = -3.0368 + 0.2218VM + 0.2601FC$	Sheng and Azvedo (2005)
6	$HHV = 0.3536FC + 0.1559VM - 0.0078Ash$	Parikh <i>et. al.</i> , (2005)
7	$HHV = 0.1905VM + 0.2521FC$	Yin (2011)
Correlations Based on Ultimate Analysis		
1	$HHV = -0.763 + 0.301C + 0.525H + 0.0640$	Jenkins and Ebeling (1985)
2	$HHV = 0.4373C - 1.6701$	Tillman (2001)
3	$HHV = 0.3491C + 1.1783H + 0.1005S - 0.10340 - 0.0151N - 0.0211Ash$	Channiwala and Parikh (2002)
4	$HHV = (3.55C^2 - 232C - 2230H + 51.2C * H + 131N + 20600)/1000$	Friedl <i>et al.</i> , (2005)
5	$HHV = 0.3259C + 3.4597$	Sheng and Azvedo (2005)
6	$HHV = -1.3675 + 0.3137C + 0.7009H + 0.03180$	Sheng and Azevedo (2005)
7	$HHV = 0.3897C + 0.2976$	Toscano and Pedretti (2009)

Correlations Based on Proximate analysis

8	$HHV = 0.2494C + 0.8250H$	Yin (2011)
9	$HHV = (C^2 + 0.60C) + 0.03CH - O + 0.53S + 0.11ON + CO^2 - 0.33SO$	Moka (2012)
10	$HHV = 0.879C + 0.3214H + 0.0560 - 24.826$	Elneel <i>et al</i> (2013)
11	$HHV = 0.335C + 1.423H - 0.154O - 0.145N$	Singh <i>et al</i> (2013)
12	$HHV = 0.9872C^{0.7587} + 0.6831H^{0.3645} + 0.1055N^{3.2688} + 0.8620$	Christoforou <i>et al.</i> , (2014)
13	$HHV = 0.251C + 1.068H + 0.011O - 1.114S - 0.328N + 0.644$	Singh <i>et al.</i> , (2015)
14	$HHV = 0.2914C + 0.8741H$	Qian <i>et al.</i> , (2016)
15	$HHV = 0.3115C + 0.7823H$	Ozyuguran <i>et al.</i> , (2018)

Development of regression Models

The experimental HHV results are plotted against different component of the proximate and ultimate to ascertain their relationships. The data in Table 2 were used as references to establish correlations between the components. The variables' contribution to the model were assessed by the R squared values. A number of combinations of the variables were developed. Models with the highest R² values are presented in equations 11-13.

$$HHV = 0.0479C + 1.4565H - 0.1557O + 0.4580N - 3.9806S + 13.742 \quad 11$$

$$HHV = -0.4340C + 4.3457H - 0.3228O + 2.7084N - 13.3969S + 0.8764MC + 0.3248VM - 0.3235FC + 0.2327Ash - 3.9756 \quad 12$$

$$HHV = 0.4746FC + 0.1889VM - 0.0246Ash - 0.0665MC - 2.3751 \quad 13$$

2.4 Prediction performances

Mean absolute error (MAE) and Average absolute error (AAE) were used to evaluate the prediction performances of the existing correlations and the developed correlations. The best correlation is that with the least error values and indicates high prediction accuracy (Sheng and Azevedo, 2017; Garcia *et al.*, 2014; Nhuchhen and Afzal, 2017)

$$MAE = \frac{1}{n} \sum_{i=1}^n |Predicted\ value - Experimental\ value| \quad 14$$

$$AAE = \frac{1}{n} \sum_{i=1}^n \left| \frac{Predicted\ value - Experimental\ value}{Experimental\ value} \right| \times 100 \quad 15$$

n is the number of sample data and i is a distinct biomass sample.

3.0 RESULTS AND DISCUSSION

The results of the proximate and ultimate analysis of the selected biomass are presented in Table 2. The experimental determination of the HHV of the selected biomass is also presented in the Table. The moisture content MC is seen to range from 1.99-9.97%; volatile matter (VM) from 55.97-85.96%; Fixed carbon (FC) 7.19-14.90% and Ash content from 0.05-22.58%. The ultimate analysis gave 39.46-67.55% Carbon content, 5.05-8.74% Hydrogen content, 24.07-52.73% Oxygen content, 0.05-2.36% Nitrogen content and 0.01-1.18% Sulphur content. The HHV value for the considered biomass ranged from 15.25-24.10kJ/kg.

Using the existing correlations presented in Table 1, HHV for each of the biomass was predicted. The prediction performances was evaluated by comparing the predicted and the experimental values given in Table 2 using equations 14 and 15. Out of the seven correlations based on proximate analysis that was considered, correlation 2 of Cordero *et al.*, (2001) has the least mean absolute error ranging from 0.12 to 5.71 and average absolute error of 0.71 to 24%. Figure 1 gives the plot of the experimental HHV and predicted HHV for all the considered biomass based on correlation 2. The correlations with the least prediction error is without ash. This is in line with the conclusion of Yin (2011). However, the correlations based on proximate analysis are not adequately predicting the experimental HHV for all the considered biomass (Xing *et al.*, 2019).

Fifteen (15) different existing correlations based on ultimate analysis were considered. The correlations were carefully chosen to include different elemental compositions, linear and non-linear equations. The correlation of Toscano and Pedretti (2009), a simple linear equation with only Carbon as the elemental composition seems to give the best HHV prediction. The Average absolute error of the correlation ranges from 0.09 to 28.9% and the Mean absolute error ranges from 0.015 to 4.71. the correlation based on elemental composition gives better prediction error (Maksimuk *et al.*, 2021). Figure 3 gives the plot of the predicted and experimental HHV based on correlation 7.

Even though, the correlation based on ultimate analysis seem to be better, the error margin can yet be improved on. There is a need to actually develop correlations that will give good representations of biomass that are typical to Nigeria.

Some linear correlations were developed in this study as given in equations 11-13. Equation 11 is based on the experimental proximate analysis of twelve biomass

considered in this study. Figure 2 depicts the comparison between the predicted HHV from equation 11 and the experimental HHV. The prediction accuracy is pretty low. Previous studies (Cordero *et al.*, (2001); Sheng and Azevedo (2005); Parikh *et al.*, (2005)) have confirmed the inadequacy of proximate analysis results to predict the HHV.

Equation 12 is a correlation from ultimate analysis while equation 13 combines both ultimate and proximate analysis variables. The R square of 0.71 for equation 12 indicates that 71% of the variables are involved in the prediction equation while that of equation 13 is 0.84.

The correlations based on a combination of both ultimate and proximate analysis has a high degree of accuracy compared to the existing and the developed ones in this study. A summary of the MAE and AAE are given in table 3 while figures 4 and 5 give the comparison of the experimental HHV and that from correlations from the study.

Table 2: Results of the Proximate, ultimate and HHV of selected biomass

Samples	Proximate Analysis				Ultimate Analysis					Higher Heating Value (KJ/Kg)
	Moisture Content (%)	Volatile Matter (%)	Fixed Carbon (%)	Ash Content (%)	Carbon Content (%)	Hydrogen Content (%)	Oxygen Content (%)	Nitrogen Content (%)	Sulphur Content (%)	
Coconut Husk	9.97	71.53	10.99	7.51	48.44	5.10	45.40	0.83	0.23	15.74
Maize Shell	8.71	72.13	14.31	4.85	48.48	6.64	44.22	0.58	0.08	17.42
Coconut Shell	6.41	80.45	7.48	5.67	54.33	5.94	38.89	0.82	0.01	19.87
Groundnut Shell	4.98	81.87	7.19	5.96	52.61	6.14	40.44	0.60	0.20	16.28
Corn Cob	5.64	85.96	5.99	2.41	46.54	4.70	48.27	0.45	0.04	16.65
Palm Kernel	1.99	83.20	10.25	4.56	44.39	8.74	43.34	2.36	1.18	18.20
Saw Dust	9.79	77.25	12.91	0.05	47.40	6.24	46.30	0.05	0.01	18.36
Walnut Shell	7.83	70.86	14.51	6.80	48.00	6.18	45.62	0.18	0.02	17.15
Bagasse	8.59	75.76	13.90	1.74	48.50	6.05	44.58	0.86	0.01	15.25
Rice Husk	7.96	55.97	13.48	22.58	40.75	5.05	52.73	1.38	0.09	13.68
Mango Pod	6.90	79.28	13.00	0.82	39.46	6.03	53.29	1.11	0.10	18.14
Cashew Shell	9.24	68.88	14.90	6.98	67.55	7.60	24.07	0.73	0.06	24.10

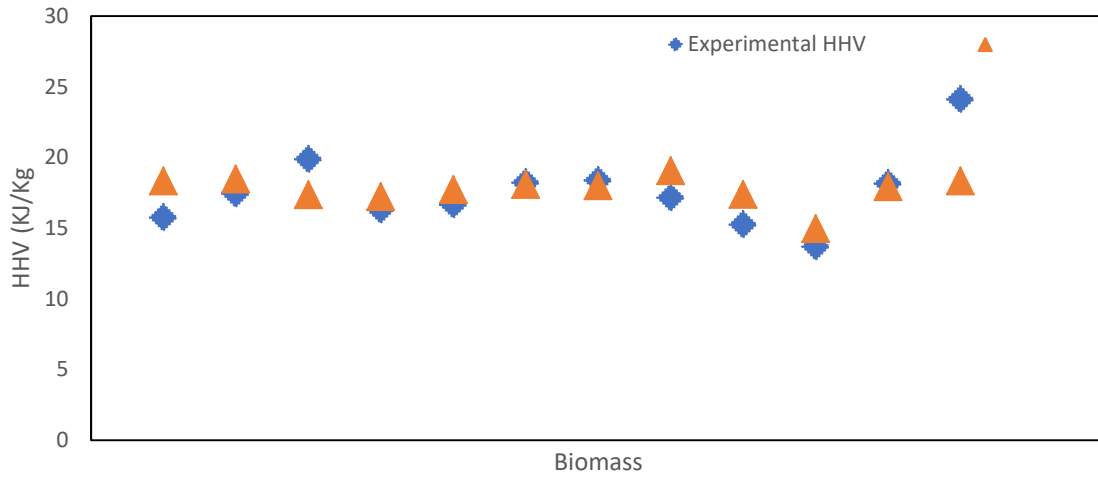
Prediction Of Higher Heating Value Of Biomass Based On Ultimate And Proximate Analyses

Figure 1: Comparison of experimental and predicted from existing models HHV based on proximate analysis

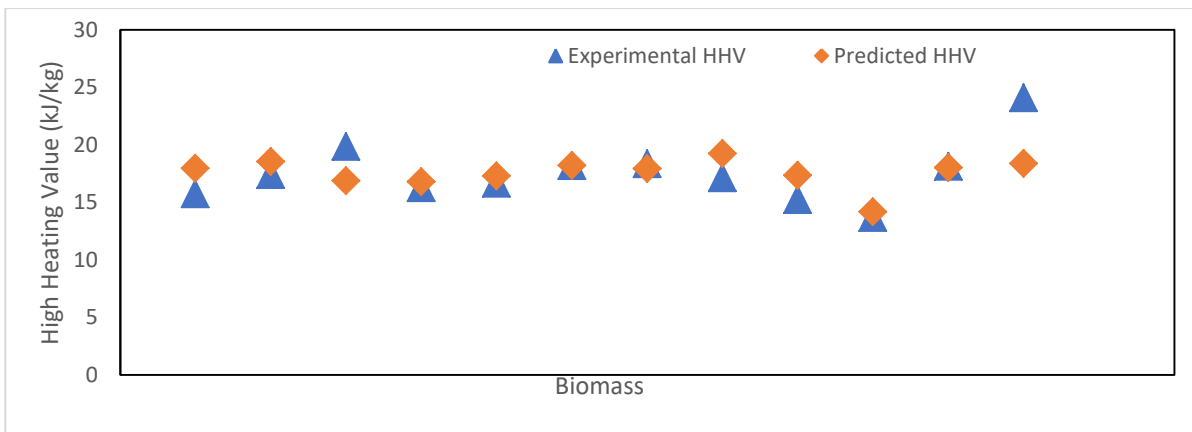


Figure 2: Comparison of experimental and predicted HHV from proximate analysis (correlation developed from this study)

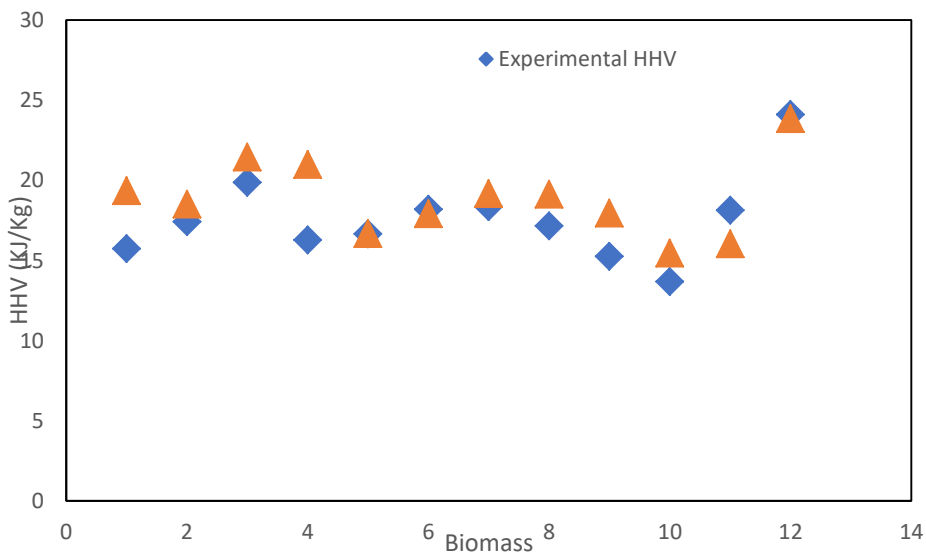


Figure 3: Comparison of experimental and predicted HHV from existing models based on ultimate analysis

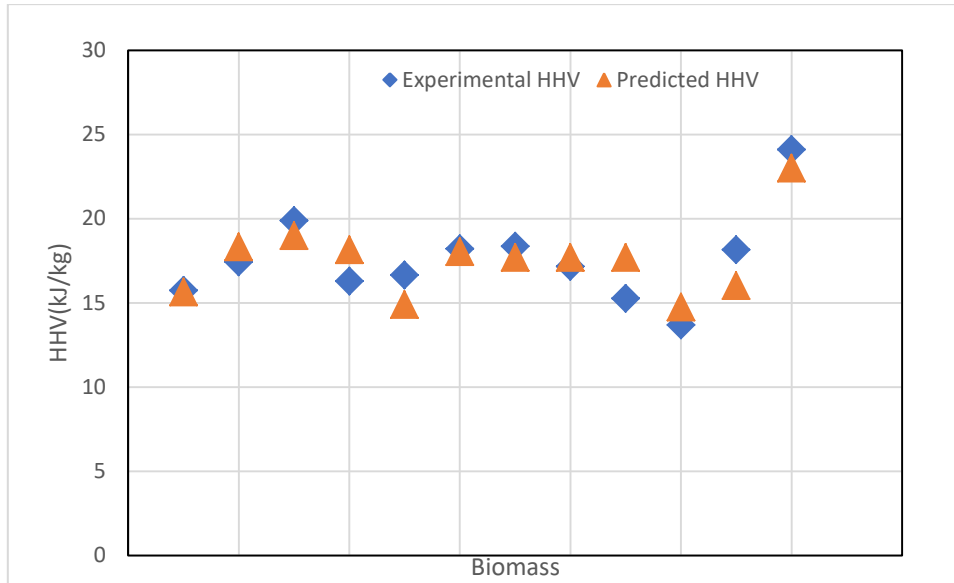


Figure 4: Comparison of experimental and predicted HHV from ultimate analysis (correlation developed in this study)

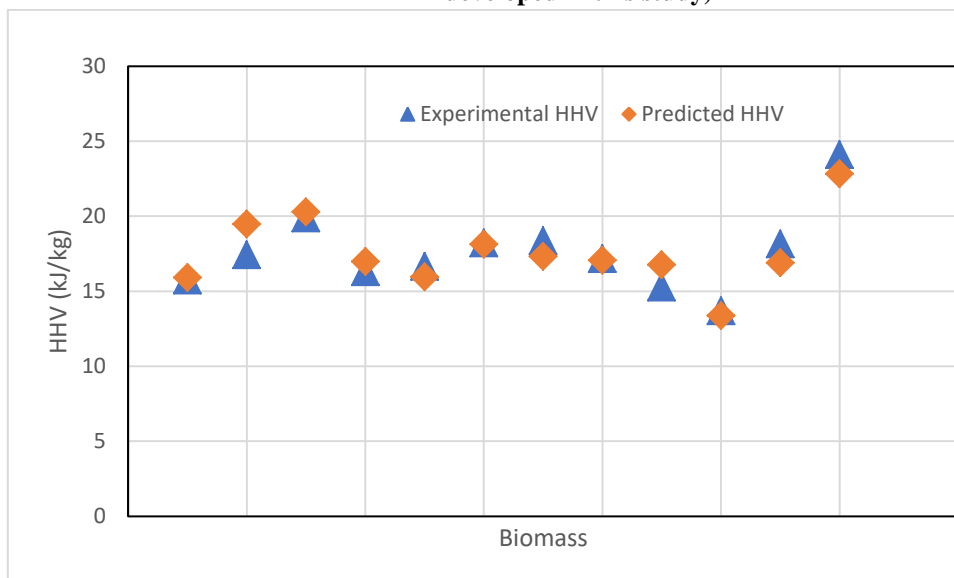


Figure 5: Comparison of experimental and predicted HHV from ultimate and proximate analysis (correlation from this study)

Table 3: Summary of prediction errors

	MAE	AAE	MAE Ranges	AAE Ranges
Existing proximate	0.1541	0.0007	0.12 to 5.77	0.0007 to 0.24
Existing ultimate	1.3013	0.0062	0.01 to 4.71	0.0009 to 0.289
This study proximate	-2.368E-15	1.1233E-17	0.02 to 5.71	0.01 to 0.24
This study ultimate	2.3684E-15	1.1233E-17	0.11 to 2.45	0.006 to 0.16
This study ultimate and proximate	2.3684E-15	1.1233E-17	0.08 to 2.05	0.01 to 0.12

4.0 CONCLUSIONS

The study presented existing correlations based on ultimate and proximate analysis to predict the HHV of biomass that are typical to Nigeria. The existing correlations based on ultimate analysis predicted the HHV with mean absolute error ranging from 0.01 to 4.71 and average absolute error ranging from 0.09 to 28.9%. The existing correlations do not seem to adequately predict the HHV. The developed correlation from this study with a mean absolute error ranging from 0.08 to 2.05 and average absolute error ranging from 0.01 to 12% seems to have good prediction accuracy. Even though, it behaves better than the existing ones, there may yet be need to improve on the predictability of the correlations.

REFERENCES

- ASTM D 3173-03 Standard test method for moisture analysis
- ASTM D 3174-04 Standard test method for ash
- Channiwala, S. A. and Parikh, P. P. (2002). A unified correlation for estimating HHV of solid, liquid and gaseous fuels, *Fuel*, Vol. 81, pp.1051–1063. [https://doi.org/10.1016/S0016-2361\(01\)00131-4](https://doi.org/10.1016/S0016-2361(01)00131-4)
- Christoforou, E. A., Fokaides, P. A., Kyriakides, I. (2014). Monte Carlo parametric modeling for predicting biomass calorific value, *J Therm Anal Calorim*, Vol. 118, pp. 1789–1796. <https://doi.org/10.1007/s10973-014-4027-5>
- Cordero, T., Marquez, F., Rodriguez-Mirasol, J., Rodriguez J. (2001). Predicting heating values of lignocellulosics and carbonaceous materials from proximate analysis, *Fuel*, Vol. 80, pp.1567–1571. [https://doi.org/10.1016/S0016-2361\(01\)00034-5](https://doi.org/10.1016/S0016-2361(01)00034-5)
- Elneel, R., Anwar, S., Ariwahjoed, B. (2013). Prediction of heating values of oil palm fronds from ultimate analysis, *J Appl Sci*, Vol. 13, pp. 491–496. doi: 10.3923/jas.2013.491.496
- Friedl, A., Padouvas, E., Rotter, H., Varmuza, K. (2005). Prediction of heating values of biomass fuel from elemental composition, *Anal Chim Acta*, Vol. 544, pp. 191–198. <https://doi.org/10.1016/j.aca.2005.01.041>
- García, R., Pizarro, C., Lavín, A. G, Bueno J. L. (2014) Spanish biofuels heating value estimation. Part I: Ultimate analysis data. *Fuel*, Vol. 117, pp. 1130–1138. <https://doi.org/10.1016/j.fuel.2013.08.048>.

- Hill, J., Nelson, E., Tilman, D., Polasky, S., Tiffany, D. (2006) Environmental, economic, and energetic costs and benefits of biodiesel and ethanol biofuels, *Proc. Natl.Acad. Sci. U. S. A.* 103 , 11206e11210. <https://doi.org/10.1073/pnas.0604600103>
- ISO 562:2010 (2010) Determination of volatile matter
- ISO 14780:2017 (2017) Solid biofuels — Methods for Sample preparation
- Jenkins, B. M., Ebeling, J. M. (1985). Correlations of physical and chemical properties of terrestrial biomass with conversion. In: Proceedings of 1985 symposium energy from biomass and waste IX IGT, California; 371.
- Jimenez, L., Gonzales, F. (1991), Study of the physical and chemical properties of lignocellulosic residues with a view to the production of fuels, *Fuel*, Vol. 70, pp. 947–950. [https://doi.org/10.1016/0016-2361\(91\)90049-G](https://doi.org/10.1016/0016-2361(91)90049-G)
- Klass, D. L.(1998). *Biomass for renewable energy, fuels, and chemicals*. San Diego: Academic Press.
- Khodaei, H., Al-Abdeli Y. M, Guzzomi F, Yeoh G. H. (2015). An overview of processes and considerations in the modelling of fixed-bed biomass combustion, *Energy*, Vol., 88, pp. 946–972. <https://doi.org/10.1016/j.energy.2015.05.099>
- Maksimuk, Y., Antonava, Z., Krouk, V., Korsakova, A., Kursevich V. (2020). Prediction of higher heating value based on elemental composition for lignin and other fuels, *Fuel*. Vol. 263, pp. 116727- <https://doi.org/10.1016/j.fuel.2019.116727>.
- Mazor, L. (1983). Quantitative elemental analysis Editor(s): Mazor, L., Comprehensive Analytical Chemistry, Elsevier, Vol.15, pp. 275-411.
- McKendry P. (2002). Energy production from biomass (part 1): overview of biomass. *Bioresour Technol* Vol. 83, pp. 37-46. [https://doi.org/10.1016/S0960-8524\(01\)00118-3](https://doi.org/10.1016/S0960-8524(01)00118-3)
- Moka, V. K. Estimation of calorific value of biomass from its elementary components by regression analysis. Thesis (BTech) 108ME062. Department of mechanical engineering of National institute of technology Rourkela. Odisha
- Nhuchhen, D. R. (2016). Prediction of carbon, hydrogen, and oxygen compositions of raw and torrefied biomass using proximate analysis, *Fuel*,

- Vol. 80, pp. 348–356.
<http://dx.doi.org/10.1016/j.fuel.2016.04.058>
- Nhuchhen, D. R., Afzal, M. T. (2017) HHV predicting correlations for torrefied biomass using proximate and ultimate analyses. *Bioengineering* Vol. 4: pp. 7.
<https://doi.org/10.3390/bioengineering4010007>.
- Ozyuguran, A., Akturk, A., Yaman S. (2018). Optimal use of condensed parameters of ultimate analysis to predict the calorific value of biomass, *Fuel*, Vol. 214, pp. 640–646.
<https://doi.org/10.1016/j.fuel.2017.10.082>
- Parikh, J., Channiwala, S. A., Ghosal, G. K. (2005). A correlation for calculating HHV from proximate analysis of solid fuels, *Fuel*, Vol. 84, pp. 487–494. <https://doi.org/10.1016/j.fuel.2004.10.010>
- Parikh, J., Channiwala, S. A., Ghosal G. K. (2007). A correlation for calculating elemental composition from proximate analysis of biomass materials, *Fuel*, Vol. 86, pp. 1710–1719.
<https://doi.org/10.1016/j.fuel.2006.12.029>
- Patterson, R. K. (1973). Automated Pregl-Dumas technique for determining total carbon, hydrogen, and nitrogen in atmospheric aerosols, *Analytical Chemistry*, Vol. 45, pp. 605–609. DOI: 10.1021/ac60325a050
- Prins, M. J., Ptasinski, K. J., Janssen F. (2007) From coal to biomass gasification: comparison of thermodynamic efficiency. *Energy* Vol. 32, pp.1248–1259.
<https://doi.org/10.1016/j.energy.2006.07.017>
- Puig-Arnabat M., Bruno J. C., Coronas A. (2010) Review and analysis of biomass gasification models. *Renew Sustain Energy Rev* Vol. 14, pp. 2841–2851. <https://doi.org/10.1016/j.rser.2010.07.030>
- Qian, H., Guo, X., Fan, S., Hagos, K., Lu, X., Liu, C. (2016) A simple prediction model for higher heat value of biomass, *J Chem Eng Data*, Vol. 61, pp. 4039–4045.
<https://doi.org/10.1021/acs.jced.6b00537>
- Sharma, S., Basu, S., Shetti, N. P., Aminabhavi, T. M. (2020) Waste-to-energy nexus for circular economy and environmental protection: Recent trends in hydrogen energy, *Sci. Total Environ*. Vol. 713, pp 136633, <https://doi.org/10.1016/j.>
- Shen, J., Zhu, S., Liu, X., Zhang, H., Tan, J. (2010). The prediction of elemental composition of biomass on proximate analysis, *Energy Convers Manage*, Vol. 51, pp. 983–987.
<https://doi.org/10.1016/j.enconman.2009.11.039>
- Sheng, C., Azevedo, J. L.T. (2005). Estimating the higher heating value of biomass fuels from basic analysis data., *Biomass Bioenergy*, Vol. 28, pp. 499–507, <https://doi.org/10.1016/j.biombioe.2004.11.008>.
- Singh, H., Sapra, P. K, Sidhu, B. S. (2013). Evaluation and characterization of different biomass residue through proximate, ultimate analysis and heating value. *Asian J Eng Appl Technology*, Vol. 2, pp. 6–10.
- Tillman D. A. (1978) Wood as an energy resource. New York: Academic Press; 1978.
- Toscano, G., Pedretti, E. F. (2009). Calorific value determination of solid biomass fuel by simplified method, *J Agric Eng*, Vol. 40, pp.1–6. <https://doi.org/10.4081/jae.2009.3.1>
- Wen X., Luo K., Jin H. H., Fan J. R. (2017) Large eddy simulation of piloted pulverized coal combustion using extended flamelet/progress variable model. *Combust Theor Model* Vol., 21, pp. 925–953. <https://doi.org/10.1080/13647830.2017.1314552>
- Xing, J., Luo, K., Wang, H., Gao, Z., and Fan, J. (2019). A comprehensive study on estimating higher heating value of biomass from proximate and ultimate analysis with machine learning approaches. *Energy* Vol. 188, pp. 116077–116088.
<https://doi.org/10.1016/j.energy.2019.116077>.

CURRENT TRENDS AND NEW PERSPECTIVES IN BIODIESEL PRODUCTION: A FOCUSED REVIEW ON INTERESTERIFICATION REACTION

*Aderibigbe, F. A.¹, **Bello, B. T.¹, Adebayo, R. O.¹, Olufowora, F. O.¹, Saka, H. B.²,
Amosa, M. K.³ and Karimu, O. S.³

¹ Department of Chemical Engineering, University of Ilorin, Ilorin, Nigeria

² Quality Control Department, Segmax Oil Nigeria Limited, Kere-Aje, Ogbondoroko, Kwara State, Nigeria

³ HSEC Directorate, Nigerian Upstream Petroleum Regulatory Commission (NUPRC), 7, Sylvester Ugoh Crescent, Jabi, Abuja-FCT, Nigeria

Email addresses of the corresponding authors:

*aderibigbe.fa@unilorin.edu.ng, ** bisolabello128@gmail.com

ABSTRACT

The consumption of energy has risen to 12 billion tons/year due to the ever-increasing population and urbanization which has directly led to more energy demand. Hence, there is an obvious need for an alternative source of fuel energy. One of the best alternatives is the use of renewable fuel energy. Biodiesel is an example of a renewable fuel energy which is produced from biomass by different technologies such as direct blending of oil, emulsification, pyrolysis, and transesterification. However, the drawback of these methods has propelled research experts to persistently search for better technologies. Over the years, transesterification reaction methods have been globally identified for in biodiesel production. Nonetheless, its by-product named glycerol has limited its utilization in biodiesel production. Therefore, it has been reported that the integration of glycerol into biodiesel composition may be a better option. In this review, the latest biodiesel production technology discussed is the interesterification reaction. This method integrates the by-product (glycerol) by producing a glycerol free Fatty Acid Methyl Esters (FAME), triacetin which is a useful fuel additive is produced instead. After the production of biodiesel and triacetin through the interesterification reaction route, there is always no need to separate both products which makes this process interestingly more sustainable and economical. The current trends of this production technology are also expounded.

Keywords: Energy; FAME; Fuel; Interesterification; Triacetin

1. INTRODUCTION

Within the past three decades, several international conventions have been organized to globally address the potentialities and plans of replacing fossil fuels by other alternative energy sources and technologies such as the renewable energy (Estevez *et al.*, 2019). There has been a very fast depletion of the sources of these fossil fuels and oil reserves which have additionally been found to be one of the major contributors of the greenhouse gases (GHG) emissions that has led to loss of biodiversity, rise in sea level, climate change, amongst other environmental concerns (Manley *et al.*, 2017; Martins *et al.*, 2019). Due to the high demand for fossil fuel, there is an increase in the price of crude oil which also affects global economic activities (Gaurav *et al.*, 2017). Affordable and clean energy provision is one of the seventeen Sustainable Development Goals (SDGs) and it is economically and environmentally

important in the majority of the African countries such as Nigeria (Adewuyi, 2020; Antwi-Agyei *et al.*, 2018; Davies *et al.*, 2019). For energy stability, the best alternative of fossil fuels from social, economic and environmental point of view is biofuel (Ayadi *et al.*, 2016; Mizik and Gyarmati, 2021). Also, annual world energy consumption has been projected to hit, by 2050, over 900 EJ, close to 1100 EJ in 2100 and also giving a pointer that global warming could be limited shown in Figure 1 (Moriarty and Honnery, 2019).

In principle, the energy enriched chemicals that are produced through biological processes or that are basically obtained from biomass of living organisms such as plants, bacteria etc. are termed "biofuels" (Rodionova *et al.*, 2017). Universally, great attention has been given to biofuel as an alternative fuel because of its ability to be revamped with gasoline for as much as 85%

volume blend without any engine modification (Hossain *et al.*, 2019). Biofuel that are principally produced from

biomass can be in solid, liquid and gaseous fuel forms (Afolalu *et al.*, 2021).

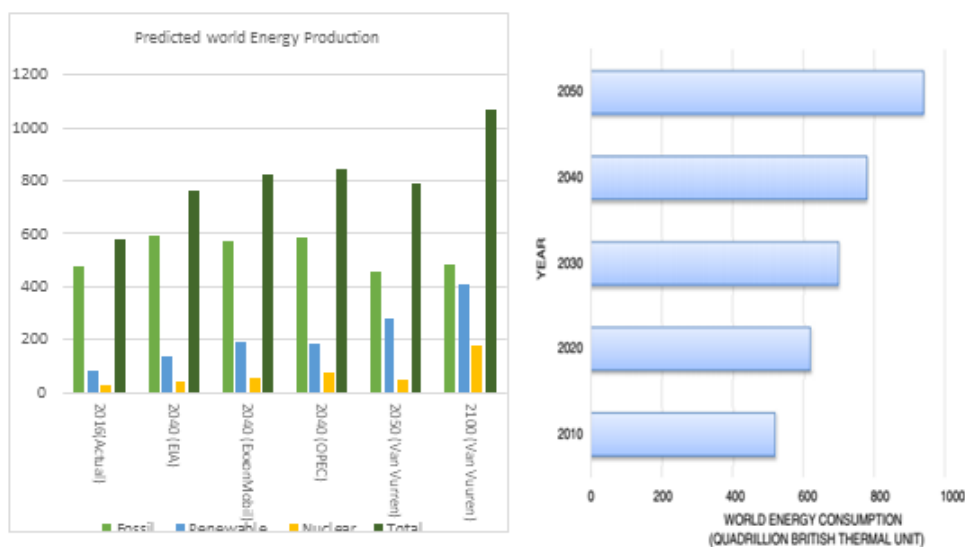


Figure 1. Predicted World Energy Production (2016 – 2100) and Consumption (2010- 2050) (Esan *et al.*, 2021; Moriarty and Honnery, 2019).

*EIA- Energy Information Administration; *OPEC- Organization of the Petroleum Exporting Countries.

They can basically be classified into three generations i.e. the first, second and third generations based on complex and chemical nature of the biomass used in the biofuel production (Sharma and Sharma, 2018). Biodiesel produced from crop plants is an example of the first-generation fuels, bioethanol and bio-hydrogen produced from agricultural by-products and energy that needs a lush land for growth is an example of the second-generation biofuel and cyano-bacteria, seaweeds, marine resources are examples of the third generation biofuels which produces large biomass within a short period of time and no lush land is needed for growth (Adewuyi, 2020; Gaurav *et al.*, 2017).

Samuel and Adekomaya (2012) stated that, biodiesel is a renewable fuel for diesel engines that meet the specification of ASTM D 6751. It is produced from oils like canola, palm kernel, waste cooking oil etc. It has been severally reported as a type of fuel that can serve as a replacement for diesel fuel in engines. It produces lesser carbon dioxide and reduced emission to the atmosphere when compared to fossil diesel. The cost of production of biodiesel basically depends on three things; the cost of feedstock, the capital cost and the by-product, which is majorly the glycerol (Roick *et al.*,

2021)). The price of feedstock is almost same as the price of refined production cost of biodiesel. This is because the capital cost to produce biodiesel is minimal but, the value of the by-product i.e., glycerol is low. Hence, this novel review revolves around the discussions on the prospects of integrating glycerol into biodiesel composition. This integration process is capable of increasing the production efficiency of biodiesel by 10% (Macario *et al.*, 2011). However, the use of catalyst to propagate the reaction is pertinent towards achieving the desired optimized product

2. BIOFUELS

For West Africa, biofuel is a fascinating source of energy because the economy can be protected or shielded against the skyrocketed crude oil prices in the world market. It is a feasible source of climate-friendly energy (Samuel and Adekomaya, 2012). Biofuels can be divided into two class i.e., the primary and secondary biofuels. The biofuels produced directly from firewood, plants, animal waste, crop residue and so on are called the primary biofuels while the biofuels produced from plants, micro-organisms, etc. are called secondary fuels which can be further subdivided into three generations; the first, second and third generation biofuels (Rodionova *et al.*, 2017). Biofuels would not only replace the global demand of fuel, but they would be able to cover an increasing part of the demand, which

can drastically reduce the dependence on fossil fuel, prolonging the life of the existing oil reserves, thus making easy the transition to a predictable world without fossil fuels (Luna *et al.*, 2016)

2.1 Historical background of biodiesel

The term “biodiesel” was first used in 1988 but from history, the use of vegetable oil to replace diesel as fuel could be traced back to 1900. The genesis of what became known as biodiesel stretches back to the discovery of diesel engine by Rudolf Diesel. At the 1900 world’s fair in Paris (Exposition Universelle), the first demonstration of diesel engine happened, French Otto’s company built a diesel engine which was tested at the event using peanut oil (Songstad *et al.*, 2009). More biodiesel history has been reported by Balasubramanian and Steward (2019) De Oliveira and Coelho (2017) and Rouhany and Montgomery (2019).

2.2 Biodiesel production

Biodiesel comprises of fatty acids methyl esters produced from free fatty acids (FFA), diacylglycerols (DAG), triacylglycerols (TAG) and phospholipids which are commonly gotten from animal fats and vegetable oils (Chen *et al.*, 2012). Several technologies have been used in previous research works to produce biodiesel. Some of the accepted technologies are direct use and blending, micro-emulsion, pyrolysis, transesterification (Estevez *et al.*, 2019) and interesterification (Kusumaningtyas *et al.*, 2016). This section would talk about all the technologies laying more emphasis on interesterification method and using data from already existing publications both analytically and empirically.

2.2.1 Direct use and blending

V. K. Mishra and Goswami (2018) reported that considerations were made in 1980 to use vegetable oil as fuel. Research was conducted using sunflower in South Africa due to the oil embargo. In 1980, Caterpillar Brazil made use of pre-combustion engines mixed with 10 % vegetable oil to maintain maximum power without making any change to the engine. At the end, it was found that it was not practical to totally replace 100 % vegetable oil with diesel fuel but to make use of 80 % diesel fuel and 20 % vegetable oil as blend. The use of this method was not satisfactory for both direct and indirect diesel engine because of the high viscosity, free fatty acid content, acid deposition, gum formation due to polymerization and oxidation during storage. Also, there were problems of lubricating oil thickening and carbon deposits.

2.2.2 Micro-emulsion

Since there are limitations to direct use and blending method. Further research was undertaken and it birthed the micro-emulsion method. Micro-emulsion was basically known as thermodynamically stable, water and surfactant, isotropic liquid mixtures of oil. Using this method solved the problems of viscosity and atomization properties of oil. Nonetheless, if a micro-emulsified diesel is used in a diesel engine there would be problems of incomplete combustion, nozzle failure and carbon deposits (Dze and Buyinda, 2020; Rajalingam *et al.*, 2016).

2.2.3 Pyrolysis

Pyrolysis can be defined as a thermochemical process of converting biomass that is in abundance and cheap into useful materials such as chemicals, fuels, gases in an oxygen deficient environment under inert conditions (Hassan *et al.*, 2020). Rajalingam *et al.* (2016) stated that pyrolysis is the conversion of hydrocarbons with complex structure into its simplest structure with or without a catalyst. Some of the challenges experienced in pyrolysis are bad quality of the bio-oil produced as a result of high water and oxygen content present in the oil which is not suitable for fueling engines directly. Also, the process of removal of water and oxygen contents gives rise to a bio-oil with high quality i.e. expensive and this might find it difficult to compete with fossil fuels (Zadeh *et al.*, 2020).

2.2.4 Transesterification

Transesterification is splitting of chemicals of heavy molecules to produce simple esters. Fatty acid triglycerides are esters of fatty acids. A very suitable alcohol is reacted with this triglyceride making use of a controlled temperature in the presence of a catalyst at a specified time. When the reaction has taken place, it produces Alkyl esters and glycerin. The alkyl ester is the main product which would possess properties as that of a fuel which is used in diesel engines and the glycerin (glycerol) is the by-product (B. K. Mishra *et al.*, 2012). There are many published articles on the transesterification of sunflower oil (Yin *et al.*, 2012), waste cooking oil (Maneerung *et al.*, 2016), neem oil (Sathya and Manivannan, 2013), castor oil (Sánchez *et al.*, 2019), waste canola oil (AlSharifi and Znad, 2020) and so on. However, it was stated by Macario *et al.* (2011) that we have so many economic and environmental processes associated with transesterification such as saponification reaction which

reduces the efficiency of biodiesel production, amongst other processes. Also, the transesterification of lipids with mono-alcohol in the presence of enzymatic, acidic, alkaline catalysts would produce Fatty Acid Methyl Ester (FAME) and glycerol (Rezania *et al.*, 2019). One of the problems associated with transesterification reaction is the production of glycerol in the process which sometimes results to 10 % by weight of the total biodiesel produced, this glycerol needs to be completely removed. To remove the glycerol, several washes with water needs to be done which then makes the process tedious and expensive (Estevez *et al.*, 2019). Furthermore, the washing phase usually requires high energy cost, and high-water consumption. To solve this problem, a biodiesel production method capable of integrating glycerol in the form of a soluble derivative called inter-esterification is needed (Hurtado *et al.*, 2019).

The most recent replacement for transesterification reaction is the interesterification reaction (Simões *et al.*, 2020). Interesterification reaction as defined is the reaction that takes place between triglyceride and methyl acetate to produce biodiesel and triacetin. Triacetin is soluble in biodiesel Nunes and Castilhos (2020) and it can also be used as additives in fuel to upgrade pour point, cloud point, cold filter plugging point generally known as cold flow properties, as substrate in confectionary manufacture, pharmaceutical products Akkarawatkhosith *et al.* (2020) as plasticizer, and gelatinizing agent in explosives, additives in the cosmetics production (Dhawan *et al.*, 2020). The difference between the reaction that occurs in transesterification and interesterification reaction is represented in Figure 2 and also a stepwise interesterification reaction represented in Figure 3 below.

2.2.5 Interesterification

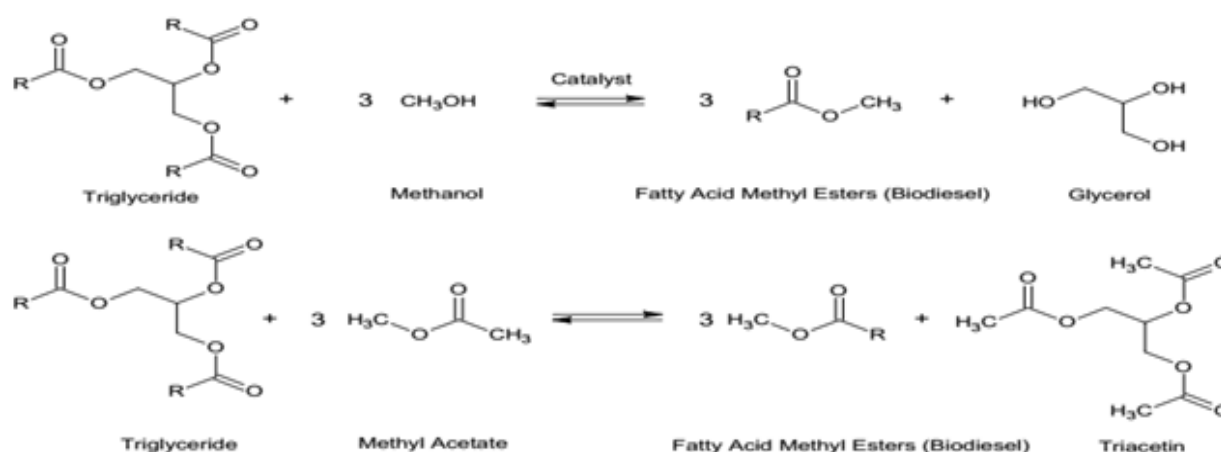


Figure 2. Reaction that occurs in Transesterification(up) and Interesterification (down) (Casas *et al.*, 2021)

Table 1 below shows the comparison between transesterification and interesterification in terms of reaction, products, product value, processes, cost and reaction time.

Table1. Comparison between Transesterification and Interesterification Reaction

Factor	Transesterification	Interesterification	Reference
Reaction	Triglyceride + Methanol	Triglyceride + Methyl acetate	(Maneerung <i>et al.</i> , 2016; Nunes and Castilhos, 2020)
Products	FAME + Glycerol	FAME + Triacetin	
Product Value	Glycerol is a by-product and has to be removed to achieve an impurity free biodiesel	Triacetin can be incorporated in the obtained product and the value is higher	(Ansori and Mahfud, 2021; Postaua <i>et al.</i> , 2019)

Processes	Separation and washing are required to achieve a good quality biodiesel	No separation is needed	(Ansori and Mahfud, 2021)
Cost	Higher production cost as a result of product separation from by-product (glycerol)	Reduced production expenses	(Abelniece <i>et al.</i> , 2020)
Reaction time	Longer reaction time is required	Ester can be obtained within the shortest reaction time	(Ansori and Mahfud, 2021; Postau <i>et al.</i> , 2019)

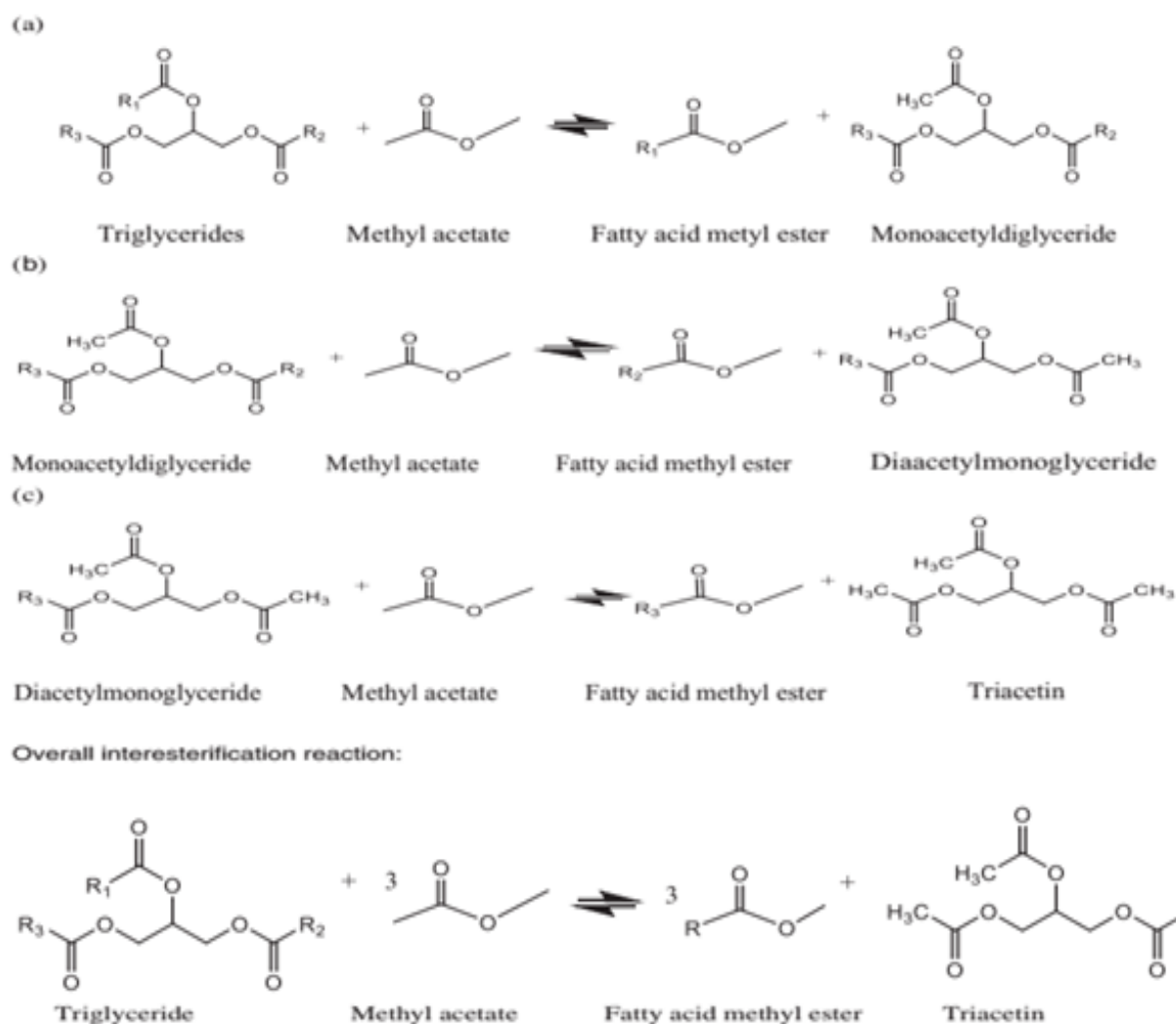


Figure 3. A Stepwise Interesterification Reaction Between Triglyceride And Methyl Acetate (Esan *et al.*, 2021).

3. BIODIESEL PRODUCTION BY DIFFERENT INTERESTERIFICATION REACTIONS

The interesterification reaction that occurs between triglycerides and methyl acetate (replacing methanol used in transesterification reaction) produces triacetin

instead of glycerol (Casas *et al.*, 2021). This section gives an overview of various published articles that have used the interesterification method to produce biodiesel from different feedstocks using different catalyst under different conditions. Macaw oil was reported to have

been interesterified with methyl acetate using a heterogeneous catalyst and was carried out in a 500 mL batch reactor (PARR 4575, IL, USA) that was made of stainless steel and attached to a pressure indicator, rotation indicator and temperature controller. Macaw oil and methyl acetate was introduced into the reactor at a molar ratio of 1:30 (oil to methyl acetate ratio) and a 55 w/w of catalyst. After the reactor has been closed, the stirrer was set to about 600 rpm at an approximate pressure of 345 kPa applied using a nitrogen gas. At a temperature of 250 °C, the reaction time started and after 2 h the reactor was cooled and opened. The catalyst used was separated from the reaction mixture using a centrifuge (Fanem Excelsa Baby 206-R) and a 0.45 mm syringe was used to filter the liquid phase removing the remaining particles. The excess methyl acetate and acetic acid was also removed. The products obtained after proper quantification of its components was corresponding to FAME and triacetin based on the European standard EN 142103. Additionally, the catalyst's regeneration/reusability was analyzed (dos Santos Ribeiro *et al.*, 2017).

It was reported by Esan *et al.* (2021) that biodiesel was produced through the interesterification reaction crambe oil and methyl acetate. The extraction of crambe oil from crambe seed was carried out using pressurized liquid extraction technique (PLE). The PLE of crambe seeds took place in a semi continuous experiment making use of temperature of 140 °C and a pressure of 10 kPa. A commercial crambe oil was employed as well. The ester yield of the commercial crambe oil to the PLE oil was in the ratio of 53.7% and 66.59% respectively at a temperature of 375 °C and 35 mins. 5.01% triacetin content was gotten in 35 mins at a temperature of 325 °C while 3% was the maximum triacetin content gotten from crambe oil at 375 °C in 15 mins. The crambe oil extracted with PLE method was observed to have higher ester and triacetin yields and this was due to the fact that using the PLE method can extract significant percentage of antioxidant. Also, it was reported that there was no significant change in the ester yield even if the molar ratio of methyl acetate and crambe oil was increased.

The interesterification of soybeans oil and methyl acetate in the presence of calcium oxide catalyst was carried out in a batch reactor of 500 mL that is made of stainless steel (PARR, model 4575), temperature controller, rotation and pressure indicators. The reactor was initially filled with soybeans oil, methyl acetate and catalyst at an initial reaction volume of 300 mL. Closing the reactor, the rate at which it was stirred was set to 600 rpm, the heat was switched on and the reaction time

started counting. The samples from the reaction was collected and the catalyst was separated from the liquid phase by centrifugation. To further discard all solid, the liquid phase was filtered using 0.45 µm syringe and the filtrate was introduced into a vacuum evaporator to remove excess methyl acetate at a temperature and time of 80 °C and 20 mins, respectively. To check and compare the calcination temperature of the catalyst the reaction was carried out with oil to methyl acetate molar ratio of 1:40 with catalyst relative to oil mass of 6% at 275 °C for 120 mins. A reaction without the use of catalyst was also performed to check the effect of catalyst on interesterification. Statistica software (StatSoftInc) was used to perform Tukey test ($p < 0.05$), to statistically analyze the conversion results. With the procedure used, the most suitable calcination temperature of calcium carbonate was determined for the reaction. From the experiments carried out, at the temperature of 250 °C and 325 °C, oil to methyl acetate molar ratio of 1:40 and 1:10, catalyst content of 6 wt% and 10 wt% for 360 mins, the kinetic behavior was checked. The optimum calcination temperature was 800 °C. The highest FAME content achieved was 62.3 wt% at 325 °C, 10 wt% of catalyst and methyl acetate to oil ratio of 40:1 (Nunes and Castilhos, 2020). Also, the interesterification reaction of soybean oil to investigate the potential of using heterogenous catalyst was reported by (Simões *et al.*, 2020).

The interesterification of cotton oil with methyl acetate assisted by an ultrasound biodiesel production was reported by (Medeiros *et al.*, 2018). The objective of the paper was to analyze the behavior of cotton oil when used as a feedstock for interesterification reaction. A 150 mL cylindrical reactor was coupled with a reflux condenser which would help prevent the loss of methyl acetate, thermostatic bath, thermocouple and an ultrasound with a probe to help aid the emulsion of solution. The use of response surface methodology (RSM) along with statistical techniques can be applied to study complex processes, being used to evaluate the importance of independent variables. Therefore, a central composite planning was used to optimize experimental conditions of the cotton oil interesterification reaction. The evaluated parameters were the molar ratio of oil/acetate with 1 second cycle. Other variables used in the study are catalyst concentration of (0.1%, 0.4%, 0.7%, 1.0%, 1.3%), ultrasonic concentration in percentage (30, 45, 60, 75, 90), vibration pulse in percentage (50, 60, 70, 80, 90) in which the values were set based on some previous studies. The interesterification of cotton seed oil showed

a very promising alternative transesterification and using RSM made it possible to study several variables that has an influence on the process and the model developed was proficient enough in accomplishing optimization. Also, a comparison was done between an experiment which was performed using a mechanical agitation i.e. the conventional way of producing biodiesel and using ultrasound method. A 14% increase in triglyceride was obtained using the ultrasound method

The interesterification of rapeseed oil catalyzed by a low surface area tin (II) oxide heterogeneous catalyst was reported. The catalyst recovery was found to be a serious challenge practically and due to this the catalyst was heterogenized using several supports. But unfortunately, in cases that effectual bonding was achieved there was reduction in the catalyst performance. Since the tin (II) based insoluble heterogenous catalyst proves difficult to separate tin (II) oxide powder was sourced commercially for the interesterification reaction. It was noticed that the commercially sourced homogeneous tin (II) octanoate showed similar performance with heterogenous supported tin (II) oxide without any trace of leaching of the ion even when it possesses low surface. The research aimed to study the effect of selected operative parameters on the performances of tin (II) oxide in the interesterification of rapeseed oil. The experiments were performed in a batch reactor that has a free volume of 20 mL. The research included a magnetic stirrer that was used to provide the mixture with agitation. Also, a type K thermocouple that was used to measure temperature value, a pressure transducer used to measure the pressure value, a valve that was connected to the system which was used to purge argon into the system. A certain amount of the oil and methyl acetate were mixed together to form a homogenous solution and tin (II) oxide (catalyst) was rapidly weighed and loaded into the reactor alongside the mixture and the reactor was then sealed. Low pressure argon was used to wash the free volume of the reactor six times and the reactor was then put into a metal block and it was heated to a desired temperature while stirring started. The experimental temperature was 483 K, therefore, the majority of the experiments were carried out at this temperature. Also, the average heating rate of the reactor is 9 K/min and the operating temperature was achieved in 20 mins. Since the effect of temperature was studied on the performance of catalyst, it was deduced that at any temperature lesser than 443 K the rate of reaction is negligible and following experimental information, the

exact transient time was achieved about 5 mins because of this singular reason it is unwise to consider the total heating period and when the temperature reached the desired temperature the reaction time measurement commenced. The FAME and triacetin yield at oil to methyl acetate ratio of 1:20, 1:40, 1:60 are 60% and 30%, 90% and 70%, 90% and 83% respectively. The average rate of generation was then calculated to be 0.7 mol/h.mol_{cat}, 1.0 mol/h.mol_{cat} and 1.0 mol/h.mol_{cat} for each run. It was then concluded that the highest FAME yields were obtained at a temperature between 473 and 503 K, at oil to methyl acetate molar ratio of 1:40 (Interrante *et al.*, 2018).

3.1 Feedstock for biodiesel production by interesterification

Most production of biodiesel uses edible food crops as feedstock i.e., about 95 %, but using edible oil for biodiesel production subjects the world to a greater risk which the supply of food could be affected awhile putting economy at a negative balance. If food and fuel are in competition for resources like lush land availability then the small land that is available for growing food crops would be compromised (Mardhiah *et al.*, 2017). With this fact the use of non-edible oils is greatly encouraged. We can then classify feedstock into non-edible and edible oil, algal oil, waste oils, animal fats and oils from microorganism. Feedstock compositions varies from the way it is refined and the source of the oil. The required composition of oils needed for biodiesel production are triglycerides, diglycerides, monoglycerides, and free fatty acid (FFA). The production of biodiesel from low cost non-edible vegetable oil is an effective way to handle the issues accompanied with energy crisis and environmental concerns and the overall cost reduction of the system and also from using non-edible feedstock, it is also desirable if the non-edible feedstock is a no or low-cost waste material to have double benefits to the environment; reduce waste pollution and produce environmental friendly fuel (Amini *et al.*, 2017).

Interesterification process using non-edible oil have been reported in some published works like cotton seed oil (Hognon *et al.*, 2014), karanja oil (Kashyap *et al.*, 2019), Macaw oil (dos Santos Ribeiro *et al.*, 2017; Ribeiro *et al.*, 2018), macauba pulp oil (Ciftci *et al.*, 2017), jathropa oil (Campanelli *et al.*, 2010; Niza *et al.*, 2011). Table 2 shows the classification of different feedstocks oil into edible oils, non-edible oils, animal fats/waste oils, solar biodiesel and others.

Table 2. Classification of Various Feedstock Oil (Delvi *et al.*, 2019; Singh *et al.*, 2020).

Types	Sources
Edible oils	Safflower, Canola, Coconut, Sunflower, African oil palm, Corn, Rapeseed, Sesame, Rice bran oil, Soybeans, Barley, Sorghum, Groundnut, Wheat.
Non-edible oils	Salmon oil, Cotton seed, Karanja, Rubber seed tree, Jatropha curcas, Pongamia, Cynara, Cumaru, Coffee ground, Passion seed.
Animal fats/Waste oils	Chicken fat, Fish oil, Pork lard, Beef tallow, Poultry fat, waste cooking oil
Solar biodiesel	Electro biofuels, Synthetic cell, Photobiological solar biodiesel
Others	Switch grass, Terpenes, Latexes, Bacteria, Microalgae, Fungi, Algae, Poplar.

3.2 Catalyst used for biodiesel production by interesterification

Different catalyst can be used in the production of biodiesel ranging from homogenous, heterogenous to enzyme catalysts.

3.2.1 Homogeneous catalysis

The homogenous catalyst can be further subdivided into acidic and basic catalyst (Abbaszadeh *et al.*, 2012). The homogenous catalyst is a catalyst widely used in the commercial industry (Nnaji, 2020), a basic homogenous catalysis such as sodium hydroxide can be used in biodiesel production and it produces a high conversion to FAME in approximately 1 h but the FAME produced from this type of catalyst has to undergo further purification to remove excess impurities with water from it. Also, the basic catalyst would dissolve in this phase, making the overall process more expensive and the residence time of the reaction is increased and also there is generation of wastewater that needs to undergo further treatment before it is discarded (Soria-Figueroa *et al.*, 2020). Also, the catalyst cannot be used again i.e. no room for reusability (Mansir *et al.*, 2017).

3.2.2 Heterogenous catalysis

Heterogenous catalyst can be defined as catalyst that give room for active sites with its reactants constantly during a reaction. (Rizwanul Fattah *et al.*, 2020). Heterogenous catalyst is better than the homogenous catalyst because of the advantages it possesses such as mild reaction conditions, reusability, improved product yield, selectivity, simple workup. Then, we can boldly say it is a better replacement for homogenous catalyst

(Maheswari *et al.*, 2020). The usage of heterogenous catalyst lowers the processing cost, there is easy separation of the catalyst, the process of biodiesel production also becomes less corrosive and toxic, less intensive and energy intake is reduced. Also, for biodiesel production from high acid oil the catalyst can be used without need to do any further pre-treatment for FFA content reduction (Mardhiah *et al.*, 2017).

For the production of biodiesel, we can classify heterogenous catalyst as solid acid or base catalyst (Amini *et al.*, 2017). Metal oxides such as magnesium oxide, calcium oxides and so on are classified as basic heterogenous catalyst. Taking Calcium oxide (CaO) for example, it has so many advantages because of this it is a widely used catalyst. CaO can also be gotten from wastes such as egg shells, fish scales, fish bones and many more (Patil *et al.*, 2021). The shells contained calcium carbonates that would be calcined which then produce a basic calcium oxide which can be used as catalyst in biodiesel production. Also, the addition of metallic element to the surface of the produced catalyst increases the basis characteristics and can produce 9% FAME yield during biodiesel production (Borges and Díaz, 2012). So, the idea of an acid base heterogenous catalyst would yield a better result.

3.2.3 Catalyst Derived from Waste Biomass

Apart from the chemical catalyst we generally use, we also have biocatalyst or bio-based catalyst. These are catalyst produced from biomass and can be grouped under the heterogenous catalyst and they are gaining world recognition (Chua *et al.*, 2020). The heterogenous

catalyst produced from waste materials such as industrial waste, agricultural waste, animal parts and their use in organic transformation is emerging as an interesting area in recent research and using this method also help solve waste disposal problem and also produces highly active catalyst (Maheswari *et al.*, 2020). Correspondingly, some published articles talks about the

production of catalyst from waste fish scales (Paul *et al.*, 2017), *luffa cylindrica* (Shih *et al.*, 2019), waste sludge (Acosta *et al.*, 2016), tobacco petiole (Zhang *et al.*, 2018) and many more. Table 3 below summarized the advantages and disadvantages of using various types of catalyst.

Table 3. Summary of the Advantages and Disadvantages of Various Catalyst

Catalyst	Advantages	Disadvantages	Reference
Homogeneous acid catalyst	No formation of soap and it has a good catalytic activity using mild conditions. It can be utilized for processes with high FFA content.	The reaction with the use of this catalyst is corrosive, requires high reaction temperature and methanol to oil ratio. The reaction is slow	(Chua <i>et al.</i> , 2020; de Lima <i>et al.</i> , 2016)
Homogeneous base catalyst	It has the tendency to produce high biodiesel yield. The reaction can be carried out using mild reaction temperature, atmospheric pressure and minimal methanol to oil ratio. It is non-corrosive and has high activity site	It is not good with feedstock that has high free fatty acid content. The neutralization reaction is cost intensive and requires more energy.	(Clohessy and Kwapinski, 2020; de Lima <i>et al.</i> , 2016)
Heterogenous acid catalyst	It can produce biodiesel under mild conditions. It has environmental benefits and produces an ASTM standard biodiesel	it possesses weak catalytic activity. It takes longer reaction time to produce the needed biodiesel.	(Mardhiah <i>et al.</i> , 2017)
Heterogenous base catalyst	The catalyst can be reused i.e. it possesses reusability properties. It reduces effluent generation.	It is expensive	(de Lima <i>et al.</i> , 2016)
Acid-base bio-based Catalyst	It helps improve environmental stability. It gives room for the production of low-cost biodiesel.		(Aderibigbe <i>et al.</i> , 2021)

4. FUTURE OUTLOOK

Much work has not been done on interesterification reaction for biodiesel production and has not been carried out on some oils such as catfish oil, *Dioclea reflexa* (Agbaarin) oil, amongst others. The interesterification reaction of *Dioclea reflexa* oil with methyl acetate using a biobased heterogenous catalyst of fish scale and *Luffa cylindrica* in the production of biodiesel would be feasible research investigation using some methodologies from previous published works. It

would also produce a glycerol free oil which is the solution to one of the problems productions of biodiesel by transesterification reaction created.

Biochemical/Biotechnology research group, Chemical Engineering Department, University of Ilorin, Ilorin, Nigeria is currently undertaking some research investigations in this area. Globally, there is a common interest of finding new and alternative fuel against fossil fuels due to the oil reserve reduction and over consumption of hydrocarbons which has been resulting

in the accumulation of greenhouse gases in the atmosphere which invariably causes global warming and researchers all over the world are putting lots of efforts to the search towards finding a sustainable and renewable energy that could help reduce carbon emission on earth. Adopting the methodology of dos Santos Ribeiro *et al.* (2017), *Dioclea reflexa* oil is currently been interesterified with methyl acetate using a bio-based heterogenous catalyst which is carried out in a magnetic stirrer connected to a temperature controller, agitation controller and an automatic stop watch at a reaction time of 1 h, temperature of 75 °C, catalyst loading of 5 w% (with respect to oil), Oil to Methyl acetate ratio of 1:30, pressure of 103 kPa (15 Psi) and constant agitation of 600 rpm . The bio-based heterogenous catalyst was obtained from wastefish scale and *Luffa cylindrica* (Luffa sponge) which was calcined and sulfonated respectively to obtain an acid base catalyst. At the preliminary stage of the research different catalyst combination was used to get the catalyst with the best combination. The best catalyst combination was found out to comprise of 40% calcined fish scale and 60% sulfonated *Luffa cylindrica* which produced a biodiesel and triacetin yield of 80.01%. This catalyst combination and the above stated conditions is being currently optimized to get the optimal condition which would further be used for the kinetics studies.

5. CONCLUSION

The review has substantially elucidated the use of interesterification reaction method for the production of biodiesel. Transesterification reaction has been widely used for biodiesel production compared to other methods of production. Despite that, the production of glycerol alongside biodiesel has increased its cost of production and also reduced the yield of the biodiesel production. Therefore, this review has shown that interesterification reaction methods could eradicate the production of glycerol in biodiesel production which would in turn reduce its cost of production, reaction time, amongst other pertinent variables and enhance biodiesel production. Also, with the aid of bio-based heterogeneous catalyst in interesterification reaction, it is worthy to state that the overall production cost of biodiesel could significantly decrease as the yield increases. However, there is a need that further research investigations be carried out in order to optimize the process operating conditions as well as the potential economics for commercialization purposes.

6. REFERENCE

- Abbaszaadeh, A., Ghobadian, B., Omidkhah, M. R., & Najafi, G. (2012). Current biodiesel production technologies: A comparative review. *Energy conversion and management*, 63, 138-148.
- Abelniece, Z., Laipniece, L., & Kampars, V. (2020). Biodiesel production by interesterification of rapeseed oil with methyl formate in presence of potassium alkoxides. *Biomass Conversion and Biorefinery*, 1-9.
- Acosta, R., Fierro, V., De Yuso, A. M., Nabarlantz, D., & Celzard, A. (2016). Tetracycline adsorption onto activated carbons produced by KOH activation of tyre pyrolysis char. *Chemosphere*, 149, 168-176.
- Aderibigbe, F. A., Saka, H. B., Ajala, E. O., Mustapha, S. I., Mohammed, I. A., Amosa, M. K., . . . Solomon, B. O. (2021). *Development of Bi-Functional Heterogeneous Catalyst for Transesterification of Waste Cooking Oil to Biodiesel: Optimization Studies*. Paper presented at the Advanced Materials Research.
- Adewuyi, A. (2020). Challenges and prospects of renewable energy in Nigeria: A case of bioethanol and biodiesel production. *Energy Reports*, 6, 77-88.
- Afolalu, S. A., Yusuf, O. O., Abioye, A. A., Emetere, M. E., Ongbali, S. O., & Samuel, O. D. (2021). *Biofuel; A Sustainable Renewable Source Of Energy-A Review*. Paper presented at the IOP Conference Series: Earth and Environmental Science.
- Akkarawatkhosith, N., Kaewchada, A., Ngamcharussrivichai, C., & Jaree, A. (2020). Biodiesel production via Interesterification of palm oil and ethyl acetate using ion-exchange resin in a packed-bed reactor. *BioEnergy Research*, 13(2), 542-551.
- AlSharifi, M., & Znad, H. (2020). Transesterification of waste canola oil by lithium/zinc composite supported on waste chicken bone as an effective catalyst. *Renewable Energy*, 151, 740-749.
- Amini, Z., Ilham, Z., Ong, H. C., Mazaheri, H., & Chen, W.-H. (2017). State of the art and prospective of lipase-catalyzed transesterification reaction for biodiesel production. *Energy conversion and management*, 141, 339-353.
- Ansori, A., & Mahfud, M. (2021). *Ultrasound assisted interesterification for biodiesel production from palm oil and methyl acetate: Optimization using RSM*. Paper presented at the Journal of Physics: Conference Series.
- Antwi-Agyei, P., Dougill, A. J., Agyekum, T. P., & Stringer, L. C. (2018). Alignment between nationally determined contributions and the

- sustainable development goals for West Africa. *Climate Policy*, 18(10), 1296-1312.
- Ayadi, M., Sarma, S. J., Pachapur, V. L., Brar, S. K., & Cheikh, R. B. (2016). History and global policy of biofuels. In *Green Fuels Technology* (pp. 1-14): Springer.
- Balasubramanian, N., & Steward, K. (2019). Biodiesel: History of Plant Based Oil Usage and Modern Innovations. *Substantia*, 3(2), 57-71.
- Borges, M. E., & Díaz, L. (2012). Recent developments on heterogeneous catalysts for biodiesel production by oil esterification and transesterification reactions: A review. *Renewable and Sustainable Energy Reviews*, 16(5), 2839-2849.
- Campanelli, P., Banchemo, M., & Manna, L. (2010). Synthesis of biodiesel from edible, non-edible and waste cooking oils via supercritical methyl acetate transesterification. *Fuel*, 89(12), 3675-3682.
- Casas, A., Pérez, Á., & Ramos, M. J. (2021). Purification of Methyl Acetate/Water Mixtures from Chemical Interesterification of Vegetable Oils by Pervaporation. *Energies*, 14(3), 775.
- Chen, L., Liu, T., Zhang, W., Chen, X., & Wang, J. (2012). Biodiesel production from algae oil high in free fatty acids by two-step catalytic conversion. *Bioresource Technology*, 111, 208-214.
- Chua, S. Y., Goh, C. M. H., Tan, Y. H., Mubarak, N. M., Kansedo, J., Khalid, M., . . . Abdullah, E. (2020). Biodiesel synthesis using natural solid catalyst derived from biomass waste—A review. *Journal of Industrial and Engineering Chemistry*, 81, 41-60.
- Ciftci, D., Ubeyitogullari, A., Huerta, R. R., Ciftci, O. N., Flores, R. A., & Saldaña, M. D. (2017). Lupin hull cellulose nanofiber aerogel preparation by supercritical CO₂ and freeze drying. *The Journal of Supercritical Fluids*, 127, 137-145.
- Clohessy, J., & Kwapinski, W. (2020). Carbon-based catalysts for biodiesel production—A review. *Applied Sciences*, 10(3), 918.
- Davies, I., Nwankwo, C., Olofinnade, O., & Michaels, T. (2019). *Insight review on impact of infrastructural development in driving the SDGs in developing nations: a case study of Nigeria*. Paper presented at the IOP Conference Series: Materials Science and Engineering.
- de Lima, A. L., Ronconi, C. M., & Mota, C. J. (2016). Heterogeneous basic catalysts for biodiesel production. *Catalysis Science & Technology*, 6(9), 2877-2891.
- De Oliveira, F. C., & Coelho, S. T. (2017). History, evolution, and environmental impact of biodiesel in Brazil: A review. *Renewable and Sustainable Energy Reviews*, 75, 168-179.
- Delvi, M. K., Soudagar, M. E. M., Khan, H., Ahmed, Z., & Shariff, I. M. (2019). Biodiesel production utilizing diverse sources, classification of oils and their esters, performance and emission characteristics: A research. *International Journal of Recent Technology and Engineering (IJRTE)*, 8.
- Dhawan, M. S., Barton, S. C., & Yadav, G. D. (2020). Interesterification of triglycerides with methyl acetate for the co-production biodiesel and triacetin using hydrotalcite as a heterogenous base catalyst. *Catalysis Today*.
- dos Santos Ribeiro, J., Celante, D., Simões, S. S., Bassaco, M. M., da Silva, C., & de Castilhos, F. (2017). Efficiency of heterogeneous catalysts in interesterification reaction from macaw oil (*Acrocomia aculeata*) and methyl acetate. *Fuel*, 200, 499-505.
- Dze, K. C., & Buyinda, G. F. (2020). MODERN METHODS OF BIODIESEL PRODUCTION: A REVIEW.
- Esan, A. O., Olabemiwo, O. M., Smith, S. M., & Ganesan, S. (2021). A concise review on alternative route of biodiesel production via interesterification of different feedstocks. *International Journal of Energy Research*.
- Estevez, R., Aguado-Deblas, L., Bautista, F. M., Luna, D., Luna, C., Calero, J., . . . Romero, A. A. (2019). Biodiesel at the Crossroads: A Critical Review. *Catalysts*, 9(12), 1033.
- Gaurav, N., Sivasankari, S., Kiran, G., Ninawe, A., & Selvin, J. (2017). Utilization of bioresources for sustainable biofuels: a review. *Renewable and Sustainable Energy Reviews*, 73, 205-214.
- Hassan, N., Jalil, A., Hitam, C., Vo, D., & Nabgan, W. (2020). Biofuels and renewable chemicals production by catalytic pyrolysis of cellulose: a review. *Environmental Chemistry Letters*, 1-24.
- Hognon, C., Dupont, C., Grateau, M., & Delrue, F. (2014). Comparison of steam gasification reactivity of algal and lignocellulosic biomass: influence of inorganic elements. *Bioresource Technology*, 164, 347-353.
- Hossain, N., Mahlia, T., & Saidur, R. (2019). Latest development in microalgae-biofuel production with nano-additives. *Biotechnology for biofuels*, 12(1), 125.
- Hurtado, B., Posadillo, A., Luna, D., Bautista, F. M., Hidalgo, J. M., Luna, C., . . . Estevez, R. (2019). Synthesis, performance and emission quality assessment of ecodiesel from castor oil in diesel/biofuel/alcohol triple blends in a diesel engine. *Catalysts*, 9(1), 40.

- Interrante, L., Bensaid, S., Galletti, C., Pirone, R., Schiavo, B., Scialdone, O., & Galia, A. (2018). Interesterification of rapeseed oil catalysed by a low surface area tin (II) oxide heterogeneous catalyst. *Fuel Processing Technology*, 177, 336-344.
- Kashyap, S. S., Gogate, P. R., & Joshi, S. M. (2019). Ultrasound assisted intensified production of biodiesel from sustainable source as karanja oil using interesterification based on heterogeneous catalyst (γ -alumina). *Chemical Engineering and Processing-Process Intensification*, 136, 11-16.
- Kusumaningtyas, R. D., Pristiyani, R., & Dewajani, H. (2016). A new route of biodiesel production through chemical interesterification of jatropha oil using ethyl acetate. *International Journal of ChemTech Research*, 9(6), 627-634.
- Luna, C., Luna, D., Calero, J., Bautista, F. M., Romero, A. A., Posadillo, A., & Verdugo-Escamilla, C. (2016). Biochemical catalytic production of biodiesel. In *Handbook of Biofuels Production* (pp. 165-199): Elsevier.
- Macario, A., Giordano, G., Bautista, F., Luna, D., Luque, R., & Romero, A. (2011). Production of glycerol-free and alternative biodiesels. In *Handbook of Biofuels Production* (pp. 160-176): Elsevier.
- Maheswari, C. S., Ramesh, R., & Lalitha, A. (2020). Antibacterial Evaluation of Some 3-Amino-1 H-Pyrazolo [1, 2-b] Phthalazine-2-Carboxamides by using Fish Scale Hydroxyapatite as a Heterogeneous Catalyst. *Polycyclic Aromatic Compounds*, 1-17.
- Maneerung, T., Kawi, S., Dai, Y., & Wang, C.-H. (2016). Sustainable biodiesel production via transesterification of waste cooking oil by using CaO catalysts prepared from chicken manure. *Energy conversion and management*, 123, 487-497.
- Manley, D., Cust, J. F., & Cecchinato, G. (2017). Stranded nations? the climate policy implications for fossil fuel-rich developing countries. *The Climate Policy Implications for Fossil Fuel-Rich Developing Countries (February 1, 2017). OxCarre Policy Paper*, 34.
- Mansir, N., Taufiq-Yap, Y. H., Rashid, U., & Lokman, I. M. (2017). Investigation of heterogeneous solid acid catalyst performance on low grade feedstocks for biodiesel production: A review. *Energy conversion and management*, 141, 171-182.
- Mardhiah, H. H., Ong, H. C., Masjuki, H., Lim, S., & Lee, H. (2017). A review on latest developments and future prospects of heterogeneous catalyst in biodiesel production from non-edible oils. *Renewable and Sustainable Energy Reviews*, 67, 1225-1236.
- Martins, F., Felgueiras, C., Smitkova, M., & Caetano, N. (2019). Analysis of fossil fuel energy consumption and environmental impacts in European countries. *Energies*, 12(6), 964.
- Medeiros, A. M., Santos, Ê. R., Azevedo, S. H., Jesus, A. A., Oliveira, H. N., & Sousa, E. M. (2018). Chemical interesterification of cotton oil with methyl acetate assisted by ultrasound for biodiesel production. *Brazilian Journal of Chemical Engineering*, 35(3), 1005-1018.
- Mishra, B. K., Kumar, R., & Kumar, R. (2012). Eco-friendly Biodiesel as an Alternative Fuel for Diesel-engine. *IOSR J. Appl. Chem*, 2(4), 41-45.
- Mishra, V. K., & Goswami, R. (2018). A review of production, properties and advantages of biodiesel. *Biofuels*, 9(2), 273-289.
- Mizik, T., & Gyarmati, G. (2021). Economic and Sustainability of Biodiesel Production—A Systematic Literature Review. *Clean Technologies*, 3(1), 19-36.
- Moriarty, P., & Honnery, D. (2019). Ecosystem maintenance energy and the need for a green EROI. *Energy Policy*, 131, 229-234.
- Niza, N., Tan, K., Ahmad, Z., & Lee, K. (2011). Comparison and optimisation of biodiesel production from Jatropha curcas oil using supercritical methyl acetate and methanol. *Chemical papers*, 65(5), 721-729.
- Nnaji, J. (2020). ADVANCES IN BIODIESEL SYNTHESIS: THE ROLE OF VARIOUS CATALYSTS. *Open Journal of Engineering Science (ISSN: 2734-2115)*, 1(1), 53-71.
- Nunes, A., & Castilhos, F. d. (2020). Chemical interesterification of soybean oil and methyl acetate to FAME using CaO as catalyst. *Fuel*, 267, 117264.
- Patil, A. M., Gite, V. V., Jirimali, H. D., & Jagtap, R. N. (2021). Fully biobased nanocomposites of hyperbranched-polyol and hydroxyapatite in coating applications. *Journal of Polymers and the Environment*, 29(3), 799-810.
- Paul, S., Pal, A., Choudhury, A. R., Bodhak, S., Balla, V. K., Sinha, A., & Das, M. (2017). Effect of trace elements on the sintering effect of fish scale derived hydroxyapatite and its bioactivity. *Ceramics International*, 43(17), 15678-15684.
- Postaue, N., Trentini, C. P., de Mello, B. T. F., Cardozo-Filho, L., & da Silva, C. (2019). Continuous catalyst-free interesterification of crambe oil using methyl acetate under pressurized conditions. *Energy conversion and management*, 187, 398-406.

- Rajalingam, A., Jani, S., Kumar, A. S., & Khan, M. A. (2016). Production methods of biodiesel. *J. Chem. Pharm. Res*, 8(3), 170-173.
- Rezania, S., Oryani, B., Park, J., Hashemi, B., Yadav, K. K., Kwon, E. E., . . . Cho, J. (2019). Review on transesterification of non-edible sources for biodiesel production with a focus on economic aspects, fuel properties and by-product applications. *Energy conversion and management*, 201, 112155.
- Ribeiro, J. S., Celante, D., Brondani, L. N., Trojahn, D. O., da Silva, C., & de Castilhos, F. (2018). Synthesis of methyl esters and triacetin from macaw oil (*Acrocomia aculeata*) and methyl acetate over γ -alumina. *Industrial Crops and Products*, 124, 84-90.
- Rizwanul Fattah, I., Ong, H., Mahlia, T., Mofijur, M., Silitonga, A., Rahman, S., & Ahmad, A. (2020). State of the Art of Catalysts for Biodiesel Production. *Front. Energy Res*, 8, 101.
- Rodionova, M. V., Poudyal, R. S., Tiwari, I., Voloshin, R. A., Zharmukhamedov, S. K., Nam, H. G., . . . Allakhverdiev, S. I. (2017). Biofuel production: challenges and opportunities. *International Journal of Hydrogen Energy*, 42(12), 8450-8461.
- Roick, C., Otun, K. O., Diankanua, N., & Joshua, G. (2021). Non-Edible Feedstock for Biodiesel Production. *Biodiesel Technology and Applications*, 285-309.
- Rouhany, M., & Montgomery, H. (2019). Global biodiesel production: the state of the art and impact on climate change. *Biodiesel*, 1-14.
- Samuel, O. D., & Adekomaya, S. (2012). Challenges confronting sustainability of biodiesel in Nigeria. *Energy*, 1(1).
- Sánchez, N., Encinar, J. M., Nogales, S., & González, J. F. (2019). Biodiesel Production from Castor oil by Two-Step Catalytic Transesterification: Optimization of the Process and Economic Assessment. *Catalysts*, 9(10), 864.
- Sathya, T., & Manivannan, A. (2013). Biodiesel production from neem oil using two step transesterification. *International Journal of Engineering Research and Applications*, 3(3), 488-492.
- Sharma, N., & Sharma, N. (2018). Second generation bioethanol production from lignocellulosic waste and its future perspectives: A review. *Int J Curr Microbiol Appl Sci*, 7(5), 1285-1290.
- Shih, Y.-J., Dong, C.-D., Huang, Y.-H., & Huang, C. (2019). Electro-sorption of ammonium ion onto nickel foam supported highly microporous activated carbon prepared from agricultural residues (dried *Luffa cylindrica*). *Science of the Total Environment*, 673, 296-305.
- Simões, S., Ribeiro, J., Celante, D., Brondani, L., & Castilhos, F. (2020). Heterogeneous catalyst screening for fatty acid methyl esters production through transesterification reaction. *Renewable Energy*, 146, 719-726.
- Singh, D., Sharma, D., Soni, S., Sharma, S., Sharma, P. K., & Jhalani, A. (2020). A review on feedstocks, production processes, and yield for different generations of biodiesel. *Fuel*, 262, 116553.
- Songstad, D., Lakshmanan, P., Chen, J., Gibbons, W., Hughes, S., & Nelson, R. (2009). Historical perspective of biofuels: learning from the past to rediscover the future. *In Vitro Cellular & Developmental Biology-Plant*, 45(3), 189-192.
- Soria-Figueroa, E., Mena-Cervantes, V. Y., García-Solares, M., Hernández-Altamirano, R., & Vazquez-Arenas, J. (2020). Statistical optimization of biodiesel production from waste cooking oil using CaO as catalyst in a Robinson-Mahoney type reactor. *Fuel*, 282, 118853.
- Yin, X., Ma, H., You, Q., Wang, Z., & Chang, J. (2012). Comparison of four different enhancing methods for preparing biodiesel through transesterification of sunflower oil. *Applied Energy*, 91(1), 320-325.
- Zadeh, Z. E., Abdulkhani, A., Aboelazayem, O., & Saha, B. (2020). Recent insights into lignocellulosic biomass pyrolysis: A critical review on pretreatment, characterization, and products upgrading. *Processes*, 8(7), 799.
- Zhang, X., Fu, W., Yin, Y., Chen, Z., Qiu, R., Simonnot, M.-O., & Wang, X. (2018). Adsorption-reduction removal of Cr (VI) by tobacco petiole pyrolytic biochar: Batch experiment, kinetic and mechanism studies. *Bioresource Technology*, 268, 149-157.

OPTIMIZATION OF PROCESS VARIABLES TO OBTAIN QUALITY SHEA KERNELS FROM SHEA NUT

Saba, A. M.¹, Baba, A. H.¹, Mohammed, I. Y.² and AbdulQadir, M.³

¹Department of Chemical Engineering, The Federal Polytechnic P. M. B. 65 Bida

²Department of Chemical Engineering, Abubakar Tafawa Balewa University, P. M. B 0248, Bauchi

³Science Department, Government Girls' Science College P.M.B 41 Bida

Corresponding authors E-mail: sabaam2006@gmail.com, aliyuharunababa2003@gmail.com

ABSTRACT

Shea butter is a product of Shea kernel obtained from Shea tree. It has wide range of applications in pharmaceuticals, confectionaries, chocolates, and soap industries. The use of Shea butter for these applications is largely dependent upon its Free Fatty Acid (FFA) content. The resultant FFA of Shea butter produced from the Shea kernel depends largely upon the process variables applied to the kernel prior to Shea butter production. Poor and inconsistent qualities usually characterize unprocessed Nigerian Shea kernels. Thus, the need to improve Shea kernel quality in Nigeria becomes necessary. This study investigated the effects of optimizing processing factors, responses, development, and analysis of predictive response models of Shea kernel leading to its optimization. Shea fruits that have fallen to the ground were picked and the pulp removed to expose the Shea nut. Effects of Shea Nut Conditioning Period (SNCP), Shea Nut Boiling Duration (SNBD) and Shea Nut Drying Temperature (SNDT) on the FFA of Shea kernel were investigated. The boundary conditions obtained from earlier experiments were used for the Design of Experiment (DOE) by Box-Beckh method of response surface methodology. Fresh Shea kernels were then processed according to the experimental design and the responses of free fatty acid, peroxide value and percentage oil content determined. The upper, middle and lower limits obtained for SNCP were 1, 6.5, and 12 day respectively, SNBD were 0, 60, and 120 minutes respectively and SNDT were 30, 70, 110 °C respectively. The optimum conditions of SNCP, SNBD and SNDT obtained after the optimization of Shea kernel were respectively 4.0 day, 120 minutes and 86 °C and the corresponding predicted responses of PV, percentage oil content, FFA and desirability were 2.868 meq/kg, 0.628 %, 53.8 5 % and 0.878 respectively.

Keywords: Shea-kernel, Shea Nut Conditioning Period, Shea Nut Boiling Duration, Shea Nut Drying Temperature, and Optimization

1.0. INTRODUCTION

Researchers and scientist all over the world are continuously looking for ways and means of improving the yield and quality of vegetable oils to meet both domestic and industrial applications (Aculey, 2012). Shea butter is one of these numerous vegetable oils and it's a fatty extract obtained from the kernels of Shea fruit. It is also a mixture of fatty acids usually Oleic, Stearic, Palmitic, Linoleic and Arachidic acids with Oleic and Stearic acids predominating and together constituting about 85 % of the fatty acid content of Shea butter (Coulibaly *et al.*, 2009 and Julius *et al.*, 2013). The presence of these fatty acids in Shea butter varies in proportion depending on the source of the Shea nuts. The nut is obtained from Shea tree which is a native of Africa and it is either called *Vitellaria paradoxa* or *Butyrospermum parkii* in West Africa or "*nilotica*" in East Africa. Nigeria is well endowed with this tree

accounting for about 50 to 60 % of West African Shea tree population. In Nigeria, these trees are concentrated in states of Niger, Kwara, Nassarawa, Zamfara, Adamawa, Edo, Yobe Plateau, Kaduna and some parts of Kebbi, Bauchi, Kogi, FCT and Oyo (NASPAN, 2018 and Koloche *et al.*, 2016). Koloche (2016) even though not up dated has shown that 40 -50 % of these Shea trees are found in Niger state. The tree starts flowering and fruiting in January and harvest begins between May to June through to August. After the harvest, the pulp is removed, the nuts are dried, the shell is removed and the Shea kernels processed for Shea butter. This research has suggested a solution to the problems of lack of standard methods in Shea kkernel processing and lack of proper documentation to show the variation in Shea kernel quality and processing factors.

The aim is to evaluate and optimize the process variables for Shea kernel processing with a view to obtain optimum quality parameters of Peroxide Value (PV), percentage oil content and Free Fatty Acid (FFA) for grade 'A' Shea butter production. This research shall contribute and improve the quality of traditional processing method of Shea kernel through Shea kernel optimization on the percentage oil content and quality processing method.

2.0. MATERIALS AND METHODS

2.1. Collection of Shea Fruit

The Shea fruits were collected from 4.5 hectares of experimental field housing 67 Shea trees along Sonmajigi village (N09° 11' 56"; E05° 35' 45"), in Lavun Local Government Area of Niger State, Nigeria. The Shea fruits that had matured, fallen to the ground were picked, taken to the research site and kept in the open for the required duration of time. The picking was done between the hours of 9 am to 11 am daily to ensure consistency in timing of the Shea fruits picking throughout the period of collection (July to August). On each picking day the Shea pulp were removed manually by applying hand pressure to expose the Shea fruit.

2.2. Establishment of the Boundary Conditions of Variables for Optimization of Shea Kernel

The lower, mid-point and upper boundary conditions for optimizing SNCP, SNBD and SNTD were determined as described by Saba (2019).

2.2.1. Effect of SNCP on the Free Fatty Acid of Shea Kernel

A batch of 5 kg of fresh fruits were collected as described in Section 2.1 and conveyed to the Federal Polytechnic Bida research site in Nigeria using a tricycle. The jute bags were used to reduce the heat generated within the bags to soak the surface moisture on the fruits. At the site where they were kept under a tree in the open space to mimic natural habitat conditions in the experimental site four pieces of Shea fruits considered adequate for the analysis were taken each day for 16 days. The pulp of the Shea fruits which were soft and tender were removed simply by applying hand pressure. Thereafter, the brown hard-shell enclosing the kernel were cracked using wooden pestle and mortar to expose the kernel. The kernels obtained were ground using 1.5 kW Atlas grinding machine and screened using laboratory sieve shaker to a particle size of between 0.05 mm to 0.1 mm and then analyzed for FFA as described in subsection 2.3.1. The experiment was repeated for SNCP of between 2 days to 16 days

and their corresponding FFA calculated using equation 1 and the results shown on Table 1

2.2.2. Effect of Boiling Duration on the FFA of Shea Kernel

Five kilogram of Shea fruits were collected as described in Section 2.1, and measured using diamond weighing balance. The pulp was removed as described in sub-section 2.2.1. The fresh Shea nuts obtained were washed severally with water to remove all the left - over pulp and then carefully poured into boiling water in an aluminium pot heated on a laboratory hot plate. As the boiling was continued, 4 pieces of Shea nuts considered adequate for the FFA analysis were collected randomly from the lot at intervals of 20 minutes for up to 120 minutes. The nuts collected were then cooled in a medium size desiccator. The hard shells of the cooled Shea nuts were then cracked to expose the kernel, the kernels were ground, screened to between 0.05 mm to 0.1 mm size and then analyzed for FFA as described in sub -section 2.3.1. The experiment was repeated for SNBD of 40 minutes, 60 minutes, 80 minutes, 100 minutes and 120 minutes and their corresponding FFA was calculated using equation 1 and the results shown in Table 2

2.2.3. Effect of Drying Temperature on FFA of Shea Kernel

Five kilogram of Shea fruits collected from the experimental field was measured using Diamond weighing balance. The fruits were de-pulped and washed as described in sub-section 2.2.2. The nuts were fed into the cylindrical chamber of the designed and fabricated rotary dryer with the aid of a removable feed-in hopper, then temperature was first set at 30 °C, and the power button was switched on and as the cylindrical chamber rotates at a speed of 13.3 rpm, the blower attached to the burner was switched on and hot air from the burner convected to the chamber. Inside the chamber, heat was transferred from the wall and to the pipes through conduction to the nuts. The heat produced in the burner was generated by the Shea shell briquette. At intervals of one hour, the power button was switched off; the Shea nut was rolled out through the discharge slot by jacking up the cylindrical chamber of the dryer with the aid of a manually operated hand crank. The weight of the Shea nut was measured using diamond weighing balance to check for moisture loss. The drying was continued until two successive constant weights were obtained. The shell of the Shea nut was then cracked using wooden pestle and mortar to expose the

dried kernels. The dried kernels were ground using a 0.75 Solitaire laboratory blender and screened to between 0.05 mm - 0.1 mm using laboratory sieve shaker. 2 g of the screened ground kernels was measured using Mettler Toledo balance and was analyzed for FFA as described in sub-section 2.3.1. The experiment was repeated for Shea nut drying temperatures set at 50 °C, 70 °C, 90 °C, and 110 °C and their respective FFAs were calculated using equation 1 and the result shown in Table 3.

2.3. Methods of Analysis

2.3.1. Determination of FFA of Shea Kernel

This was done according to American Oil Chemists Society (AOCS) (1994) and the volume of NaOH consumed was recorded and used in equation (1) to calculate the free fatty acid content of the kernel.

$$FFA = \{(V - B) \times N_f \times 28.2\} / W \quad (1)$$

Where FFA is the free fatty acid (%), V is the Volume of NaOH ethanolic solution used for titration (mL), B, Volume of NaOH consumed during FFA determination blank titration (mL), N_f , Normality of NaOH factor, W, Weight of Oil sample (g).

2.3.2. Percentage Oil Content Determination and Extraction Efficiency

$$Y_0 = (W_u - W_e) / W_u \times 100 \quad (2)$$

Where:

Y_0 = percentage oil yield; W_u = weight of sample before pressing (g), W_e = weight of sample after pressing (g)

2.3.3. Determination of PV of Shea Kernel:

The Peroxide Value (PV) was determined according to International Organization for Standardization (ISO) (2005) and as in equation (3):

$$PV = (T \times M \times 1000) / W \quad (3)$$

Where: PV = peroxide value (mequiv/kg) T = Titre value of Na_2SO_3 (cm^3), M = Molarity of Na_2SO_3 (M) and W = weight of Oil sample (g)

2.4. Optimization Procedure and Validation of Responses from Shea Kernel Processing

Box–Behnken Design (BBD) response surface methodology was used for the Design of Experiment (DOE) for the Shea kernel optimization and model development for good quality Shea kernel processing.

Validation of the optimum responses obtained from the optimum quality of Shea kernel was carried out by collecting fresh Shea nut and processed according to the optimum conditions obtained from Design Expert 11.2.1.0

3.0. RESULTS AND DISCUSSION

3.1. The Result of Preliminary Experiment

Prior to the optimization of Shea kernel, preliminary experiments were conducted to show the effects of SNCP, SNBD and SNDT on the percentage FFA of Shea kernel. The results of these experiments are shown in Tables 1,2 and 3 respectively.

Table 1: Effect of SNCP on FFA of Shea kernel

SNCP (day)	FFA (%)
1	1.81
2	4.68
4	5.89
6	6.93
8	6.26
10	10.99
12	13.03
14	14.60
16	14.96

Table 1 shows the changes in FFA of Shea kernel as the SNCP increases from the initial period of day 1 to day 16. Within this period the FFA increases from 1.81 % to 14.96 %. The high value of FFA on the 16th day may be as a consequence of slow drying rate which enhanced activity of enzyme lipase present in the kernel. This observation is consistent with the findings of Aculey *et al.* (2012). The drop observed on the 8th day, may also result from partial activation of phenolic compounds during kernel degradation (Nahm, 2011). This drop as observed may also suggest the upper range of SNCP within which the Shea nut should be processed. Above the 8th day, the FFA builds up at a higher rate. This effect of SNCP on FFA is modelled by quadratic equation (4) with correlation coefficient, $R^2 = 0.941$. A co-relation co-efficient of 0.941 shows that 94.1 % of the variability in SCNP affects the amount of FFA produced

$$Y_{FFA} = 0.00x^2 + 0.817x + 1.908 \quad (4)$$

The effect of SNBD on the FFA of Shea kernel is depicted in Table 2

The effect of SNBD on the FFA of Shea kernel is depicted in Table 3

Table 2: Effect of SNBD on FFA of Shea kernel

SNBD (min)	FFA (%)
0	1.81
20	1.38
40	1.09
60	1.01
80	1.01
100	0.98
120	1.36

Table 2 shows that as the SNBD increases from 0 minute to 100 minutes, the FFA decreases from 1.810 % to 0.980 %, indicating leaching out of FFA as boiling is done. This trend favours the processing of higher quality Shea kernel since low FFA is desired in high quality Shea kernel. This increases the chances of getting high quality Shea butter. Further increase in SNBD to 120 minutes shows significant increase in the FFA of Shea kernel from 0.980 % to 1.360 %. This trend suggests that higher boiling duration do not favour lower FFA. It can be deduced that SNBD can both decrease and increase FFA of Shea kernel and hence should be controlled within 100 minutes. This observation is consistent with the findings of Lovett (2012) which suggest moderate SNBD for good quality Shea kernel. The effect of SNBD is adequately represented with quadratic equation (5) with correlation coefficient of $R^2 = 0.972$. A co-relation co-efficient of 0.972 shows that 97.2 % of the variability in SNBD affects the amount of FFA produced.

$$Y_{FFA} = 0.001x^2 + 0.023x + 1.801 \quad (5)$$

Table 3: Effect of SNBD on FFA of Shea kernel

SNBD (°C)	FFA (%)
30	6.42
50	6.00
70	4.56
90	5.40
110	8.33

Table 3 shows how SNBD affects the FFA of Shea kernels. As SNBD increases from 30 °C to 70 °C, the FFA of Shea kernel decreases from 6.420 % to 4.560 % and from 70 °C to 110 °C the FFA increases from 4.560 % to 8.330 %. The lower the SNBD, the longer it takes the Shea kernel to dry and hence more FFA is produced within the kernel as a result of increase in lipase activity and moisture content in the kernel. Also, with high SNBD (above 70 °C) thermal degradation of fatty acids begins to occur thereby producing more FFA. This variation suggests that moderate SNBD of about 70 °C favours lower FFA in Shea kernel. The effect of SNBD is modelled by quadratic equation (6) with correlation coefficient of $R^2 = 0.866$. A co-relation co-efficient of 0.866 shows that 86.6 % of the variability in SNBD affects the amount of FFA produced

$$Y_{FFA} = 0.001x^2 + 0.214x + 11.82 \quad (6)$$

3.2. Experimental Results of Shea kernel Processing

Table 4: Responses obtained from experimental design of Shea kernel processing using Box-Behnken Design Method

Std	Run	Factor 1 A:SNCP (day)	Factor 2 B:SNBD (hrs)	Factor 3 C:SNBD (°C)	Response 1 PV (meq/kg)	Response 2 Oil Content (%)	Response 3 FFA (%)
10	1	1	60	30	1.40 ± 0.01	52.00±1.23	7.98±0.19
14	2	12	60	30	2.70±0.03	51.67±1.22	5.57±0.13
7	3	6.5	120	30	1.80±0.02	53.67±1.27	5.49±0.13
8	4	6.5	60	70	3.20±0.03	48.67±1.15	2.26±0.05
11	5	6.5	60	70	3.40±0.03	52.67±1.25	1.68±0.04
12	6	6.5	120	110	3.80±0.04	53.33±1.26	1.04±0.02
9	7	6.5	0	30	1.45±0.01	54.67±1.29	5.98±0.14
6	8	6.5	60	70	3.50±0.04	48.33±1.14	1.48±0.03
5	9	6.5	0	110	3.10±0.03	50.00±1.18	1.12±0.03

Std	Run	Factor 1 A:SNCP (day)	Factor 2 B:SNBD (hrs)	Factor 3 C:SNDT (°C)	Response 1 PV (meq/kg)	Response 2 Oil Content (%)	Response 3 FFA (%)
4	10	12	0	70	3.31±0.03	56.00±1.32	3.37±0.08
15	11	1	120	70	1.45±0.01	53.67±1.27	2.24±0.05
2	12	1	0	70	1.29±0.01	47.67±1.13	2.00±0.05
17	13	6.5	60	70	3.50±0.04	52.33±1.24	1.63±0.04
1	14	1	60	110	1.90±0.02	45.33±1.07	0.60±0.01
13	15	12	120	70	4.50±0.05	52.00±1.23	2.52±0.06
3	16	6.5	60	70	3.80±0.04	52.00±1.23	1.53±0.04
16	17	12	60	110	4.90±0.05	49.67±1.17	4.85±0.11

Response values are means \pm std. dev ($n = 3$). The FFA $\leq 3\%$; percentage Oil content $\geq 50\%$ and PV ≤ 5 meq/kg, Megan G, (2013),

Run 12 in Table 4, shows that the lowest PV of 1.29 meq/kg and FFA of 2.00 % are within grade 'A' threshold of Shea kernel obtained but the percentage oil content of 47.67 % is lower than the realizable % oil content (ARSO, 2017). Run 10 in Table 4 gave the highest percentage oil content of 56 %, which is above the realizable standard and the PV of 3.31 meq/kg is within and the FFA of 3.37 % is outside the grade 'A' threshold. Run 14 also gave the lowest FFA of 0.60 % and its PV of 1.90 meq/kg fell inside the grade 'A' obtained from the analysis.

threshold of Shea kernel and the percentage oil content is lowest 45.33 %. To improve the percentage oil content and the quality parameters of FFA and PV of Shea kernel the process variables can be optimized.

3.2.1. Analysis of Variance (ANOVA) for Shea kernel Processing

Tables 5, 6 and 7 shows the ANOVA for response surface quadratic model of PV, percentage oil content and FFA of Shea kernel and statistical parameters

Table 5: Analysis of Variance for Response Surface Quadratic Model of PV for Shea kernel

Response Source	Sum of Squares	df	Mean Square	F-value	p-value
PV					
Model	20.35	9	2.26	40.99	<0.0001 Significant
A-SNCP	10.97	1	10.97	198.93	0.0001
B-SNBD	0.7200	1	0.7200	13.05	0.0086
C-SNDT	5.04	1	5.04	91.36	0.0001
AC	0.7225	1	0.7225	13.10	0.0085
A ²	0.4516	1	0.4516	8.19	0.0243
B ²	1.12	1	1.12	20.24	0.0028
C ²	0.7695	1	0.7695	13.95	0.0073
Residual	0.3862	7	0.0552		
Lack of Fit	0.1982	3	0.0661	1.41	0.3639 Not significant
Pure Error	0.1880	4	0.0470		
Cor Total	20.74	16			
Fit Statistics					
Std. Dev.	0.2349		R ²		0.9814
Mean	2.88		Adjusted R ²		0.9574
C.V. %	8.15		Predicted R ²		0.8330
PRESS	3.46		Adeq Precision		21.8159

From Tables 5, the models for PV had F-values of 40.99, which implied that it is statistically significant and had only 59.01 % chance that its magnitude could

occur due to noise (induced variation under normal operating conditions by uncontrollable factors). The "Lack of Fit F-value" of 1.41 for PV implies the Lack of Fit is not significant relative to the pure errors of 0.047.

There is 36.39 % chance that the 'lack of fit (F value)' of this large level of significance could be due to noise. The model have p-value < 0.0001 for PV. This is able to explain 99.99 % variation in PV, thus, suggesting that the model shows a good fit. The significant model terms are as shown in Tables 5.

Table 6: Analysis of Variance for Response Surface Quadratic Model of % oil content for Shea kernel

Response	Source	Sum of Squares	df	Mean Square	F-value	p-value	
% oil Content	Model	101.62	9	11.29	3.86	0.0444	Significant
	C-SNDT	23.39	1	23.39	8.00	0.0255	
	AB	25.00	1	25.00	8.54	0.0222	
	B ²	24.10	1	24.10	8.24	0.0240	
	Residual	20.48	7	2.93			
	Lack of Fit	2.57	3	0.8553	0.1910	0.8975	Not significant
	Pure Error	17.92	4	4.48			
Cor Total	122.10	16					

Fit Statistics

Std. Dev.	1.71	R ²	0.8323
Mean	51.39	Adjusted R ²	0.6166
C.V. %	3.33	Predicted R ²	0.4345
PRESS	69.05	Adeq Precision	7.7530

From Tables 6, the models for Percentage oil content had F-values of 3.86, which implied that it is statistically significant and had only 96.14 % chance that its magnitude could occur due to noise (induced variation under normal operating conditions by uncontrollable factors). The "Lack of Fit F-value" of 0.1910 for Percentage oil content implies the Lack of Fit is not significant relative to the pure errors of 4.48. There is

89.75 % chance that the 'lack of fit (F value)' of this large level of significance could be due to noise. The model have p-value < 0.0444 for Percentage oil content. This is able to explain 99.96 % variation in Percentage oil content thus, suggesting that the model shows a good fit. The significant model terms are as shown in Tables 6.

Table 7: Analysis of Variance for Response Surface Quadratic Model of FFA for Shea kernel

Response	Source	Sum of Squares	df	Mean Square	F-value	p-value	
FFA	Model	73.04	9	8.12	97.50	< 0.0001	Significant
	A-SNCP	1.52	1	1.52	18.29	0.0037	
	C-SNDT	37.89	1	37.89	455.20	< 0.0001	
	AC	11.09	1	11.09	133.22	< 0.0001	
	A ²	4.91	1	4.91	58.95	0.0001	
	C ²	16.08	1	16.08	193.24	< 0.0001	
	Residual	0.5826	7	0.0832			
	Lack of Fit	0.1877	3	0.0626	0.6338	0.6312	Not significant
	Pure Error	0.3949	4	0.0987			
	Cor Total	73.62	16				

Fit Statistics

Std. Dev.	0.2885	R ²	0.9921
Mean	3.02	Adjusted R ²	0.9819
C.V. %	9.55	Predicted R ²	0.9508
PRESS	3.62	Adeq Precision	34.7195

From Table 7 FFA had F-value of 97.50 which implied that it is statistically significant and had only 2.50 % chance that its magnitude could occur due to noise (induced variation under normal operating conditions by uncontrollable factors). The "Lack of Fit F-value" of 0.6338 for FFA implies the Lack of Fit is not significant relative to the pure errors of 0.0987. There is 63.12 % chance that the 'lack of fit (F value)' of this large level of significance could be due to noise. The models have p-value < 0.0001 for FFA. This is able to explain 99.99 % variation FFA. Thus, suggesting that the model shows a good fit. The significant model terms are as shown in Table 7.

3.2.2. Fit Statistic for PV, percentage oil content and FFA of Shea kernel Processing

From Tables 5, 6 and 7 the quadratic regression model showed satisfactory value of determination coefficient; R² of 0.9814, 0.8323 and 0.9921 for PV, percentage oil content and FFA respectively. No significant lack of fit at $p > 0.05$, which means that the calculated models were able to explain 98.14 %, 83.23 % and 99.21 % of the results. The results indicated that the models used to fit response variable were significant ($p < 0.0001$, 0.0444 and 0.0001) and adequate to represent the relationship between the response and the independent variables. R² adj (adjusted determination coefficient) is the correlation measure for testing the goodness-of-fit of the regression equation, (Li-Chun *et al.*, 2012); Hossain *et al.*, (2012) and Kim *et al.*, (2012). The R² adj value of these models were 0.9574, 0.6166 and 0.9819 which indicates that only 4.26 %, 38.34 % and 1.81 % of the total variations

could not be explained by the models. The "Pred R-Squared" and the "Adj R-Squared" are in reasonable agreement there differences less than 0.2. Meanwhile, relative lower value of CV < 10 % showed a better precision and reliability of the experiments carried out with 8.15, 3.33 and 9.55 for each of the responses. This means that the deviation between predicted and experimental values were not much as reported by Maran and Manikanda (2012). "Adeq Precision" of 21.816, 7.7530 and 34.7195 all indicates an adequate signal ratio greater than 4 which are desirable and it shows that this model can be used to navigate the design space.

3.2.3. Analysis of PV for Shea Kernel Quality

$$Y_{\text{Peroxide}} = 3.48 + 1.17125 \cdot \text{SNCP} + 0.3 \cdot \text{SNBD} + 0.79375 \cdot \text{SNDT} + 0.425 \cdot (\text{SNCP} \cdot \text{SNDT}) - 0.3275 \cdot (\text{SNCP})^2 - 0.5158 \cdot (\text{SNBD})^2 - 0.4275 \cdot (\text{SNDT})^2 \quad (7)$$

The desired objective is to minimize the PV of the Shea kernel which indicates the oxidation of fat/oil and possible formation of off flavour. Equation (7) suggests that decreasing any of the three quadratic terms influenced the other by causing decrease in PV. Table 8 also showed the interaction between SNCP and SNDT (Shown in Figures. 1 and 2) on the PV of Shea kernel at optimum 60 min SNBD. The PV with the desired objective to obtain good quality Shea kernel that can produce grade 'A' Shea Butter should be around $10 \leq \text{PV} \leq 0$ (Megan, 2013).

Design-Expert® Software
Version 11.1.2.0.

Factor Coding: Actual

PV (meq/kg)

● Design points above predicted value

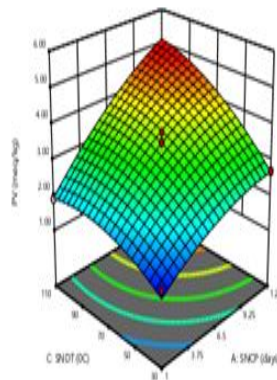
○ Design points below predicted value

1.29  4.90

X1 = A: SNCP

X2 = C: SNTD

Actual Factor



Design-Expert® Software

Version 11.1.2.0.

Factor Coding: Actual

PV (meq/kg)

● Design Points

-- 95% CI Bands

X1 = A: SNCP

X2 = C: SNTD

Actual Factor

B: SNBD = 60

C- 30

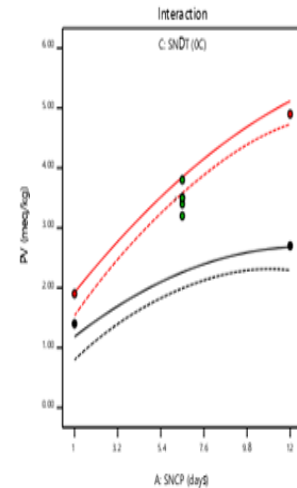


Figure 1: 3D RSP showing double effects of SNCP and SNBD on percentage oil content

Figure 2: Interactive Plot showing effects of SNCP and SNBD on percentage oil content

Table 8: Design point of interaction between SNCP and SNTD on PV at confidence interval bands of 95 % and optimum 60 minutes of SNBD

Lower limit		PV	Upper limit		PV
SNCP	SNTD		SNCP	SNTD	
LL-1	LL-30	1.40	UL-12	LL-30	2.70
Lower limit		PV	Upper limit		PV
LL-1	UL-110		1.90	UL-12	

Note: Equilibrium point of zero SNCP per SNTD

Table 8 shows that the Shea kernel processed at one day SNCP; 30 °C SNTD and of 60 minutes SNBD had the lowest Peroxide Value (PV) of 1.40 meq/kg. This might result from the kernels that had not been exposed to other active variables such as O₂, moisture contents and UV rays from sunlight since they were collected on the first day, with minimum FFA and hence low PV. Also the Shea kernel processed at SNCP of 12 day, constant 110 °C SNTD and 60 minutes SNBD gave the highest PV of 4.9 meq/kg; which is 3 times the PV obtained at constant 1 day SNCP, 110 °C SNTD and 60 minutes SNBD and almost twice the PV obtained at 12 day SNCP, 30 °C SNTD and 60 minutes SNBD. These differences in PV may be due to combining effect of prolonged SNCP of 12 day and constant 110 °C SNTD as described in preliminary experiment shown on Tables 1 and 3. This indicates that an increase in SNTD up to 70 °C resulted in reduction of FFA and by implication the PV. This observation is similar to the findings of Afaf (2003) which states that the decomposition of hydro-peroxides and other side reactions are minimized around 70 °C. This might give the moderate temperature

value of the graph, where lowest PV was measured and no generation of hydro-peroxides above 70 °C. Thus, suggesting that SNCP of 1.00 day or less and SNTD of 30 °C must be maintained in order to obtain the lowest Peroxide Value.

3.2.4. Analysis of Percentage Oil Content of Shea Kernel

$$Y_{\text{Oil content}} = 50.80 - 1.71 * (\text{SNTD}) - 2.50 * (\text{SNCP} * \text{SNBD}) + 2.39 * (\text{SNBD})^2 \quad (8)$$

The percentage oil content was significant ($P < 0.0444$) and positive to quadratic effect of SNBD as shown in equation (8). This leads to maximum percentage oil content of 56.00 % at 12 - day, 0 minute and 70 °C SNTD. Table 9 shows the interaction between SNCP and SNBD (extracted from figures 3 and 4) on the percentage oil content of Shea kernel at optimum 70 °C SNTD. The objective is to obtain Shea kernel with the maximum possible oil content ≥ 50 %.

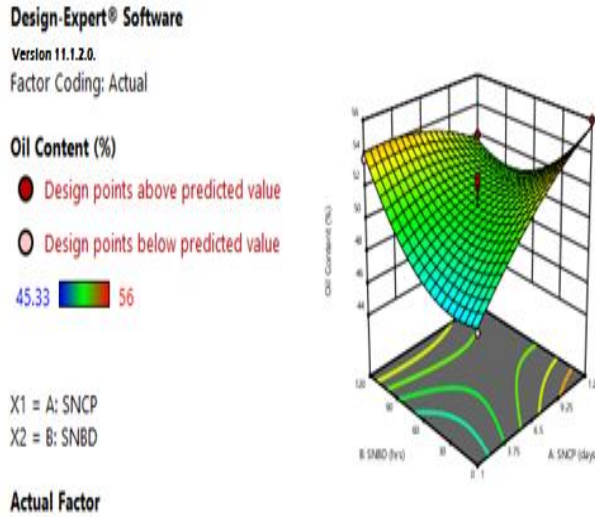


Figure 3: 3D RSP showing double effects of SNCP and SNBD on percentage oil content

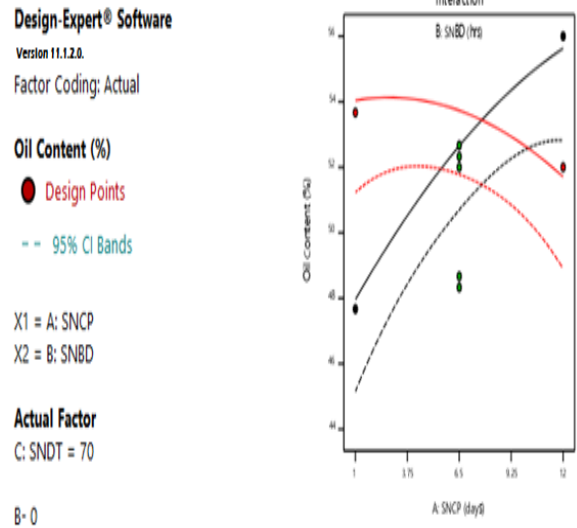


Figure 4: Interactive Plot showing effects of SNCP and SNBD on percentage oil content

Table 9: Design point of interaction between SNCP and SNBD on percentage oil content at confidence interval bands of 95 % and optimum 70 °C of SNTD

Lower limit		% Oil content	Upper limit		% Oil content
SNCP	SNBD		SNCP	SNBD	
1	0	47.67	12	0	56.00
Lower limit		% Oil content	Upper limit		% Oil content
1	120		53.67	12	

Note: Equilibrium point of 7.875 SNCP per SNBD

Table 9 shows that the Shea kernel processed at SNCP of one day, 0 minute SNBD and optimum 70 °C of SNTD produced the lowest percentage oil content of 47.67 %. This may be due to high retention of the proteins binding the fibres; holding the moisture and lipids at 1 day SNCP thereby making the fresh nut difficult to dry causing unavailability of the total fats content for the extraction of oil content (Lovett, 2005; Harris, 1998 and Hyman, 1991). Similarly, the Shea kernel processed at 12 day SNCP, 0 minute SNBD and SNTD of 70 °C had the highest percentage oil contents of 56.00 %. This high percentage oil content of 56.00 % obtained might be due to prolonged SNCP of 12 day which might have allowed polymerization of more oil in the Shea kernel at constant SNTD of 70 °C. Also, as a result prolonged SNCP moisture content contained in the kernel must have reduced, hence increasing the percentage oil content. According to Yonas *et al.* (2016) the highest percentage oil content obtained from the Shea kernel may result from constant SNTD of 70 °C at prolong SNCP of 12 day which might also be attributed

to thermal polymerization and decarboxylation of the oil. The high percentage oil content obtained may also result from denaturing of the proteins binding the fibres; and holding the moisture and lipids, thus making the fresh nut easier to dry and increasing the availability of the total fats content for extraction (Lovett, 2005; Harris, 1998 and Hyman, 1991).

3.2.5. Analysis of FFA for Shea Kernel Quality

$$Y_{FFA} = 1.72 + 0.4363*(SNCP) - 2.18*(SNTD) + 1.67*(SNCP*SNTD) + 1.08*(SNCP)^2 + 1.95*(SNTD)^2 \quad (9)$$

The negative linear coefficient term of SNTD was the only significant term in single effect in relation with FFA; thus leading to minimum value of FFA 0.60 % around SNCP. Table 16 shows the interaction between SNCP and SNTD (extracted from figures 8 and 9) on FFA of Shea kernel at optimum 60 minutes of SNBD.

The objective is to obtain a grade 'A' Shea kernel with $3 \leq \text{FFA} \leq 0$.

Design-Expert® Software

Version 11.1.2.0.

Factor Coding: Actual

FFA (%)

● Design points above predicted value

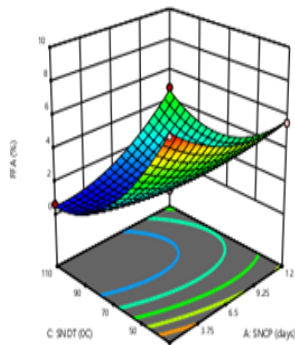
○ Design points below predicted value

0.6  7.98

X1 = A: SNCP

X2 = C: SNTD

Actual Factor



Design-Expert® Software

Version 11.1.2.0.

Factor Coding: Actual

FFA (%)

● Design Points

-- 95% CI Bands

X1 = A: SNCP

X2 = C: SNTD

Actual Factor

B: SNBD = 60

C-30

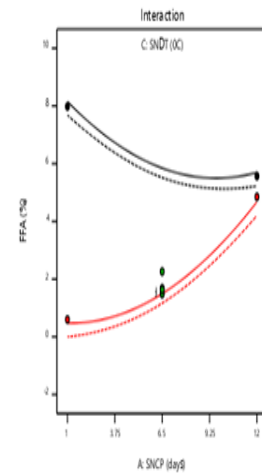


Figure 5: 3D RSP showing effects of SNCP and SNTD on Free Fatty Acid

Figure 6: Interactive plot showing effect of SNCP and SNTD on Free Fatty Acid

Table 10: Design point of interaction between SNCP and SNTD for FFA at confidence interval bands of 95 % and constant optimum conditions of 60 °C SNBD

Lower limit		FFA	Upper limit		FFA
SNCP	SNTD		SNCP	SNTD	
1	30	7.98	12	30	5.57
Lower limit		FFA	Upper limit		FFA
1	110		0.60	12	

Table 10 shows that the kernels obtained at 1 day SNCP and 30 °C SNTD has the highest FFA value of 7.98 %. At this low SNTD of 30 °C the enzymes and micro - organisms that would catalyze the formation of free fatty acids are active and can lead to the formation of more FFA, (Badoussi *et al.*, 2015). Similarly, the kernel obtained at 12 day SNCP and 30 °C SNTD gave the FFA value of 5.57 %. This slight decrease in FFA might be as a result that the Shea fruits had been exposed to a lower temperature (<30 °C) for 12 day before the commencement of drying at 30 °C. On the other hand, the kernel obtained at 1 day SNCP and 110 °C SNTD gave the lowest FFA value of 0.60 %. This might be as result of inactivation of enzymes and faster rate of moisture removal from the kernel leading to lower FFA value.

3.3. Optimization of Shea kernel using Response Surface Methodology

When all the factors investigated were combined, it was observed that the highest required percentage oil content and quality responses of grade 'A' Shea kernel were not met. Thus, the factors were optimised to guarantee high

percentage oil content, low PV and low FFA, a multi objective optimization was carried out by Design expert (11.1.2.0) to estimate the individual desirability using BBD of RSM

3.4. Optimization Result

3.4.1. Numerical Optimization Result

The goal is to determine the optimum conditions that will maximize percentage oil content from 45.33 % to 56 %, minimizes the PV from 4.9 meq/kg to 1.29 meq/kg and FFA from 7.98 % to 0.60 %. The optimum conditions of the factors were found to be 4.333 day of SNCP, 120 minutes of SNBD, 86.056 °C of SNTD while the responses are 2.869 of PV, 53.58 % of percentage oil content and 0.628 of FFA (%) with high desirability of 0.878 (87.8%) were selected.

3.4.2. Validation of PV, % oil content and FFA of Shea kernel quality

The peroxide value, percentage oil content and free fatty acid were validated and results shown in Table 11.

The results obtained from optimization were validated by carrying out three parallel experiments under the same optimal conditions and the average experimental

values of the responses obtained from Shea kernel processed as shown in Table 11 were compared. On comparison of predicted figures of PV, % oil and FFA with those of the actual values gave a standard deviation of ≤ 1.02 which is consistent with the findings of

Mohammed *et al.* (2017). This implies that the optimization in this study is reliable as shown on Table 11.

Table 11: Validation of Shea kernel Optimization

Shea kernel		SNCP (day)	SNBD (min)	SNDT (° C)	PV	% Content	Oil FFA
Optimum (predicted)	conditions	4.3333	120.00	86.00	2.87	53.579	0.627754
Experimental (Actual)	conditions	4.30	120.00	86.00	2.887	52.14	0.663913
Standard deviation					0.012021	1.017527	0.025568

4.0. CONCLUSION

The optimization of these processing factors using Box-Behnken method of response surface methodology was carried out, which led to Grade 'A' Shea kernel obtained at a processing condition of 4.0 day of SNCP, 120 minutes SNBD and 86 °C of SNDT giving Shea kernel with 2.868 meq/kg of PV, percentage oil content of 53.82 %, 0.628 % of FFA and desirability of 0.878.

The results from the optimization compares favourably with African Organization for Standardization Standards (ARSO, 2017).

5.0. ACKNOWLEDGEMENTS

Our appreciation goes to Tertiary Education Trust Fund (TETFund) for funding the research and also the Management of Federal Polytechnic Bida for providing an enabling environment for the research.

REFERENCES

- Aculey, P.C.; Lowor, S.T.; Kumi, W.O. and Assuah, M.K. (2012): The Effect of Traditional Primary Processing of the Shea Fruit on the Kernel Butter Yield and Quality. *American Journal of Food Technology*, 7 (2): 73-81
- Afaf, Kamal-Eldin (2003): Lipids Oxidation Pathways, AOCS Press, Department Food Science, Swedish University of Agricultural Sciences Uppsala, Sweden Champaign, Illinois
- ARSO, (2017). African Organization for Standardization; Building capacity to help Africa trade better, <https://www.tralac.org/news/article/11646-activities-of-the-african-organisation-for-standardisation-arso-related-to-the-work-of-the-wto-tbt-committee.html>
- Badoussi E., Azokpota P., Madode Y. E., Tchobo F. P., Amoussou B.F., Kayode A. P. P., Soumanou M.M., & Hounhouigan D. J. (2015). Cooking and Drying Processes Optimisation of *Pentadesma butyracea* Kernels during Butter Production, *African Journal Biotechnology*, 14(39) 2777-2785, <http://www.academicjournals.org/AJB>.
- Coulibaly, Y., Ouédraogo, S. and Niculescu, N. (2009): Experimental Study of Shea Butter Extraction Efficiency Using a Centrifugal Process. *Asian Research Publishing Network (ARPN)*, 4(6), 14-19
- Harris, R. (1999). Market and Technical survey: Washington DC. *Shea nuts*. pp. 45-70.
- Hyman, E.L. (1991). A Comparison of Labour Saving Technologies for Processing Shea Nut Butter in Mali. *World Development* 19 (9), 1247 – 1268
- Hossain, M.B., Brunton, N.P., Patras, A., Tiwari, B., O. Donnell, C.P., Martin-Diana, A.B. and Barry-Ryan, C. (2012). Optimization of ultrasound assisted extraction of antioxidant compounds from marjoram (*Origanum majorana* L.) using response surface methodology. *Ultrason. Sonochem*, 19, 582–590.
- Kim, H. K., Do, J.R., Lim, T.S., Akram, K., Yoon, S.R., Kwon, J.H. (2012). Optimisation of microwave assisted extraction for functional properties of *Vitis coignetiae* extract by response surface methodology. *J. Sci. Food Agric.*, doi 10.1002/jsfa.5546.
- Koloche, I. M., Olaleye, R. S., Adeniji, O. B., Yahaya, S.A., Umar, S. I. M. and Tsado, J. H. (2016). Socio-Economic Characteristics and Constraints Associated with the Adoption of the Improved Shea Nut Processing Technologies in Niger

- State, Nigeria. *Greener Journal of Agricultural Sciences*, 6(1), 001-009.
- Julius, K. I., Lilly, N., and Ayangealumun, I. (2013): Effects of Extraction Methods on the Yield and Quality Characteristics of Oils from Shea nut. *Journal of Food Resource Science*, 2(1), 1-12.
- Li-Chun Zhao, Ying He, Xin Deng, Geng-Liang Yang, Wei Li, Jian Liang, and Qian-Li Tang (2012). Response Surface Modeling and Optimization of Accelerated Solvent Extraction of Four Lignans from Fructus Schisandrae, *Molecules*, V (17), pp 3618-3629; doi:10.3390/molecules17043618
- Lovett, P. N. (2005). Shea Processing Technical Inventory and Recommended Improved Processing Methodology. Technical Report to the World Agroforestry Centre (ICRAF-WCA).
- Lovett, P. (2013). Quality @ Quantity @ Price: A Report Submitted to USAID. *Shea 2013* (pp. 1-20). Abuja, Nigeria: Global Shea Alliance.
- Maran, P. J. and Manikanda S. (2012). Surface Modelling and Optimization of Process Parameters for Aqueous Extraction of Pigment from Pea Fruit Dye Pigin, 95, pp 465 - 472.

LAB-SCALE CONTINUOUS ADSORPTIVE SEPARATION OF Cd (II) ION FROM AQUEOUS EFFLUENT USING MAGNETIC NANOCELLULOSIC ADSORBENT

Etuk, V. E., Oboh, I. O., Etuk, B. R.

Department of Chemical and Petroleum Engineering, University of Uyo, Nigeria

*Email of corresponding author: victoretuk@uniuyo.edu.ng

ABSTRACT

Haphazard disposal of industrial effluents into the environment has negatively impacted the global water security sector. Some of the accompanying chemical pollutants are reported to be carcinogenic when ingested or inhaled. Cadmium had been linked with several cancers in humans. Batch-wise adsorption technique is the commonly practiced separation procedure due to its lack of ambiguity and the potential for sorption of low concentration pollutants from effluent streams. The frequently used activated carbon adsorbent can be restrictive due to excessive sludge generation. The essence of this research interest is in the development of sustainable, renewable and environmentally friendly adsorbents based on advances in nanotechnology. In this study, 91.31 % recovery of Cd²⁺ was recorded when 3.0 mg of the solute was treated using novel magnetic nanofibrillated cellulose in fixed bed adsorption process.

Key words: Breakthrough curve, Environment, fixed bed, Nanoadsorbent, wastewater

1. INTRODUCTION

In accordance with several World Health Organization sources cobalt, chromium, zinc, lead, mercury, cadmium, copper, aluminum, iron, manganese and nickel are catalogued among the most unsafe if mistakenly ingested (Mousa *et al.*, 2013; Sylwan and Thorin, 2021). The indiscriminate exposure of these toxic metallic ions to the environment had been blamed on unethical disposal of various industrial effluents and other anthropogenic and geological activities. Such substances are known to be non-digestible, bio-accumulative and highly hazardous when unwittingly permitted into the menu via the sources of water supply. Such obnoxious occurrences had been reported to have detrimental impacts on human beings which occupy the zenith of the food chain, as well as partly account for the global ecological lopsidedness observed in the ecosystem nowadays (Tanveer, 2020; Putro *et al.*, 2017). Moreover, the turmoil witnessed in the correct application of relevant legislation or EPA guidelines *vis-à-vis* effective monitoring by assigned personnel and inappropriate attitude of stakeholders has negatively affected the strict compliance to wastewater disposal ethics by the operators of some of these companies in some countries (Ordinioha, 2015; Oladipupo *et al.*, 2016, Yakubu, 2017).

Consequently, modern environmental conservationists, engineers and scientists advocate the application of green/clean technological approaches for the conversion of raw materials to products, provision of services,

management of industrial/ municipal wastes and recycling of wastes (Tanveer, 2020; Sylwan and Thorin, 2021). The overall intention of clean technology is to conserve the natural resources and fix environmental damage that may have occurred in the past. These can eventually lead to systematic environmental protection.

Specifically, it had been reported that undesirable human exposure to cadmium primarily occurs through the ingestion of contaminated food and water. Cadmium accumulates in plants and animals with a long half-life of about 20–35 years (Leyssons *et al.*, 2017; WHO., 2008). Cadmium occurs naturally in the environment by the gradual process of erosion and abrasion of rocks and soils, and from climatic or geological events such as forest fires and volcanic eruptions (Rao *et al.*, 2010). The best-known cadmium mineral is greenockite cadmium sulfide (77.6% Cd). Other minerals are otavite, cadmium carbonate (61.5% Cd) and pure cadmium oxide (87.5% Cd). Greenockite (CdS) is nearly always associated with sphalerite (ZnS). This metal is of special concern because of its non-degradable and therefore persistent nature. The main anthropogenic pathway through which cadmium enters the environment is via wastes from industrial processes such as electroplating, smelting, alloy manufacturing, plastic, cadmium-nickel batteries, fertilizers, pesticides, mining, pigments/dyes, textile operations and refining. Also, there has been disturbing nexus between the epidemiological data of environmental and occupational cadmium exposure and various types of cancer including breast, lung, prostate,

nasopharynx, pancreas and kidney cancers (Genchi, *et al.*, 2020).

Activated carbon, which is popularly employed in traditional adsorption processes for wastewater treatment is exorbitant and sometimes opposed to the removal of heavy metals (Gunatilake, 2015, Shafiq, Alazba and Amin, 2018). This has led to the multiplicity of interest in recent times on the possibilities of magnetic modification of low cost agro-based adsorbents for application in the removal of hazardous metallic pollutants from wastewater due to its cost effectiveness and eco-friendly attributes (Sylwan and Thorin, 2021; Contruvo, 2017; WHO, 2017).

However, based on the surveyed literature, only few of the numerous novel adsorbent candidates from biomass sources has emerged in the realms of commercialization (Crini *et al.*, 2018). In this study, novel nanocellulose enabled magnetic adsorbent was fabricated, modified by magnetite ($\text{Fe}^{2+}/\text{Fe}^{3+}$) and assessed for the separation of Cd^{2+} from aqueous effluent, whose WHO and SON permissible limits were reported as 0.003 mg/ L by continuous fixed bed adsorption process (WHO, 2008).

2. MATERIALS AND METHOD

2.1 Preparation of adsorbent:

This was accomplished in two sets of processes, namely;

(a) **Costus Afer Nanofibrillated Cellulose (C-NFC):** - The mature *costus afer* stems used for this study were obtained from the bushes around the main campus of University of Uyo, Akwa Ibom State, Nigeria. Selected samples were labeled and taken to Botany Department of the University of Uyo for identification. The stems were cut to small sizes of approximately 1cm, washed several times with clean water to get rid of dust and water-soluble impurities and soaked in re-distilled water. The soaked material was separated and pulverized into pulp to expose its vascular tissues and then placed in the sun to dry sufficiently. The residual moisture in the sun-dried pulp was further treated to crispness in the WiseVen oven at 101 °C for about 3 hours. The dried crisp *Costus afer* stem pulp was then ground by several passes and screened with 2500-Tyler mesh size to obtain C-NFC particle sizes of 5µm with the aid of a Heavy-Duty Warring blender equipped with a static grinding stone and a rotating one revolving at about 1000 rpm. The obtained particles were subjected to further pulverization until particle sizes in the nano-range were obtained. The powdery product shown in Figure 1 was collected and stored in a desiccator for further use.

(b) **Magnetic Nanofibrillated Cellulose (C-MNFC):** - Measured amount of the powdery product (C-NFC) obtained in sub-section 2.1 and re-distilled water at the ratio of 1:10 were introduced into 250ml conical flask and placed on a magnetic stirrer with heating capability and maintained at 40 °C for 1 hr.

Then 4.9g of anhydrous ferric chloride and 4.2g of ferrous sulphate heptahydrate salts were added to the obtained suspension and stirred vigorously, accompanied by gradual rise in temperature from 40 – 90 °C at the rate of 2 °C/min. Meanwhile, 50 ml an alkaline solution comprising a mixture of 4.08g NaOH and 0.52g M KNO_3 such that its pH remained above 9 was prepared and its temperature was raised rapidly from ambient to about 60 °C. This was followed by the dropwise addition of the alkaline mixture to the iron solution mixture which resulted in the formation of the required black precipitate *Costus-afer* magnetic nanofibrillated cellulose (C-MNFC) (Galland *et al.*, 2017). The obtained adsorbent shown in Figure 2 was filtered, rinsed and dried at 105 °C and stored in a desiccator for further use. The entire steps of the process spanned 7 hrs.

Preparation of stock solution: Stock solutions of Cobalt was prepared with redistilled water as solvent from analytical grade of cobalt (II) sulphate heptahydrate dissolution. All working solutions were obtained by dilution of the stock solutions with re-distilled water into 50, 100, 150mg/l respectively for each experimental run. The concentration of metal ions in solutions was analyzed by Atomic Absorption Spectrophotometer.

Continuous Adsorption Studies: The continuous adsorption study was conducted with 400mm x 2mm OD column packed with a known quantity of the C-MNFC adsorbent to the desired bed height of the adsorbent 4, 8 and 12 cm. Re-distilled water was passed through the column in order to remove air bubbles and impurities from the bed of adsorbent. The influent was pumped to the top of the packed column with the aid of a solenoid dosing pump at three different flow rates (4, 8 and 12 mL/min) with different initial solute concentrations (50, 100 and 150 mg/L). The treated effluent was collected at regular intervals for subsequent analysis with AAS. The practical feasibility of the sorption column performance was verified through the dynamic response of the operation with respect to initial pollutant concentration, specific bed height and flow rate, based on the analysis of its breakthrough time (t_b), exhaustion time (t_{ex}) as well as the characteristic curvilinear shape of the breakthrough curve.



Figure 1: *Costus afer* Nanofibrilated Cellulose (C-NFC)



Figure 2: *Costus afer* Magnetic Nanofibrilated Cellulose

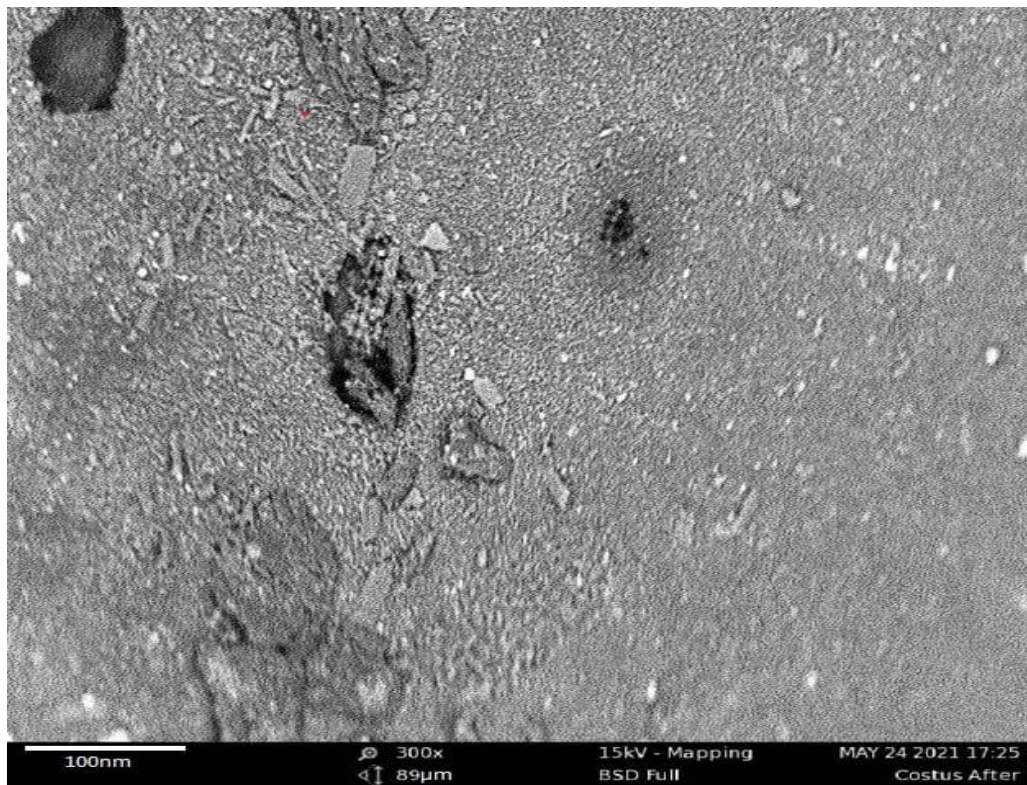


Figure 3: SEM image of C-NFC

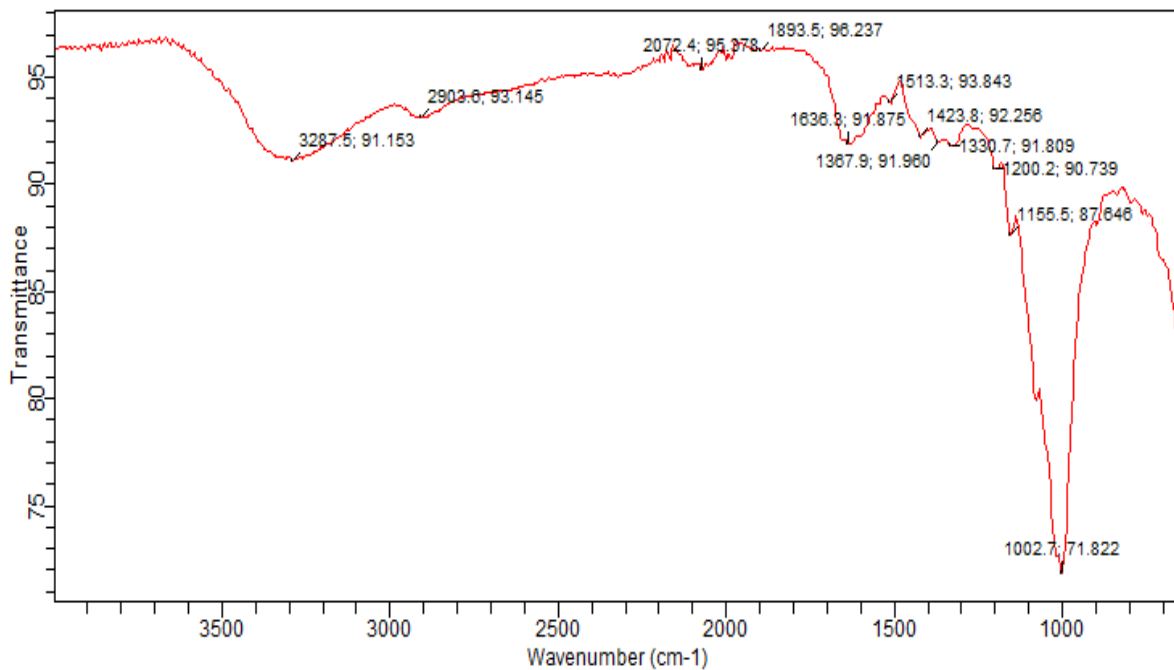


Figure 4. FTIR SPECTRA of C-MNFC before Cd (II) ion adsorption

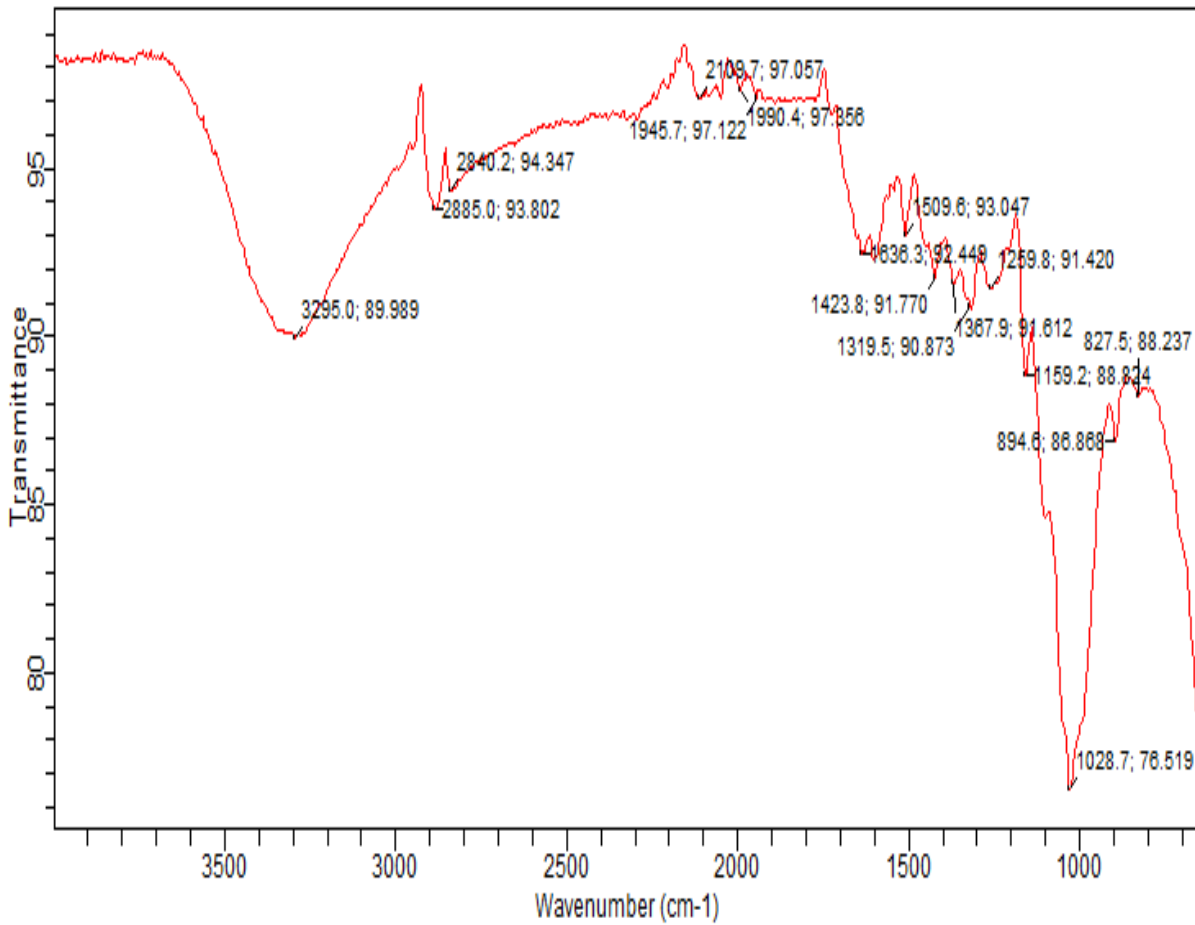


Figure 5. FTIR SPECTRA of C-MNFC after Cd (II) ion adsorption

Table 1: Physical properties of C-MNFC

Physical properties	Values
C-NFC Specific surface area (m ² /g)	816.417
C-NFC Pore diameter range (nm)	1.200 – 6.000
C-NFC Pore volume range (cc/nm/g)	0.000 – 0.1700
C-MNFC Specific surface area (m ² /g)	1219.544
C-MNFC Pore diameter range (nm)	1.400 – 6.000
C-MNFC Pore volume range (cc/nm/g)	0.000 – 0.2300
C-NFC Bulk density (g/cm ³)	1.22
C-MNFC Bulk density (g/cm ³)	1.59
C-MNFC Average particle diameter (nm)	3.54

Table 2: Elemental compositions of C-NFC obtained from proximate analysis

	Element Symbol	Element Name	Atomic Conc.	Weight Conc.
19	K	Potassium	32.48	37.05
47	Ag	Silver	4.17	13.12
30	Zn	Zinc	5.88	11.21
20	Ca	Calcium	8.02	9.37
6	C	Carbon	18.17	6.37
16	S	Sulfur	5.19	4.85
15	P	Phosphorus	5.36	4.84
14	Si	Silicon	5.00	4.09
8	O	Oxygen	6.54	3.05
13	Al	Aluminum	3.09	2.43
12	Mg	Magnesium	2.18	1.55
11	Na	Sodium	1.75	1.18
7	N	Nitrogen	2.17	0.89
26	Fe	Iron	0.00	0.00
22	Ti	Titanium	0.00	0.00

Table 3: Summary of column performance

Summary of fixed bed adsorption parameters for Cd (II) ion removal by C-MNFC at different operating conditions of bed height, flow rate and initial solute concentration

Adsorbent type	m (g)	H (cm)	Q (ml/min)	C0 (mg/L)	tb (min)	te (min)	qttotal(mg)	qe(mg/g)	m total (mg)	%R (mass%)
C-MNFC	4	4	8	100	30	195	0.5668	0.1417	1.522	37.45
C-MNFC	8	8	8	100	115	300	1.248	0.156	2.328	53.60
C-MNFC	12	12	8	100	222	387	2.742	0.1879	3.003	91.31
C-MNFC	4	4	4	100	138	348	0.7963	0.1909	1.319	60.37
C-MNFC	4	4	12	100	15	126	0.3467	0.0872	1.397	24.82
C-MNFC	4	4	8	150	15	95	0.1814	0.0426	0.988	18.36
C-MNFC	4	4	8	50	85	373	1.3158	0.319	2.279	57.82

Table 4: Adsorption capacities of Cd²⁺ by various plant-based adsorbents

S/N	Adsorbent	Initial concentration (g/L)	Adsorption capacity (mg/g)	% Recovery	Reference
1	Wheat straw biochar	2	–	90	Naeem <i>et al</i> , 2019
3	Chlorella vulgaris biomass	0.025	–	76.448	El-Sheekh <i>et al</i> , 2019
4	Cassava stem	-	10.47	-	Prapagdee <i>et al</i> , 2014

S/N	Adsorbent	Initial concentration (g/L)	Adsorption capacity (mg/g)	% Recovery	Reference
5	Dracaena draca	0.01		79.60	Masoudi <i>et al</i> , 2018
6	Hazelnut-shells		5.45		Masoudi <i>et al</i> , 2018
7	Sugarcane-bagasse	–	2	–	Masoudi <i>et al</i> , 2018
8	C-MNFC	3.0	2.4	91.31	Present study

3. RESULTS AND DISCUSSION

The BET result indicated that the surface area of the magnetic nanofibrillated cellulose was 721.544 m²/g while the bulk density was evaluated as 1.22g/cm³ by tapped density procedure. The Java ImageJ particle size analysis revealed that the average particle diameter of C-MNFC was 3.54 nm as shown in Table 1.

The proximate analysis conducted with 92.82% dry matter of the C-NFC adsorbent indicated the presence of >60% carbohydrates, 18.55% crude fat, 5.75% crude protein and 5.03% ash. Further test results showed that the ash comprised various trace quantities of inorganic salts of potassium, calcium, magnesium, zinc, sodium, silver, etc. as indicated in Table 2.

However, trace amount of iron and zirconium salt were noticed in the C-MNFC adsorbent after treatment with magnetite which provided additional binding sites for the adsorbates (Galland *et al.*, 2017). These trace elements were contributions from the impurities in the iron salts used.

Scanning Electron Microscopy (SEM) morphologies of adsorbent before and after adsorption revealed the deposition of Cd (II) ion onto the nanocellulosic substrate during the dynamic contacting. This was also confirmed by the differences in the values of the peaks of FTIR spectra before and after adsorption shown in Figures 4 and 5.

Currently, the FTIR spectrum is divided into three wavenumber regions: far-IR spectrum (<400 cm⁻¹), mid-IR spectrum (400-4000 cm⁻¹), and near-IR spectrum (4000-13000 cm⁻¹). The mid-IR spectrum is the most widely used in the sample analysis, but far- and near-IR spectrum also contribute in providing information about the samples analysed (Asep *et al.*, 2019; Ibrahim and Faruruwa, 2020). This study focused on the analysis of FTIR in the mid-IR spectrum. Thus, the outstanding

single bond region corresponds to the spectra range between 2050-2900 cm⁻¹ where C-H stretch, C-C combination and CH₂ were the possible vibrational peaks detected. The broad adsorption band in the area between 3250 – 3000 cm⁻¹ indicated the presence hydrogen bond as well as confirmed the existence hydroxyl (-OH stretch) in C-NFC adsorbent. The occurrence of a peak between 3100 and 3000 cm⁻¹ suggested the existence of aromatic structure while the narrow bond at 2903.6 cm⁻¹ confirmed the existence of C-C bond. The shallow peak between the band range 1513.3 and 1900 cm⁻¹ represented the existence of NH-stretch, C-H, organic or aliphatic nitro bond while the sharp peak observed at 1002.9 cm⁻¹ correspond to the existence phosphate or silicate ion, whereas the peaks between 1367.9 to 1423.8 cm⁻¹ correspond to O-H and C-H combination.

Column Performance: The continuous adsorption of cadmium ion from aqueous effluent was carried out in three different bed heights of 4, 8 and 12 cm corresponding to mass of 4, 8 and 12g respectively while the wastewater inlet flow rate and initial solute concentration was kept at 8ml/min and 100mg/L respectively at the pH 6.9 and temperature of 301 k (28 ±1 0C). The breakthrough curves for different bed heights were plotted as the ratio of effluent concentration to influent concentration (C_t/C_o) against time (t). It can be observed from Table 3 that the breakthrough time t_b (time at which 1% of the initial solute concentration appeared in the effluent) and exhaustion or saturation time t_e (time at which 90% of initial solute concentration appeared in the effluent) increased with increasing bed height which resulted in increase of the residence time of the adsorption process

Effects of Bed height on breakthrough curve: Increase in bed height enhanced the removal efficiency of the adsorbate due to the corresponding increase in adsorption sites and the residence time of the wastewater as well as its throughput volume in the fixed bed

column. Also, the slope of breakthrough curve appeared to decreased with increasing bed height, which resulted in a broadened mass transfer zone while the breakthrough time and the exhaustion time were increased from 30 to 220 minutes and 195 to 387 minutes respectively, as the flow rate increased from 4 mL/min to 12 mL/min.

Effect of Flow rate on Breakthrough Curve: The effect of the flow rate on the adsorption of C-MNFC was investigated by varying the flow rate of the influent at 4, 8 and 12 mL/min respectively while the initial solute concentration and bed height were kept at 100 mg/L and 8 cm respectively as shown by the breakthrough curve in figure (3b). These curves were obtained for the various flow rates from the plot of the normalized concentration (C_t / C_o) against time. It was observed that the breakthrough time was approached much faster at higher flow rate than at a lower one because of the correspondingly lower residence time of the influent in the column, which in turn reduced the contact time between cadmium ion adsorbate and the C-MNFC adsorbent and vice versa at lower flow rate for the saturation time. The longer the approach of saturation point from breakthrough time the higher the percentage recovery of the pollutant. In this case, the breakthrough time and the exhaustion time increased from 15 to 138 minutes and 126 to 348 minutes respectively, as the bed height passed from 4 to 12 cm). This behavior of the variations of the slopes of the breakthrough curves and the respective adsorption capacity is supported by the principle of mass transfer since the rate of mass transfer increased at higher flow rate which resulted in faster approach of the saturation point due to decreased residence time.

Effect of Initial Solute Concentration: The fixed bed study was carried out at different initial solute concentration of 50 mg/L, 100 mg/L and 150 mg/L respectively while the bed height and flow rate were kept constant at 8 cm and 8 mL/min respectively. The breakthrough curves for all initial solute concentrations of the wastewater were plotted as the normalized concentration (C_t / C_o) against time as shown in Table 2. It can be observed that the breakthrough time and the exhaustion time were increased from 35 to 215 minutes and 195 to 385 minutes respectively, as the initial adsorbate concentration increased from 50mg/L to 150mg/L.

The results implied that the change in concentration gradient affects the saturation rate, bed exhaustion time

and breakthrough time. Thus, the breakthrough time, exhaustion time and breakthrough volume decreased with increased initial adsorbate concentration because of the low mass-transfer profile from the bulk solution to the adsorbent surface.

CONCLUSION

This study showed that magnetic nanofibrillated cellulose can be used as an efficient and ecofriendly adsorbent candidate for the separation of Cd (II) ion from industrial effluent streams. The removal of this adsorbate was dependent on flow rate, initial solute concentration of influent stream and bed height; it was seen to increase with increasing bed height but decreased with increasing flow rate and increasing initial Cd (II) ion concentration of influent. The practical feasibility of sorption column performance was verified through the dynamic response of the its operation parameters based on the analysis of breakthrough time (t_b), exhaustion time (t_e) and the characteristic curvilinear shape of the breakthrough curve.

Thus, increasing initial adsorbate concentration and flow rate can reduced the residence time but not necessarily enhance the pollutant recovery efficiency of the of C-MNFC. 91.31 % recovery of Cd^{2+} was obtained when 3.0 mg of the solute was treated with novel magnetic nanofibrillated cellulose in a 12 cm fixed bed column. This method is suitable for the treatment of large volume of wastewater and can easily be adaptable to industrial scale operation compared to batch adsorption approach.

REFERENCES

- Asep, N., Rosi, O., Risti, R. (2019). How to Read and Interpret FTIR Spectroscopy of Organic Material. *Indonesian Journal of Science & Technology*. 4 (1): 97-118.
- Chinedu, E., Chukwuemeka, C. (2018). Oil Spillage and Heavy Metals Toxicity Risk in the Niger Delta, Nigeria. *Journal of Health and Pollution*. ResearchGate. 8 (19): 1 – 9.
- Contruvo, J. A., (2017). WHO Guidelines for drinking water quality: First addendum to the fourth edition. *J. American water works Association*. 7(109); 44 – 51.
- Crini, G., Lichfouse, E., Wilson, L., Morin-Crini, N. (2018). Conventional and non-conventional adsorbents for wastewater treatment. *Environmental Chemistry Letters*, Springer, 8: 1-20.
- El-Sheekh, M., El Sabagh, S., El-Souod, G., Elbeltagy, A. (2019). Biosorption of Cadmium from

Lab-Scale Continuous Adsorptive Separation Of Cd (II) Ion From Aqueous Effluent Using Magnetic Nanocellulosic Adsorbent

- Aqueous Solution by Free and Immobilized Dry Biomass of *Chlorella vulgaris*, *International Journal of Environmental Research*, 13:511–521
- Galland, S., Richard L., Andersson, R., Salajkov, M., Ström, V., Olsson, R., Berglund, L. (2017). Cellulose nanofibers decorated with magnetic nanoparticles – synthesis, structure and use in magnetized high toughness membranes for a prototype loudspeaker. United States Patent: Patent No : US 9 , 767 , 944 B2(45)
- Genchi, G., Sinicropi, M., Lauria, G., Carocci, A., Catalano, A. (2020). Review: The Effects of Cadmium Toxicity. *Int. J. Environ. Res. Public Health*. 17(3782): 1 – 24. doi:10.3390/ijerph17113782.
- Gunatilake, S. K. (2015). Methods of removing heavy metals from industrial wastewater. *Journal of Multidisciplinary Engineering Science Studies*. 1(1): 12 – 18.
- Ibrahim, Z.; Faruruwa, D. (2020). Biosorption Studies of Cd²⁺ and Cr⁶⁺ from Aqueous Solution Using Cola-Nut Leaves as Low-Cost Biosorbent, *Journal of Chemistry*, Hindawi, Article ID 6042398, 10 pages <https://doi.org/10.1155/2020/6042398>
- Leysens, L., Vinck, B., Straeten, C., Wuyts, F., Maes, L. (2017). Cobalt toxicity in humans. A review of the potential sources and systemic health effects, *Toxicology*, Elsevier, 387: 264 – 279.
- Mamoud, A., Fawzy, M., Radwa, A. (2016). Optimization of cadmium (Cd²⁺) removal from aqueous solutions by novel biosorbent. *Int. J. Phytoremed.* 18 (6) 619–625. <https://doi.org/10.1080/15226514.2015.1086305>
- Masoudi, R., Moghimi, H., Ramezan E., Taheri, A. (2018). Adsorption of cadmium from aqueous solutions by novel Fe₃O₄- newly isolated *Actinomucor* sp. bionanoadsorbent: functional group study, *Artificial Cells, Nanomedicine, and Biotechnology*, 46 :1092 – 1101
- Mousa, W., Soliman, S., El-Bialy, A., Shier, H. (2013). Removal of some heavy metals from aqueous solutions using rice straw. *Journal of Applied Sciences Research*, 9(3): 1696-1701.
- Naeem, M., Imran, M., Amjad, M., Abbas, G., Tahir, M., Murtaza, B., Zakir, A., Shahid, M., Bulgariu, L., Ahmad, I. (2019). Batch and Column Scale Removal of Cadmium from Water Using Raw and Acid Activated Wheat Straw Biochar, *Water*, 11, 1438; doi:10.3390/w11071438.
- Nwankwoala, H., Amadi, Y., Ameh, M. (2017). Contamination Risk Assessment of Physico-chemical and Heavy metal Distribution in Water and Sediments of the Choba Section of the New Calabar River, Nigeria. ResearchGate Article. P. 1 -16.
- Oladipupo, S., Mudashiru, O., Oyeleke, M., Bakare, S. (2016). Review of some Impact of Oil Exploration and Production in Niger Delta, Nigeria. *International Conference of Science, Engineering & Environmental Technology*. 1 (13): 90 – 103.
- Ordinioha, B. (2015). The Human Health Effects of Oil Exploration and Exploitation in the Niger Delta Region of Nigeria. ResearchGate Article. DOI 1013140/RG2.1.1973.2320
- Putro, J., Kurniawan, A., Ismadji, S., Jua, Y. (2017). Nanocellulose based biosorbents for wastewater treatment: Study of isotherm, kinetic, thermodynamic and reusability. *Environmental Nanotechnology, Monitoring & Management*, Elsevier. 8: 134 – 149.
- Rao, K., Mohapatra, M., Anand, S., Venkateswarlu, P. (2010). Review on cadmium removal from aqueous solutions. *International Journal of Engineering, Science and Technology*, 2 (7): 2010, pp. 81-103
- Standard Organization of Nigeria. (2007). Nigerian Standard for Drinking Water Quality.
- Shafiq, M., Alazba, A., Amin, M. (2018). Removal of Heavy Metals from Wastewater using Date Palm as a Biosorbent: A Comparative Review. *Sains Malaysiana*. 47 (1): 35 – 49.
- Sylwan, I., Thorin, E. (2021). Removal of Heavy Metal during Primary Treatment of Municipal wastewater and Possibility of Enhanced Removal: A Review. *Water*. 13: 1121 – 1147.
- Tanveer, M. A. (2020). Adsorption of Pb (II) from Wastewater by Natural and Synthetic Adsorbent. *Biointerface Research in Chemistry*. 10 (5): 6522 – 6539.
- WHO (2017). Guidelines for drinking-water quality. Fourth edition incorporating the first addendum. WHO, Geneva.
- WHO (2008). Guidelines for drinking-water quality. Third edition incorporating the first and second addenda. WHO, Geneva.

PRACTICAL ENGINEERING SKILLS TRANSFER IN THE NIGERIAN UNIVERSITY SYSTEM: A REVIEW OF EDO STATE UNIVERSITY UZAIRUE

Aluyor. E. O. ¹ and *Otoikhian, K. S. ²

^{1,2}Edo University Iyamho, Edo State, Nigeria

KM 7 Auchi-Abuja Express Way Iyamho, Uzairue, Etsako West LGA, 312102, NIGERIA

¹eoaluyor@yahoo.com and ^{2,*}Otoikhian.kevin@edouniversity.edu.ng

Corresponding Author: ^{2}Kevin Shegun Otoikhian (Otoikhian.kevin@edouniversity.edu.ng)

ABSTRACT

The contemporary engineer is required to manage environmental, cultural, and social issues while resolving complex technical problems that call for the work of inter-professional collaboration. The technological, ICT, and soft skills needed by an engineer have been separated into these three categories. Numerous routine job positions would not only be threatened by the market growth for, and use of these technological innovations in the engineering industry, but it would also drive innovative and exciting opportunities and call for authentic intelligence and creativity. This review therefore, using a tactical methodological approach, discloses the significance of effecting workable engineering expertise in the Nigerian Institutions whilst also suggesting that, unless efforts are made to continually develop and foster the acquisition of engineering skills, the daunting new fad with the use of technological innovations within the engineering industry will inevitably lead in the joblessness of engineering graduates and professionals. This suggestion is, in fact, expected to generate so much prospects for engineers with an entrepreneurship and innovation perspective whilst take creating an enabling environment for innovations via the use of emerging technologies.

Keyword: Skills, framework, engineers, practical, technologies, entrepreneurial.

1.0 INTRODUCTION

Engineering is generally described as a profession in which the experiential and study-based knowledge of mathematics, science, and technology is practiced and implemented to find ways to economically utilize and manipulate materials and forces for the benefit of man (Akinsanya & Omotayo, 2013). Engineers are generally called problem solvers because of their ability to think critically and analytically about problems with the assurance of getting a solution. The uniqueness of the engineering discipline is the unparalleled response to events which is also closely related to their capacity to anticipate and plan. Hence, the deep understanding of societal problems coupled with an engineer's broad scope of reasoning places them in an advantageous position. Engineers are therefore expected to solve several societal problems in sustainable ways. To do so, they must be well-versed in engineering ideas and the application of engineering theoretical principles to real issues (Falade, 2008). Engineering students must therefore be trained not just for the present but also for a future that may be significantly different from the present in a world of rapid technological advancement. The balance of emphasis must be tilted towards those fundamental skills as well as skills of emerging immense relevance necessary for progressive

engineering in current and future times (National academy of Science, 2012). With the rapid advances in science, technology and Information Technology (IT) and the exponential rise in unemployment, comes the need for highly skilled and entrepreneurial engineers with the requisite competence to maximize these gains in delivering valuable solutions to the world's problems that are more effective, faster and/or cheaper. The present global work environment is significantly different from that of fifty (50) years ago, notably, it is almost unthinkable these days for any engineer to function effectively as required by the present work environment, without the aid of computers/ work stations running relevant software. Over 60 percent of the Nigerian populace (over 200 million) are under 24 years and this figure is likely to increase significantly come 2050 (Onyeiwu, 2021). However, in another fifty (50) years from now, the work environment will be significantly different than it is right now with certain skills of emerging relevance such as advanced computer and digital literacy, applications of machine learning, artificial intelligence and other disruptive technologies becoming essential skills requirements for many engineering professionals (Bakhshi *et al.*, 2017). The engineering professionals will not have to be without jobs, but they will have to constantly upgrade their skill set (Fulgence, 2015). There will also be a need for more

engineers with an entrepreneurial outlook to adequately take advantage of the opportunities for innovation that these new technologies present. Furthermore, as the work environment and operations of even small firms and organizations go global, there will be an increasing demand for soft skills such as communication, teamwork, leadership, time management, lifelong self-learning and so on (Chikumba, 2011; Choudary, 2014; Cukierman and Palmieri, 2014). There has been a growing problem of skills mismatch of engineering graduates with (Pitan and Adedeji, 2012) reporting a skills mismatch of 60.6% with major weaknesses in soft skills. In the midst of all these, the ever relevant and fundamental engineering skills and requirements such as sound knowledge of the fundamental science principles as well concepts, techniques and principles of the specific engineering disciplines in addition to technical problem solving, critical thinking, numeracy etc. will remain as relevant as they have always been. The question then is how can these ever-increasing demands for advanced computer skills and soft skills in addition to the fundamental technical skills and know-how be imbued in the teaching and training of the modern-day engineer?

2.0 PRACTICAL ENGINEERING SKILLS FOR THE 21ST CENTURY

Before presenting and discussing a strategy for imparting the practical engineering skills needed for the modern engineer, there is a need for some clarity about what these skills are to be imparted. These skills, are divided into three broad categories which are technical skills, computer skills and soft skills.

2.1 Technical Skills

These are traditional engineering skills that form the bedrock of the engineering discipline. Employers and recruiters have consistently invested significant resources in addressing this technical skill gap among engineering graduates worldwide (Kalbande *et al.*, 2022; Syam *et al.*, 2021). The relevance of these skills will always remain well in place and highly transferrable. These skills include an in-depth grasp of relevant science fundamentals; an in-depth grasp of fundamentals, and applications of disciplinary principles, and the capability for independent scientific research. Others are ability to prepare and interpret engineering drawings, engineering design, systems thinking and analysis (Aluyor, 2020).

2.2 Computer Skills

In recent times, the importance of the computer in engineering practice has been on an exponential increase. Fully interactive realities in engineering education has recognizable psychological and pedagogical benefits, which in turn enhances students' comprehension of the subject areas, efficiency and scores, and an overall learning quality. The advantages of using VR as a substitute for physical laboratories also extend to the university or institution in terms of decreased liability, infrastructure, and cost (Soliman *et al.*, 2021). Computer skills that are relevant for the modern-day engineer include computer-aided design, modelling, simulation and control of systems, processes and devices; computer programming, data analytics, applications of artificial intelligence, and machine learning in engineering, among others (Aluyor, 2020). Studies have shown that workers exposed to computer application courses in experimental and control groups perform significantly differently in the long run, demonstrating the effectiveness of a computer-based instructional model (Kardipah and Wibawa, 2020).

2.3 Soft Skills

The unemployable status of most graduates is due to the lack of industry-relevant or basic skills from the university (Adekola *et al.*, 2016; Oloyede *et al.*, 2018; Ruth *et al.*, 2014). Oftentimes, these skills could include both hard and soft skills. It should be noted that though most employers are philanthropists and are involved in "community development" also known as "corporate social responsibility" which helps develop their immediate residents by providing amenities, training and employing indigenes, engaging the services of semi-skilled workers within the community, etc. while making a profit from the community either through their natural resources or other means. Companies are not just looking for people to be show liberality or prove their philanthropic nature too. They need skilful individuals that will foster organizational growth while churning out more profit and this is the primary goal of every profit-making enterprise. Hence, Most Nigerian graduates have been bereft of this ability even after specialized training. Professionals must therefore possess a variety of relevant soft skills, including problem-solving skills, teamwork, consistent learnability, analytical thinking, and communication. These competencies are required for a comprehensive academic background in engineering (Aluyor, 2020; Cukierman and Palmieri, 2014; Kalbande *et al.*, 2022).

3.0 A STRATEGIC FRAMEWORK FOR IMPARTING THESE SKILLS

As can be reasonably deduced, there is the need for a well-thought out strategy for delivering the skills outlined in the previous section within the engineering

education system. Engineering education can no longer be business as usual and there is a need for innovation based on an effective strategy in the way engineering education is delivered in order to obtain engineers that are qualified for the modern day world and are globally competitive.

3.1 Aimed Strategic Framework

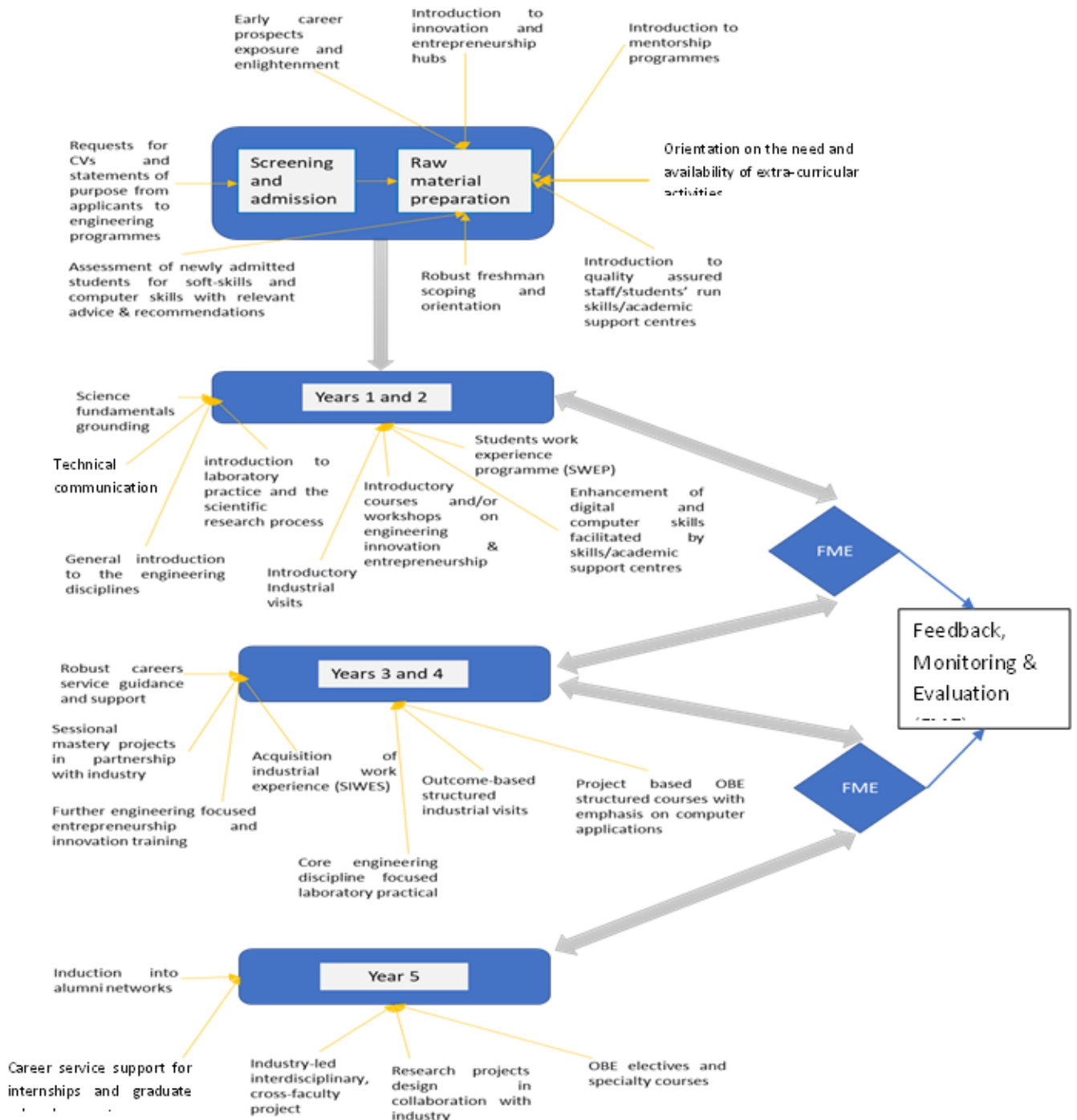


Figure 1: Aimed Strategic Framework for Imparting Practical Engineering Skills (Aluyor, 2020; Aluyor and Otoikhian, 2022)

Figure 1 shows a proposed strategic framework for imparting the technical, digital, and soft skills required of engineers in the 21st century. The framework consists of four stages represented by the four blue squares with curved edges as shown in figure 1. The four stages of the strategic framework are discussed below.

3.1.1 Stage 1: Raw material selection and preparation

The quality of input into any process to a large extent affects the quality of outputs that can be obtained. The task of producing engineering graduates with the required skills for the 21st century requires vital co-operation between academia, students, alumni, and industry.

At the candidate screening and admission part of stage 1, it is recommended that another layer of screening requirement be added, in requesting that applicants submit briefs and statements of purpose in support of their application to be admitted to an engineering programme. This additional layer of screening requirements could go a long way in raising awareness and fostering efforts to develop some of the soft skills and basic computer skills required for an engineering degree by applicants. A statement of purpose, for example, will compel applicants to research, reflect upon, and communicate why they want to study engineering. This singular exercise which can be conducted and/or evaluated along with other application documents by the university, faculty, or departmental admissions board will prove vital to the rest of the students' engineering journey giving a sense of purpose, consciousness of will, and a direction for individualized goals.

At the conclusion of the screening and admission phase of stage 1, the next phase is termed, raw material preparation, this is relatively a brief phase in terms of duration as it is expected to last only a couple of weeks, usually the first few weeks of the start of the engineering programme and its impact is going to be far-reaching. The major components and key activities of this phase are as highlighted in figure 1. One of the key activities is labelled, robust freshman scoping/orientation, this entails detailed orientations at the university, faculty and departmental levels of the purpose and aim of university education. The vision of the kind of graduates that are intended to be produced at the end of the engineering programme should be clearly communicated to the new students at this stage. Furthermore, the need for students to take responsibility for their own learning and begin to

cultivate the skill of lifelong self-learning should be communicated at this stage. This will serve to give an apt sense of purpose, focus and motivation to the students for their engineering education journey. The relevant skills that they are expected to acquire through their time in the university and how the university, faculty and department intends to impart these skills should be clearly spelt out. This will help to engender co-operation with the process amongst the students.

Entrepreneurship and innovation hubs, career service units, skills/academic support centres and mentorship program are key requirements that should be in place to enable the engineering programmes achieve its aim and objectives. These units, programmes and/or centres are to be established and operated via a synergy between academia, alumni, industry, and older students. Also, at this stage, an assessment of the computer and soft skills level of newly admitted students is appropriate. This will serve to assess the level of support that these students need to thrive in their studies towards achieving the aim and objectives of the engineering programmes. It is probably superfluous to state here that an engineering undergraduate student in the 21st century would need a laptop or some regular access to a computer in order to develop the necessary computer and digital literacy skills intended. The students should be encouraged to participate in relevant clubs and societies and even aspire for positions of responsibility in these clubs and societies as this has been proven to improve soft skills and employers generally find such impressive (Lowden *et al.*, 2011).

3.1.2 Stage 2: Foundational Training

This stage is where foundational engineering competencies are imparted to the students. The core components and key activities of this stage are as shown in figure 1 which is quite self-explanatory. The Students Work Experience Programme (SWEP) which is a period of about 12 weeks workshop practice training as well as exposure to the various engineering disciplines serves to impact several technical skills such as; basic equipment handling, work environment health and safety skills, basic engineering drawing skills amongst others. The soft skills to be honed include teamwork, self-learning, communication, etc.

The use of multimedia technologies and learning management systems (LMS) is key for effective delivery of courses in the 21st century.

3.1.3 Stage 3: Core Engineering Training

This is the stage at which students are trained in their core engineering disciplines of choice. The principles and techniques of the core engineering disciplines are imparted to the students at this stage. Advanced discipline-specific computer skills and applications are to be built into the delivery of the courses, which should follow the prescription of the Outcome Based Education (OBE) curriculum. As much as is feasible, assessed course projects should be included in the delivery of these courses, this will further serve to hone the technical, computer and soft skills of the students. The Student Industrial Work Experience Schemes (SIWES) should be strategically managed to ensure that the aim and objectives of the scheme are achieved. Industrial visits should be frequent at this stage with clearly defined outcomes for each visit. The attainment of these outcomes should be assessed, and the assessment scores should be included in the grades for the SIWES programme.

Furthermore, laboratory practical sessions at this stage should be highly focused and directly linked to the principles taught in the classroom. It is recommended that the lecturers who teach the various courses should be responsible for designing and supervising laboratory practical sessions that are directly aligned to the course principles taught in class. It is also recommended that this should be done in collaboration with industry partners. This will further help to ensure the engineering programme laboratory practicum is relevant to industrial practice.

The engineering entrepreneurship and innovation trainings by the entrepreneurship and innovation hubs should be much more discipline focused at this stage and should be facilitated by seasoned engineering entrepreneurs and innovators; persons who have led and/or are leading entrepreneurial initiatives and/or have made several engineering innovations. These resource persons may be within the staff base of the various departments or maybe guest lecturers/facilitators outside the full-time employ of the university. The key point here is that those who seek to impart entrepreneurial and innovation skills to engineering students must themselves be entrepreneurs and innovators. The management of the engineering programmes will have to seek out and engage qualified personnel among its staff, alumni, and industry partners as well as other personnel, if need be, across the length and breadth of the country, for such task.

A notable component included in the proposed framework in Figure 1, which is not common in the Nigerian university system, is termed ‘sessional mastery projects’ and should be administered with input from industry partners. It is a well-known fact that a key requirement for mastery is practice. The proposed sessional mastery projects are team-based projects that will require the students to draw on all the technical, computer and soft skills that they have garnered in a given academic year to solve a real-world problem, probably posed by industry partners.

Furthermore, at this stage, there should be concentrated effort by the career services units to provide necessary support and training to students to help them secure internships, graduate positions, and jobs during studies and upon graduation.

3.1.4 Stage 4: Specialisation and Finishing

At this final stage, students usually have the option of offering several electives in line with the aspects of the discipline they intend to focus on. The final year research project at this stage should be tailored towards solving real-world problems which have the potential to result in profitable spin-out companies if the research is successful.

These research projects should be designed in consultation with industry partners.

Furthermore, a recommendation is made for a final engineering design project which should be industry led, cross-faculty and interdisciplinary. The idea is to draw students from the various departments within the faculty of engineering into teams that will then tackle a problem presented by industry. This will help to simulate a typical inter-disciplinary work situation which is the norm in an industrial work environment. None of the engineering disciplines is an island of itself, expertise from the various engineering disciplines are usually needed to deliver any major engineering project. A project-based learning approach is vital in developing soft skills alongside technical and/or computer skills (Harmer, 2014; Kabouridis *et al.*, 2014).

At this stage, the careers services unit as well as the entrepreneurship and innovation hubs should be actively involved in providing necessary support to fresh graduates in securing graduate placements, internships, and/or starting their own businesses. Furthermore, these fresh graduates should be duly inducted into functional alumni networks for continuous professional development support. These alumni networks are in turn very beneficial to the university in terms of serving as a

source of additional funding, providing mentorship to undergraduates, and serving as links between the higher education institution (HEI) and the industry in which they work, amongst other benefits.

A notable and very important component of this strategic framework is the feedback, monitoring and evaluation Feedback Monitoring and Evaluation (FME) component. Quality control and assurance is key to ensuring qualitative engineering education (Oloyede *et al.*, 2018). Regular assessment of the attainment levels of the technical skills, digital/computer skills and soft skills of would-be engineers and an assessment of the overall satisfaction of all major partners in the engineering education project is vital to the success of the proposed strategic framework.

3.2 Additional Notes

In implementing the presented strategic framework above, there are several salient points that should be taken note of. First of all, the management and members of the engineering academia may need to commit to continuous training and professional development in keeping with current best practices and developments in their areas of specialty. Academics who are expected to impart advanced computer application skills and soft skills to would-be engineers must be highly competent in these skills. Furthermore, there is need for regular curriculum updates in keeping pace with global trends and developments (Aluyor *et al.*, 2019).

The need for a synergy between academia, industry, alumni networks, and students have been highlighted throughout this paper. In order for this strategic framework to be successful, the importance of such a synergy cannot be over-emphasized. Possible challenges to implementing some of the recommendations presented herein include; the natural inertia to change, inadequate levels of advanced computer application and digital literacy amongst engineering academia, challenge of establishing and sustaining strategic links and partnerships with industry, certain restrictive policies of regulatory bodies, funding, amongst others. These challenges can however be duly overcome if all parties involved catch the vision of the overwhelming benefits that are available to all parties and the society at large if engineering graduates from the Nigerian university system possess the practical engineering skills to make them thrive and be globally competitive in this 21st century. A good measure of grit and sustained motivation is needed by all parties involved if the engineering education in Nigeria is to be reformed to enable it produce engineering graduates of high calibre,

through a robust and rigorous implementation of the Outcome Based Education (OBE) curricula.

4.0 THE EDO STATE UNIVERSITY EXAMPLE

Edo State University Uzairue is one of the few universities in Nigeria that has adopted to a large extent several of the recommendations presented in this paper to ensure her engineering graduates are well equipped and prepared to excel in the modern world. The engineering programmes enjoy a full implementation of the outcome-based education (OBE) curricula with a strong emphasis on computer applications in engineering. There is a well-established entrepreneurship centre that offers courses to students on entrepreneurship. Edo State University is well equipped with multimedia teaching facilities in all the classrooms and 24/7 teaching and learning is supported by the institutional learning management system which made it possible for Edo State University to carry on with her academic calendar and successfully conclude the 2019/2020 academic session with students writing exams remotely. The laboratories are reasonably equipped, and the university maintains close links with industry and other Higher Education Institutions (HEIs) within and outside the country. There is a robust FME mechanism in place to ensure students satisfaction and quality assurance.

Notable and strategic frame work for engineers within Edo State university Uzairue include;

4.1 Entrepreneurship (Technical and Vocational Trainings)

- EDSU has expanded to accommodate an entire entrepreneurship department, disciplines, and courses which run through the curriculum from the first year to the final year with the first year entrepreneurship courses (Aluyor & Otoikhian, 2021). These courses provide general hands-on training in entrepreneurship and business and the higher-level courses between the third and fifth years provide robust and pragmatic training on entrepreneurship in engineering and technology. These courses can also be narrowed down to provide discipline-specific training on how the core technical knowledge from a given engineering discipline can be translated into entrepreneurial engagements.
- No business can survive on the strength of a single discipline (Aluyor & Otoikhian, 2021). A synergy amongst several disciplines in EDSU has been explored to facilitate the tackling of the multi-

faceted challenges in Nigeria and Africa at large and create businesses by so doing. It is therefore suggested that a good way to spur engineering graduates to begin to seriously consider and generate ideas for co-entrepreneurial exploits across multiple disciplines. This business plan pre-requisite course currently undertaken by every EDSU final year students in engineering concentrates on generating and funding ideas to tackle localized engineering problems like electricity generation through solar, agricultural (food waste and shortages), retail, waste water purification, etc. It is undertaken by an interdisciplinary team of students with each member of the team contributing her/his technical know-how to the business idea and the plan for its execution.

Institutions of higher learning could leverage existing or create mutually beneficial relationships with funding partners like banks, NGOs, governmental bodies, etc. These businesses when successful will yield a good return on investment (ROI) to the institutions of higher learning and other investors while curbing the unemployment menace and solving a real-life problem based on applied engineering and technology.

4.2 Computer Skills Integration

Edo State University Uzairue has been able to both purchase licenses and gain access to the following unique software amongst a numerous list of others in keeping with this technological paradigm to ensure IT competencies and broaden employment opportunities among its students. Some of this multi-disciplinary software is listed below with their employment opportunities.

SOFTWARE	PURPOSE	OPPORTUNITIES
Anaconda navigator	This is a desktop GUI used by the computer science and engineering department for launching and managing conda packages and the environment without the use of a CLI.	All levels of software developer roles. Data Engineer opportunities. Support engineering opportunities.
ANDROID STUDIO	This is Google's IDE for Android OS development. It is widely used by the computer science and engineering department.	Mobile application development. Remote and Physical Jobs. Wide entrepreneurship possibilities in starting small-scale remote businesses.
ASPEN Tech Software	A chemical process simulator that uses mathematics to quantitatively represent chemical processes ranging from individual activities to whole chemical plants and refineries for dynamic and steady-state simulations.	Remote or Physical Chemical Engineering Oil and Gas, processing opportunities. Sometimes, physical presence is essential. Entrepreneurship possibilities
DWSIM Software	An alternative but open-sourced chemical process simulator that quantitatively represent chemical processes ranging from individual activities to whole chemical plants and refineries for dynamic and steady-state simulations.	Remote or Physical Chemical Engineering Oil and Gas, processing opportunities. Sometimes, physical presence is essential. Entrepreneurship possibilities
Autodesk Autocad	AutoCAD is a computer-aided design (CAD) software for 2D and 3D design and drawing. Modern AutoCAD features involve a complete set of solid modelling and tools.	Civil Engineering, Structural Engineering, Mechanical Engineering, and Architecture. It can be learned as a vocational skill and possesses remote job potentials.
AUTOCAD Architecture	Is an architecture simulation software for representing objects in 2D and 3D.	Civil Engineering and Architecture. It can be learned as a vocational skill and has remote job potentials.
AUTOCAD	This software is AutoCAD based intended to help build	Electrical Engineering job

SOFTWARE	PURPOSE	OPPORTUNITIES
Electrical	electrical designs with the creation and modification of control systems. It has extended features to automate control engineering tasks, such as building circuits, numbering wires, and creating bills.	potentials. Can be remote or physical. Has a lecturing or training business opportunity
AUTODESK REVIT	Is a CAD software for building, information, and modelling (BIM) of architectural landscapes, civil and structural engineers, mechanical, electrical, and plumbing engineers, designers and contractors.	Civil Engineering, Structural Engineering, and Architecture. Can be learned as a vocational skill and has remote job potentials.
Bigblue Button, Zoom (Paid), Google meet	This is a video conferencing tool integrated with the Canvas LMS used in teleconferencing, online lectures, and training of staff.	Physical and Remote video conferencing opportunities. Easy platform for entrepreneurship scaling.
CANVAS	A Learning Management System (LMS) is used to teach, monitor, assess, grade, and analyze students and their performances.	LMS/Canvas Administrator Remote job opportunities. Canvas Admin/Instructional Designer.
CIRCUIT MAKER	This is a printed circuit board (PCB) software for making or simulating a circuit board, running and analyzing it before the actual fabrication.	Electrical knowledge and expertise for training and business development through advanced development. Opportunities to tweak (open source) and make improvements.
COREL DRAW	This is used by the University Administration and media to design our flyers, magazines, booklets, LOGO, etc.	Massive opportunities for remote and physical jobs across every sector in any Nation of the world.
DESIGN Expert	This is a mathematical modelling and simulation tool used by chemical engineers to design experiments, analyze the results and optimize the analysis.	Employment opportunities through training, project review, and proposal writing. Upwork, Fiverr, etc. potentials.
Intellij	It is an IDE used as a Java compiler by our computer science and engineering programs to maximize a developers' potentials. Other languages it can be used with include Node.js, Angular, React, Vue, Typescript, etc.	Massive opportunities in the ICT sector across the world. Remote jobs for front-end and back-end developers.
MATLAB	Software for machine and deep learning, communications and signal processing, control systems, image and video processing, model testing and measurement, computational finance, engineering design, and modelling, and computational biology.	All Engineering and some sciences job opportunities. Tech. sales engineer job roles based on skills.
MAPLE	Mathematical software that integrates the world's most powerful math engine with a user-friendly interface that easily explores, analyses, visualize and then solve mathematical problems. It is ideal because it allows for usability while solving mathematical problems in both education and research.	All Engineering and some sciences job opportunities. Tech. sales engineer job roles based on skills. Lecturing and training opportunities. Online opportunities on remote job sites. Tech. Sales

SOFTWARE	PURPOSE	OPPORTUNITIES
		opportunities.
MAPLESIM	A Modelica-based modelling and simulation tool used to generate equation models, run simulations, and analyze a system using both a symbolic and mathematical power of Maple.	All Engineering and some sciences job opportunities. Tech. sales engineer job roles based on skills. Lecturing and training opportunities. Online opportunities on remote job sites
MICROSOFT OFFICE Suite	This is the most common fundamental software used by our students for word editing, excel calculations, and graphing, programming, and slideshow presentations.	Basic for every activity to be carried out in today's world. Unending opportunities based on competencies.
Microsoft Visual Studio	This software is a development console supported by Microsoft Windows, Windows Mobile, Windows CE, .NET Framework, .NET Framework, and Silverlight. It is used to develop using Java programming language, Python, C++, etc.	Any level developer opportunities both remote and physical. Earn from your home.
Netbeans	This is a free and open-source integrated development environment (IDE) used on a Linux, Windows, or Solaris operating system for Java, C++, HTML, PHP, and other programming languages. It is used to develop web, enterprise, desktop, or mobile applications.	Opportunities for remote jobs in development roles. Open source means an opportunity to improve the software, increase personal worth, and grow a spread influence.
POSTGRES / MYSQL	This is a high-level database software for structured querying of data, programming before data analysis	Database Administrator in Fintechs, FMCGs, Financial sector, etc. Jobs could be remote or physical
PSPICE	This is a virtual circuit simulation and design tool used by our electrical engineers for evaluating analog circuits and mixed-signal circuits while maximizing performance.	Hardware and Software Electrical Engineering opportunities at all levels ranging from basic to advanced knowledge of circuit building. Remote opportunities are available.
Python 3	This is our most used programming language by engineers and scientists across all disciplines within the university. It is used for website and software development, task automation, data analysis, and data visualization.	All levels of software developer roles. Data Engineer opportunities. Support engineering opportunities. Unlimited opportunities across any sector around the world. From governmental to non-governmental.
STAR UML	This is a sophisticated software used to develop our students into Agile and Concise professional development	It Architect, Database design and development, Oracle developer, Solution Architect, etc.

5.0 CONCLUSION

A conceptual plan for teaching these relevant soft and hard skills has been reviewed, along with the competencies required of the engineer of the twenty-first

century. The guidelines for the management and implementation of these skills as referenced here may present a number of challenges, but these difficulties are not insurmountable. The suggestions reviewed and

reiterated in this article are attainable and currently being practised in Edo State University Uzairue. If this is put into effect in other institutions, it will ensure the required competencies and expertise of our engineering graduates from Nigeria's university system for workplaces now and in the future.

REFERENCES

- Adekola, P. O., Allen, A. A., Olawole-Isaac, A., Akanbi, M. A., & Adewunmi, O. (2016). Unemployment in Nigeria; A Challenge of Demographic Change? *International Journal of Scientific Research in Multidisciplinary Studies*, 2(5), 1–9.
- Akinsanya, O. A., & Omotayo, K. F. (2013). Falling Standard of Engineering Education in Nigeria- Causes and suggestions. 2(10), 4.
- Aluyor, E.O. (2020) 'IMPARTING PRACTICAL ENGINEERING SKILLS IN THE NIGERIAN UNIVERSITY SYSTEM', in Proceedings of the 2020 National Engineering Conference of the Nigeria Society of Engineers [NSE]. Conference of the Nigeria Society of Engineers [NSE], Abuja, Nigeria: Nigeria Society of Engineers [NSE], pp. 9–29.
- Aluyor, E. O., & Otoikhian, S. K. (2021). REDUCING UNEMPLOYMENT IN NIGERIA – THE ROLE OF TERTIARY INSTITUTIONS IN THE ENTREPRENEURIAL DEVELOPMENT OF ENGINEERING GRADUATES. *JOURNAL OF THE NIGERIAN SOCIETY OF CHEMICAL ENGINEERS*, 36(2), 55–60. <https://doi.org/10.51975/21360207.so>
- Aluyor, O. Emmanuel, and Shegun Kevin Otoikhian. 'Imparting Practical Engineering Skills in the Nigerian University System'. *International Journal of Multidisciplinary Research and Growth Evaluation* 03, no. 02 (12 April 2022): 570–74.
- Aluyor, E.O., Otoikhian, S.K. and Agbodekhe, B. (2019): "A Chemical Engineering Curriculum-Meeting the Nigerian Need" *Journal of the Nigerian Society of Chemical Engineers (JNSChE) NSChE Journal of Volume 34, No. 1*
- Bakhshi, H., Downing J.M., Osborne M.A., and Schneider P. (2017) *The future of skills: employment in 2030*. United Kingdom: Pearson.
- Chikumba, S. (2011) 'DEVELOPMENT OF SOFT ENGINEERING SKILLS FOR INDUSTRIAL ENGINEERING TECHNOLOGISTS THROUGH EFFECTIVE MENTORING', p. 17.
- Choudary, D.V. (2014) 'THE IMPORTANCE OF TRAINING ENGINEERING STUDENTS IN SOFT-SKILLS', p. 5.
- Cukierman, U.R. and Palmieri, J.M. (2014) 'Soft skills in engineering education: A practical experience in an undergraduate course', in 2014 International Conference on Interactive Collaborative Learning (ICL), Dubai, United Arab Emirates: IEEE, pp. 237–242. Available at: <https://doi.org/10.1109/ICL.2014.7017776>.
- Falade, F. (2008). CHALLENGES IN ENGINEERING EDUCATION IN AFRICA. 10.
- Fulgence, K. (2015) 'Employability of Higher Education Institutions graduates: Exploring the influence of Entrepreneurship Education and Employability Skills Development Program Activities in Tanzania', p. 281.
- Harmer, N. (2014) 'Project-based learning', p. 34.
- Kabouridis, G., Giannopoulos, G.I. and Tsirkas, S.A. (2014) 'Improving the skills and employability of mechanical engineering students via practical exercise', p. 8.
- Kalbande, Vijay N, Shitalkumar A Rawandale, Radheshyam H Gajghat, Arvind B Bodhe, and Chandrahans C. Handa. 'Novel Outlook to Analyzing a Gap between Industrial and Institutional Skills at Students in the Faculty of Engineering and Natural Sciences'. *International Journal of Health Sciences*, 14 May 2022, 8940–48. <https://doi.org/10.53730/ijhs.v6nS2.7329>.
- Kardipah, S., and Basuki W. (2020) 'A Flipped-Blended Learning Model with Augmented Problem Based Learning to Enhance Students' Computer Skills'. *TechTrends* 64, no. 3: 507–13. <https://doi.org/10.1007/s11528-020-00506-3>.
- Lowden, K. et al. (2011) *Employers' perceptions of the employability skills of new graduates: research commissioned by the Edge Foundation*. London: Edge Foundation.
- National academy of Science (2012) *Education for Life and Work: Developing Transferable Knowledge and Skills in the 21st Century*. Washington, D.C.: National Academies Press, p. 13398. Available at: <https://doi.org/10.17226/13398>.
- Oloyede, A.A., Ajimotokan, H.A. and Faruk, N. (2018) 'Embracing the future of engineering education in Nigeria: teaching and learning challenges',

- Nigerian Journal of Technology, 36(4), p. 991. Available at: <https://doi.org/10.4314/njt.v36i4.1>.
- Onyeiwu, S. (2021). Seeking jobs abroad isn't an option for young Nigerians: They don't have the right skills. *The Conversation*. <https://theconversation.com/seeking-jobs-abroad-isnt-an-option-for-young-nigerians-they-dont-have-the-right-skills-165978>
- Pitan, O. and Adedeji, S.O. (2012) 'Skills Mismatch Among University Graduates in the Nigeria Labor Market', *US-China Education Review*, 1, pp. 90–98.
- Ruth, H., Emmanuel, A. Y., & Ndubuisi-Okolo, P. (2014). UNDERSTANDING AND OVERCOMING THE CHALLENGE OF YOUTH UNEMPLOYMENT IN NIGERIA. 3(5), 9.
- Soliman M. et al. (2021) 'The Application of Virtual Reality in Engineering Education'. *Applied Sciences* 11, no. 6: 2879. <https://doi.org/10.3390/app11062879>.
- Syam, H. et al (2021) 'The Employability Skills of Engineering Students': Assessment at the University'. *International Journal of Instruction* 14, no. 4: 119–34. <https://doi.org/10.29333/iji.2021.1448a>.

SYNTHESIS, CHARACTERIZATION AND EQUILIBRIUM STUDY OF NITRIC ACID MODIFIED ACTIVATED CARBON ADSORBENT FROM BAMBOO CULMS

Francis, A. O.^{1}; Ochi, D.²; Osaghae, S.³

¹Department of Chemical Engineering, Edo State University, Uzairue, Nigeria

²Department of Chemical Engineering Technology, Auchi Polytechnic, Auchi, Nigeria

³Department of Mineral and Petroleum Resources Engineering Technology, Auchi Polytechnic, Auchi, Nigeria

*Email: francis.asokogene@edouniversity.edu.ng

ABSTRACT

This study evaluated the synthesis of low cost activated carbon adsorbent from waste bamboo culms collected at a construction site around Auchi Polytechnic, modified with environmentally friendly nitric acid for enhanced pore structures and improved adsorption versatility. The material was characterized by Fourier transform infrared (FTIR), Brunauer-Emmett-Teller (BET), energy dispersive X-ray (EDAX) and nickel adsorption. The FTIR result showed the characteristics O–H stretching of free hydroxyl and strong hydrogen bond group on the activated carbon surface. The BET surface area of the activated carbon displayed high specific surface area of $1.087 \times 10^3 \text{ m}^2/\text{g}$ and 71.41% mesoporosity, despite the lower activation temperature of 600 °C. The maximum adsorption capacity of the activated carbon for nickel was 20.69 mmol/g. Freundlich isotherm model best explained the adsorption behavior, suggesting heterogeneous surface adsorption due to textural properties of the activated carbon or ionic interaction between nickel molecule and the functional groups. Nitric acid modified activated carbon is a promising adsorbent candidate for heavy metal removal.

Keywords: Bamboo culms, nitric acid, adsorbent, modified, characteristics.

1. INTRODUCTION

Research has shown the development in the use of porous adsorbents from waste materials as promising method for the treatment of contaminated effluent. Adsorption of contaminants in gases and water is essential from the purification, hazardous and environmental waste disposal point of view (Tran et al. 2018; Gundogdu et al. 2012; Singh et al. 2019). Hence, agricultural waste are used for the synthesis of porous adsorbents such as activated carbon for the removal of hazardous components in exhaust gases, purification of drinking water and wastewater treatment. Demand for activated carbon is on the increase due to its wide range of use and environmental friendliness (Ani et al. 2020). Studies have shown that activated carbon are produced from various biomass such as date seed (Ogungbenro et al. 2020), peanut shells (Guo et al. 2020), corn cob (Feng et al. 2020), acai seed (Queiroz et al. 2020), phanera vahlii fruit (Ajmani et al. 2020), bamboo (Mahanim et al. 2011; Negara et al. 2020), palm-tree cob, plum kernel, cassava peel, bagasse, jute fibre, rice husk, olive stone, date pit, fruit stones and nutshell (Rex et al. 2020; Reza et al. 2020).

Bamboo which mainly comprises of cellulose, lignin and hemicellulose (Ma et al. 2014) has wide domestic and industrial application in the pharmaceutical industry, making of handicrafts and furniture, building, decorating, paper making and as firewood in most

developing world, but very little attention has been received on its application as good adsorbent (Nirmala et al. 2018; Pande and Pandey, 2008; Khalil et al. 2012; Gupta and Kumar, 2008). Bamboo occurs as a natural resource in Nigeria and it is basically used for construction purposes because of its strength, toughness and low cost (Mahanim et al. 2011). However, bamboo can be converted into activated carbon suitable for wastewater treatment through the process of pretreatment, carbonization and activation (Mahanim et al. 2011). Pretreatment enables the removal of adherent materials from the bamboo and drying, carbonization enriches the carbon content and creates initial porosity of the activated carbon adsorbent, and activation enhances the pore structures of the activated carbon adsorbent.

In this present work, nitric acid modified activated carbon adsorbent was synthesized from bamboo culms which were gathered from a construction site around Auchi Polytechnic campus, to enhance its pore structures and improve its versatility for adsorption (Deliyanni et al. 2015). The availability at little cost of these bamboos which are primary precursor for the synthesis of the activated carbon adsorbent in this study was also good alternative to patent adsorbents. The physicochemical properties of the nitric acid modified activated carbon were analyzed using BET, EDAX and FTIR, and batch adsorption of nickel ion at working

concentration of 0.196 mol/L at varying adsorbent dosage was conducted in order to broaden the existing knowledge on activated carbon utilization as adsorbent in wastewater.

2. MATERIALS AND METHODS

2.1 Chemical, reagents and instruments

Bamboo culms were collected from a construction site around Auchi Polytechnic campus. All chemicals used were of analytical grade: nitric acid (65%, Sigma-Aldrich, USA), nickel (II) nitrate hexahydrate, $\text{Ni}(\text{NO}_3)_2 \cdot 6\text{H}_2\text{O}$ (98%, Shanghai Jinshan chemical Co., China), analytical balance (Scout Pro, Ohaus, London), pH meter/thermometer (HI 9813-5portable pH/EC/TDS/ $^{\circ}\text{C}$ meter, Hanna instruments, Inc., USA), grinding mill (Biocotek, China), shaker (Ro-tap, England), magnetic stirrer with hot plate (Gallenhamp, England), stop watch (Quartz, China), Fourier transform infrared (FTIR) spectrometer (Thermo Scientific, Nicolet ISI 10, USA), energy dispersive X-ray (EDAX) (BRUKER corporation, Germany), atomic absorption spectrophotometer (AAS) (Solar 969 unicam series) and Brunauer-Emmett-Teller (BET) surfer machine (Thermo scientific, USA).

2.2 Preparation of bamboo culms nitric acid activated carbon

Nitric acid modified activated carbon was synthesized from bamboo culms, screened to 0.150 mm size and labelled as NBAC. The procedure involved pretreating the bamboo culms by cutting it into 2 cm long with a saw, washing the cut culms with distilled water to remove adherent materials and drying in an oven (Gallenhamp, England) at 110 $^{\circ}\text{C}$ for 150 min. 2 kg of the dried bamboo culms was feed into a METM-25 muffle furnace for 3 h for carbonization to take place. The carbonized culm was comminuted and sieved to 0.150 mm size. 100 g of the sieved culm was put into a beaker containing 2% HNO_3 (v/v) and stirred until a paste-like mixture was formed. The paste-like mixture was de-moisturized in an oven at 110 $^{\circ}\text{C}$ for 6 h and then transferred into a muffle furnace for 1 h at 600 $^{\circ}\text{C}$ to form activated carbon. The activated carbon was kept to cool and washed with distilled water until pH of 7 was obtained, dried in an oven for 8 h at 110 $^{\circ}\text{C}$, kept in a desiccator and labeled nitric acid modified bamboo culms activated carbon (NBAC) (Ademiluyi and Rodney, 2016; Ademiluyi et al. 2009; Shim et al. 2001).

2.3 Physicochemical characterization of nitric acid activated carbon

The surface functional groups of nitric acid modified activated carbon was characterized using a Nicolet ISI 10 FTIR spectrometer (Thermo scientific, USA). 50 mg

of the adsorbent and 120 mg of KBr were mixed and triturated using pestle and mortar, and the mixture was compacted with a hydraulic press at a pressure of 8 tons to form a disk. The disk was dried in an oven at 80 $^{\circ}\text{C}$ for 16 h before analysis. The FTIR spectrum was obtained at a frequency range of 4000 to 400 cm^{-1} .

The textural properties of nitric acid modified bamboo culm activated carbon was characterized using a Micromeritics ASAP2010 analyzer (Thermo Scientific, USA) based on Brunauer-Emmett-Teller (BET) method. The sample was outgassed at 250 ± 1 $^{\circ}\text{C}$ in a vacuum overnight to remove moisture and volatiles components which could compromise the isotherms before exposure to nitrogen at a temperature of 77 K at different incremental pressure.

The elemental composition of nitric acid modified bamboo culm activated carbon was characterized using energy dispersive X-ray (EDAX), Bruker handheld analyzer. The beam that was emitted from the front end of the analyzer interacted with the atoms in the sample and displaced the electrons from the inner orbital shells due to difference in energy between the primary X-ray and the binding energy that holds the electrons in orbits. This difference in energy (energy loss) was used to identify the elements in the sample because the amount of energy lost in the fluorescence process is unique to each element (Ghannam et al. 2016).

The adsorption potential of nitric acid modified bamboo culm activate carbon for nickel removal was evaluated in batch mode experiment at a pH of 8.0 and temperature of 55 $^{\circ}\text{C}$. A 50 mL of different concentrations of nickel solution was prepared and brought into contact with 0.5 g of nitric acid modified bamboo culm activated carbon. The flasks were sealed and shaken for 72 h at ambient temperature (Hui and Zaini 2015). After that, the solution was withdrawn and the residual concentration was determined using atomic absorption spectrophotometer (AAS) (Solar 969 unicam series). The adsorption capacity, q_e (mmol/g) was calculated from the mass balance equation as (Francis et al. 2020),

$$q_e (\text{mmol/g}) = \left(\frac{C_o - C_e}{m} \right) \times V \quad (1)$$

where, C_o and C_e (mmol/L) are the initial and equilibrium concentration, respectively, V (L) is the volume of solution and m (g) is the mass of adsorbent.

3. RESULTS AND DISCUSSION

The FTIR spectrum of nitric acid modified activated carbon from bamboo culm is presented in Figure 1. The

Synthesis, Characterization And Equilibrium Study Of Nitric Acid Modified Activated Carbon Adsorbent From Bamboo Culms

broad peak in the region of 3824–3318 cm^{-1} shows an O–H stretching of free hydroxyl and strong hydrogen bond group on the activated carbon surface. Similar result was presented by Kibami et al. 2017. The region of 2322–2102 cm^{-1} shows C=N stretching of nitriles

group. The C=O stretching in the region of 1982–1875 reflects the presence of carbonyl and carboxylic acid groups. The peak at 1558 and 1010 are C–C and C–N stretching vibration of aliphatic amine group.

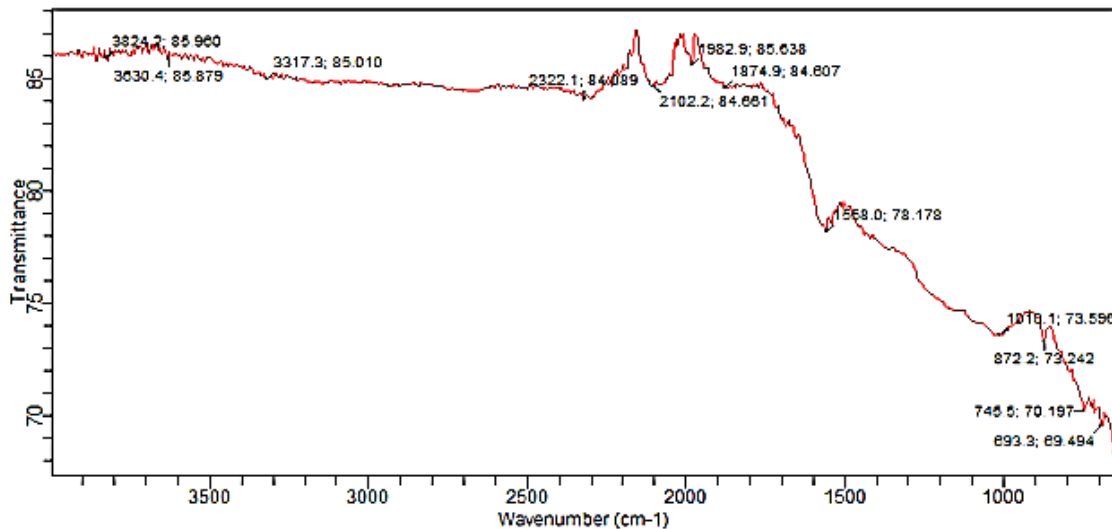


Figure 1: FTIR spectrum of nitric acid modified activated carbon from bamboo culm.

The textural property of nitric acid modified activated carbon from bamboo culm is presented in Table 1.

Table 1: Specific surface area and pore properties of NBAC

Material	Specific surface area (m^2/g)		Micropore area (A_i , m^2/g)	Pore volume (cm^3/g)		Average pore diameter (nm)	Meso-porosity (%)
	BET method (Ab)	Langmuir method		Total (v_t)	Micro (v_i)		
NBAC	1.087×10^3	1.037×10^4	1.087×10^3	5.593×10^{-1}	1.599×10^{-1}	1.847	71.41

The modified activated carbon demonstrated high specific surface area and pore volume at lower activation temperature of 600 $^\circ\text{C}$ when compared to non-modified activated carbon from bamboo as reported by Ma et al. 2014 and Lo et al. 2012 at the same temperature and higher temperature, respectively. This suggests that with nitric acid modification, lower activation temperature is required for higher specific surface area and pore volume. The mesoporosity of 71.41% recorded for the adsorbent suggests that mesoporous materials will allow ions and

macromolecular penetration easier into their pores (Budascaerechai et al. 2012). Activated carbon modification improves its specific surface area, pore volume and widens its industrial application (Deliyanni et al. 2015; Lalhruaittuanga et al. 2010).

The EDAX result of the nitric acid modified activated carbon is presented in Figure 2. The result revealed that the predominant mineral composition of the material are calcium (Ca) and silicon (Si) (Nongdam and Leimapokpam, 2014).

Analyte Concentration Table

Element	Concentration
Na2O	0.000 Wt %
MgO	4.722 Wt %
Al2O3	4.882 Wt %
SiO2	28.276 Wt %
P2O5	3.855 Wt %
SO3	3.881 Wt %
Cl	0.981 Wt %
K2O	6.294 Wt %
CaO	41.580 Wt %
TiO2	1.162 Wt %
Cr2O3	0.008 Wt %
Mn2O3	0.769 Wt %
Fe2O3	3.381 Wt %
ZnO	0.000 Wt %
SrO	0.207 Wt %

Spectra for all conditions

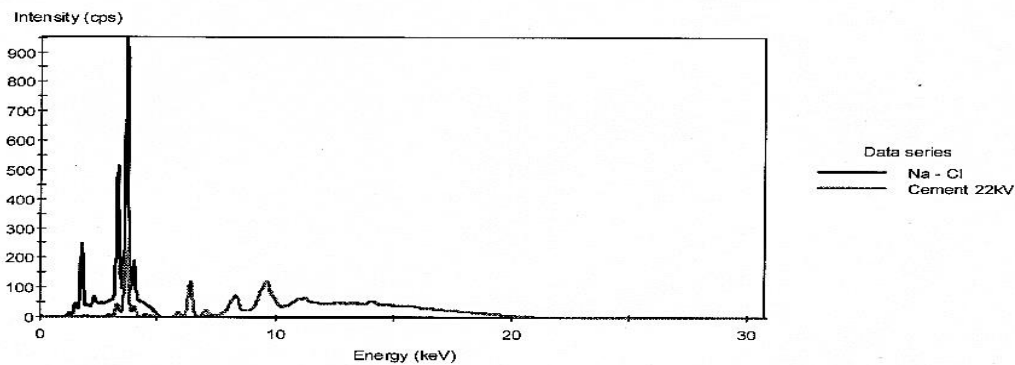


Figure 2: EDAX result of nitric acid modified activated carbon from bamboo culm.

Nickel Adsorption

The adsorption of nickel onto nitric acid modified activated carbon from bamboo culm at different initial concentration is presented in Figure 3. The adsorption capacity increased from 2.1 mmol/g at initial concentration of 0.081 mmol/L to 5.15 mmol/g at initial concentration of 0.093 mmol/L and 11.5 mmol/g at initial concentration of 0.112 mmol/L. This can be attributed to active adsorption sites of adsorbent which were easily occupied and saturated by adsorbate molecules at low initial concentrations, resulting in low adsorption capacity; meanwhile, at high initial concentrations, a higher fractional adsorbent-adsorbate adsorption ratio occurred which resulted in increased nickel uptake (Luo et al. 2019; Zhao et al. 2022; Bhumica et al. 2013).

Nonlinear Langmuir and Freundlich isotherm models were used for the validation of the adsorption experimental data for nickel uptake. Equations (2) and (3), respectively, define these models.

$$q_e = \frac{Q_m K_L C_e}{1 + K_L C_e} \quad (2)$$

$$q_e = K_F C_e^{\frac{1}{n}} \quad (3)$$

where q_e (mmol/g) is the amount of nickel removed by the adsorbent, C_e (mmol/L) is the equilibrium nickel concentration in solution, K_L (L/mmol) is the Langmuir equilibrium constant, Q_m (mmol/g) is the maximal monolayer adsorption capacity. The Freundlich adsorption constant of adsorption capacity and the frequency of surface heterogeneity are defined as K_F (mmol/g)(L/mmol)^{1/n} and $1/n$, respectively (Fosso-Kankeu et al. 2014; Zhao et al. 2022).

Table 2 shows the regression coefficient (R^2) and isotherm parameters obtained from the nonlinear regression approach. Both the Langmuir and Freundlich models fit the experimental data well from their regression coefficient values of 0.995 and 0.994, respectively. However, the Freundlich model fits better due to its closeness to the experimental data as reflected in its least error function (SSE) value of 0.28. As a result, the Freundlich model best matched this adsorption behavior at equilibrium, implying a heterogeneous nickel uptake onto NBAC involving mesopore filling and ionic interaction (Mistar et al. 2020; Luo et al. 2019). Nickel maximum adsorption capacity, Q_m was of 20.69 mmol/g.

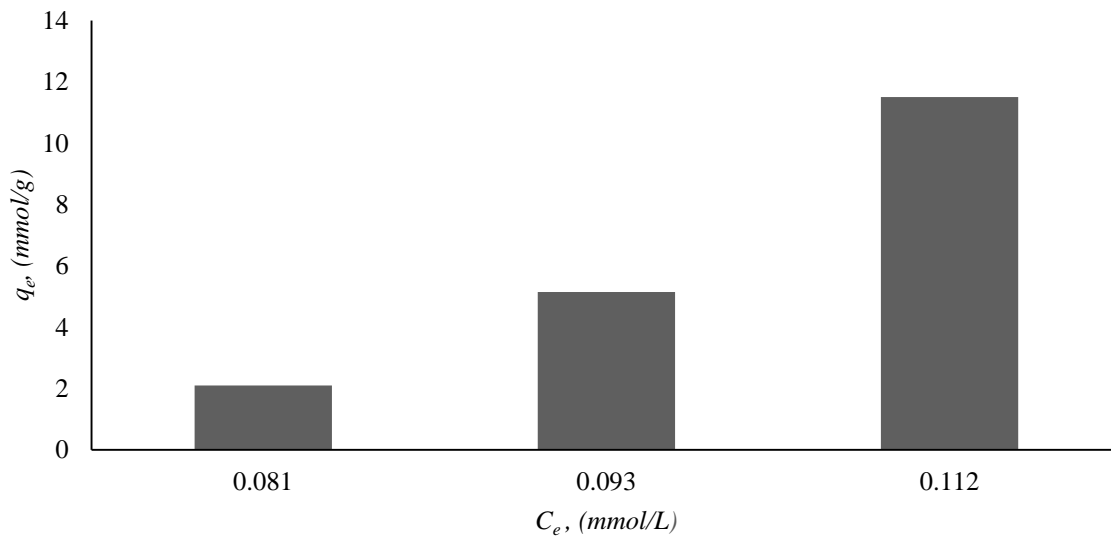


Figure 3: Nickel uptake by NBAC.

Table 2: Isotherm constants of Ni adsorption onto NBAC

Material	Langmuir model				Freundlich model			
	Q_{max} (mmol/g)	K_L (L/mol)	R^2	SSE	K_F	1/n	R^2	SSE
NBAC	20.69	0.034	0.995	28.04	36.73	4.74	0.994	0.28

4. CONCLUSIONS

Nitric acid modified activated carbon was synthesized from bamboo culm collected from a construction site around Auchu Polytechnic campus. The activated carbon was characterized for physicochemical properties and nickel adsorption at various initial concentrations, pH of 8 and temperature of 30 °C. The presence of O–H stretching of free hydroxyl and strong hydrogen bond group on the activated carbon surface suggests its promising adsorption interaction with positive charged water pollutant like metal ions and cationic dyes. The textural properties revealed increased specific surface area and pore volume due to modification at lower activation energy. Consequently, the adsorption of nickel can be attributed to the availability of larger number of adsorption sites or surface due to its high specific surface area, pore volume and mesoporosity of the nitric acid modified activated carbon. Freundlich isotherm model best described the adsorption behavior.

5. ACKNOWLEDGEMENTS

We wish to acknowledge the scientific and financial support made by Ugo Lilian, Osadolor Gideon, Ozugwor Amos and Chukwuma Kingsley. We also acknowledge the role of Prof. R. O. Onyeonwu of Martlet Environmental Research Laboratory.

REFERENCES

- Ademiluyi, F. T., Amadi, S. A., and Amakama, N. J., (2009). Adsorption and Treatment of Organic Contaminants using Activated Carbon from Waste Nigerian Bamboo. *Journal of Applied Sciences and Environmental Management*, 13(3).
- Ademiluyi, F. T., and Rodney, N., (2016). Effect of Process Parameters on the Single Adsorption of Zinc and Nickel Ions Using Activated Carbon from Waste Nigerian Bamboo. *International Journal of Engineering and Applied Sciences*, 3(1), 257734.
- Ajmani, A., Patra, C., Subbiah, S., and Narayanasamy, S., (2020). Packed bed column studies of hexavalent chromium adsorption by zinc chloride activated carbon synthesized from *Phanera vahlii* fruit biomass. *Journal of Environmental Chemical Engineering*, 8(4), 103825.
- Ani, J. U., Akpomie, K. G., Okoro, U. C., Aneke, L. E., Onukwuli, O. D., and Ujam, O. T., (2020). Potentials of activated carbon produced from biomass materials for sequestration of dyes,

- heavy metals, and crude oil components from aqueous environment. *Applied Water Science*, 10(2), 1-11.
- Bhumica, A., Priya S., and Chandraji, B., (2013). Equilibrium, kinetic and thermodynamic studies of simultaneous co-adsorptive removal of phenol and cyanide. *International Journal of Chemical, Molecular, Nuclear, Materials and Metallurgical Engineering* 7. 11.
- Budsareechai, S., Kamwialisak, K., and Ngernyen. Y., (2012). Adsorption of lead, cadmium and copper on natural and acid activated bentonite clay. *KKU Research Journal* 17. (5), 800-810.
- Deliyanni, E. A., Kyzas, G. Z., Triantafyllidis, K. S., and Matis, K. A., (2015). Activated carbons for the removal of heavy metal ions: A systematic review of recent literature focused on lead and arsenic ions. *Open Chemistry*, 13(1).
- Feng, P., Li, J., Wang, H., and Xu, Z., (2020). Biomass-based activated carbon and activators: preparation of activated carbon from corncob by chemical activation with biomass pyrolysis liquids. *ACS omega*, 5(37), 24064-24072.
- Fosso-Kankeu, E., Reitz, M. and Waanders, F. 2014. Selective adsorption of heavy and light metals by natural zeolites. *6th International Conference on Green Technology, Renewable Energy and Environmental Engineering, Cape Town (SA)*, 167-70.
- Francis, A. O., Muhammad, A. A. Z., Zainul, A. Z., Misau, M. I., Surajudeen, A., and Aliyu, E. U., (2020). Equilibrium and kinetics of phenol adsorption by crab shell chitosan. *Particulate Science and Technology*. pp 1-13. DOI:10.1080/02726351.2020.1745975
- Ghannam, H. E., S Talab, A., Dolgano, N. V., Husse, A., and Abdelmagui, N. M., (2016). Characterization of chitosan extracted from different crustacean shell wastes. *Journal of Applied Sciences*, 16(10), 454-461.
- Gundogdu, A., Duran, C., Senturk, H. B., Soylak, M., Ozdes, D., Serencam, H., and Imamoglu, M., (2012). Adsorption of phenol from aqueous solution on a low-cost activated carbon produced from tea industry waste: equilibrium, kinetic, and thermodynamic study. *Journal of Chemical & Engineering Data*, 57(10), 2733-2743.
- Guo, R., Yan, L., Rao, P., Wang, R., and Guo, X., (2020). Nitrogen and sulfur co-doped biochar derived from peanut shell with enhanced adsorption capacity for diethyl phthalate. *Environmental Pollution*, 258, 113674.
- Gupta, A., and Kumar, A., (2008). Potential of bamboo in sustainable development. *Asia Pacific Business Review*, 4(3), 100-107.
- Hui, T. S., and Zaini. M. A. A., (2015). Isotherm studies of methylene blue adsorption onto potassium salts-modified textile sludge. *Jurnal Teknologi (Science and Engineering)* 74. (7), 57-63.
- Khalil, H. A., Bhat, I. U. H., Jawaid, M., Zaidon, A., Hermawan, D., and Hadi, Y. S., (2012). Bamboo fibre reinforced biocomposites: A review. *Materials & Design*, 42, 353-368.
- Kibami, D., Pongener, C., Rao, K. S., and Sinha, D., (2017). Surface Characterization and Adsorption studies of *Bambusa vulgaris*-a low cost adsorbent. *Journal of Materials*, 8(7), 2494-2505.
- Lalhruaitluanga, H., Jayaram, K., Prasad, M. N. V., and Kumar, K. K., (2010). Lead (II) adsorption from aqueous solutions by raw and activated charcoals of *Melocanna baccifera* Roxburgh (bamboo)—a comparative study. *Journal of hazardous materials*, 175(1-3), 311-318.
- Lo, S. F., Wang, S. Y., Tsai, M. J., and Lin, L. D., (2012). Adsorption capacity and removal efficiency of heavy metal ions by Moso and Ma bamboo activated carbons. *Chemical Engineering Research and Design*, 90(9), 1397-1406.
- Luo, L., Wu, X., Li, Z., Zhou, Y., Chen, T., Fan, M. and Zhao, W. 2019. Synthesis of activated carbon from biowaste of fir bark for methylene blue removal. *Royal Society Open Science* 6(190523), 1-14
- Ma, X., Yang, H., Yu, L., Chen, Y., and Li, Y., (2014). Preparation, surface and pore structure of high surface area activated carbon fibers from bamboo by steam activation. *Materials*, 7(6), 4431-4441.
- Mahanim, S. M. A., Asma, I. W., Rafidah, J., Puad, E., and Shaharuddin, H., (2011). Production of activated carbon from industrial bamboo wastes. *Journal of Tropical Forest Science*, 417-424.
- Mistar, E. M., Alfatah, T. and Supardan, M. D. 2020. Synthesis and characterization of activated carbon from *Bambusa vulgaris striata* using two-step KOH activation. *Journal of Materials Research and Technology*, 9 (3), 6278-6286.
- Negara, D. N. K. P., Nindhia, T. G. T., Surata, I. W., Hidajat, F., and Sucipta, M., (2020). Textural characteristics of activated carbons derived from tabah bamboo manufactured by using H₃PO₄ chemical activation. *Materials Today: Proceedings*, 22, 148-155.
- Nirmala, C., Bisht, M. S., Bajwa, H. K., and Santosh, O., (2018). Bamboo: A rich source of natural antioxidants and its applications in the food and

Synthesis, Characterization And Equilibrium Study Of Nitric Acid Modified Activated Carbon Adsorbent From Bamboo Culms

- pharmaceutical industry. *Trends in Food Science & Technology*, 77, 91-99.
- Nongdam, P., and Leimapokpam, T., (2014). The Nutritional Facts of Bamboo Shoots and their Usage as Important Traditional Foods of Northeast India, *Int Sch Res Notices*. DOI, 10(2014), 679073.
- Ogungbenro, A. E., Quang, D. V., Al-Ali, K. A., Vega, L. F., and Abu-Zahra, M. R., (2020). Synthesis and characterization of activated carbon from biomass date seeds for carbon dioxide adsorption. *Journal of Environmental Chemical Engineering*, 8(5), 104257.
- Pande, S. K., and Pandey, S., (2008). Bamboo for the 21st century. *International Forestry Review*, 10(2), 134-146.
- Queiroz, L. S., de Souza, L. K., Thomaz, K. T. C., Lima, E. T. L., da Rocha Filho, G. N., do Nascimento, L. A. S., ... and da Costa, C. E., (2020). Activated carbon obtained from amazonian biomass tailings (acai seed): Modification, characterization, and use for removal of metal ions from water. *Journal of Environmental Management*, 270, 110868.
- Rex, P., Masilamani, I. P., and Miranda, L. R., (2020). Microwave pyrolysis of polystyrene and polypropylene mixtures using different activated carbon from biomass. *Journal of the Energy Institute*, 93(5), 1819-1832.
- Reza, M. S., Yun, C. S., Afroze, S., Radenahmad, N., Bakar, M. S. A., Saidur, R., ... and Azad, A. K., (2020). Preparation of activated carbon from biomass and its' applications in water and gas purification, a review. *Arab Journal of Basic and Applied Sciences*, 27(1), 208-238.
- Shim, J. W., Park, S. J., and Ryu, S. K., (2001). Effect of modification with HNO₃ and NaOH on metal adsorption by pitch-based activated carbon fibers. *Carbon*, 39(11), 1635-1642.
- Singh, S., Kumar, V., Romero, R., Sharma, K., and Singh, J., (2019). Applications of nanoparticles in wastewater treatment. In *Nanobiotechnology in bioformulations* (pp. 395-418). Springer, Cham.
- Tran, H. N., You, S. J., Hosseini-Bandegharai, A., and Chao, H. P., (2017). Mistakes and inconsistencies regarding adsorption of contaminants from aqueous solutions: a critical review. *Water research*, 120, 88-116.
- Zhao, H., Zhong, H., Jiang, Y., Li, H., Tang, P., Li, D. and Feng, Y. 2022. Porous ZnCl₂-activated carbon from Shaddock peel: methylene blue adsorption behavior. *Materials*, 15(895), 1-16 <https://doi.org/10.3390/ma15030895>

A REVIEW ON SYNTHESIS OF HIERARCHICAL ZEOLITES Y

Usman, R. A.^{1,2}, Kovo, A. S.², Abdulkareem, A. S.^{2,3}, Garba, M. U.²¹Department of Physical Planning and Development, Federal University Lokoja. PMB 1154 Lokoja, Kogi State, Nigeria²Department of Chemical Engineering, Federal University of Technology, PMB. 65, Minna, Niger State, Nigeria³Nanotechnology Research Group, Africa Center of Excellence for Mycotoxin and Food Safety, Federal University of Technology, PMB 65, Minna, Niger State, Nigeria*Corresponding author's E-mail: rukiausman3@gmail.com

ABSTRACT

Zeolites has emerged as a main heterogeneous catalyst in most chemical industries. Its diffusion limitation causes ineffective utilization of the catalyst, leading to early coking and subsequent deactivation of the zeolites. Hierarchical zeolites Y have been identified as suitable advanced material that addresses the limitations encountered with microporous zeolites in the catalytic reaction. It has an enlarged pore improved surface area and reduced channel that speed-up the reaction. The review paper focuses on two main methods of synthesizing hierarchical zeolites Y and their shortcomings. The synthesis strategies of hierarchical zeolite Y are through post-synthesis treatment (top-down) and direct synthesis with the aid of morphology modifying agents (bottom-up). However, these synthesis routes are characterized by high energy consumption and the use of expensive chemicals which are not environmentally friendly. In this review, several synthesis routes were studied and examined. The additive-free synthesis route, which involves adjustment of crystallization parameters and additional aging steps, was economically and ecologically friendly. Hierarchical zeolites Y have been extensively used in industrial applications due to their enhanced intra-crystalline diffusion and improved catalytic properties.

Keywords: Zeolite Y, Hierarchical zeolite, Top-down, Bottom-up

1. INTRODUCTION

Zeolite Y is crystalline aluminosilicates tetrahedral TO₄ structure with a FAU type framework topology. The general formula of zeolite is Mⁿ⁺, [Si_x Al_y O_z]. mH₂O, where Mⁿ⁺ is a cation, [Si_x Al_y O_z] is the main zeolite framework, and mH₂O is a water molecule in the sorbed phase. Zeolites Y framework combine a 3-dimensional network of micropores (0.74 nm). FAU-type zeolites belong to the group of large-pore zeolites. The framework composition (Si/Al ratio) can be tuned from 1 to infinite by altering the hydrothermal synthesis or post-synthetic modifications (Dorien *et al.*, 2020). It is the most widely applied zeolites in adsorption and catalysis. Zeolite Y comprises a Si/Al = 2.5 and of appreciable total acidity. Zeolite Y has beneficial properties, like a large pore diameter of 1.124nm, a three-dimensional micropore system, and high aluminum content and thus an increased number of acid sites, to use as a catalyst in different cracking processes (Bastian *et al.*, 2020). However, the catalysts showed rapid deactivation due to their insufficient thermal stability. To increase the thermal stability of zeolite Y, a

post-synthetic treatments of zeolite Y was adopted. These involve utilizing steam and/or acid treatments while maintaining crystallinity. The resulting zeolites, with a framework Si/Al ratio of 6 and higher are called 'ultrastable' due to their improved catalytic and hydrothermal stability. Zeolite Y does extremely well as catalyst in numerous petrochemical applications, such as (hydro)cracking and (shape) selectivity (Dorien *et al.*, 2020),

The zeolite micropores are responsible for superior properties to amorphous aluminosilicates. It also causes diffusion limitations inside the zeolite crystals. The crystal restricts a wide variety of bulky molecules, which can only react on the external surface, thereby causing a drop in diffusion from inter-crystalline. The shape selectivity of the zeolites Y is also affected. The class of hierarchically structured zeolites was discovered to perform optimally in the above reaction. This hierarchically structured zeolite Y has an auxiliary level of mesopores or macro-porosity to the micropores, enhancing mass transport and diffusion within the crystals while maintaining the intrinsic zeolitic

properties. The diffusion path length within the zeolitic micropore channels is also reduced.

Synthesis of hierarchical zeolites is a way of adding a mesopores to micropores zeolites in which the improvement in the surface characteristics and porous structure of the parent zeolite are enhanced to give the benefits of both easy mass transfer through the mesoporous channels and the shape selectivity of the microporous framework. Various processes are used to create additional pore system in zeolites. They are top-down (such as desilication or dealumination) or bottom-up in which hard/soft templates are used to create pores in zeolites (Dabbawala *et al.*, 2020).

The introduction of microporous crystalline structures in mesoporous materials and mesoporous or macroporous structures in zeolite crystals are among the accomplishments of synthesizing hierarchical zeolite. Many reviews have summarized various methods of the hierarchical zeolites Synthesis. This paper focuses on the different synthesis methods of hierarchical zeolites.

2. HIERARCHICAL ZEOLITES

"Hierarchical structured zeolites" are zeolites with at least two layers of pore sizes, or 2 nm (meso-/macropores). Hierarchical zeolites also exhibit mesoporosity or macroporosity in addition to their inherent microporosity. However, the secondary porosity is typically in the mesoporous range. Inter-crystalline mesopores are generally introduced into regions where nanosized zeolite crystals are intergrown to generate intracrystalline mesopores inside the microporous zeolite structure. The synthesis methods play a significant role in different levels of hierarchical porosity. Comparing hierarchical zeolites to conventional microporous zeolites, the former exhibit better catalytic activity. Large molecules are primarily responsible for this enhancement, as the secondary porosity enables them to permeate into active areas inside channels without obstruction (Jia *et al.*, 2019).

In a wide range of catalytic reactions (Jahandideh *et al.*, 2021), rearrangement, and Fischer Tropsch, hierarchically porous zeolites that combine the intrinsic micropores with an auxiliary meso- and/or

macropore network of inter- or intracrystalline structure exhibit an unhindered transport path (macropores) and improved micropore accessibility (mesopores) (Chen *et al.*, 2020). Hierarchical zeolites have been extensively studied due to their enhancement of intra-crystalline diffusion, which leads to improved catalytic activity, resistance to coking, and deactivation. The enhanced intra-crystalline diffusion of molecules broadens their applicability and performance for technical processes involving bulky molecules. An additional pore system and thus a hierarchical pore structure can be created using different preparation routes.

1.0 Methods of evaluating Hierarchical Zeolites.

The essence of synthesizing hierarchical zeolites is to improve access to the active sites located in the zeolite micropores and to reduce diffusion limitations. There are ways of relating the performance of these zeolites to the observed changes in textural properties. Some of the methods used in investigating textural properties are Scanning Electron Microscopy (SEM), Transmission Electron Microscopy (TEM), N₂ physisorption and Hierarchy Factor. SEM is used in investigating the topology of porous zeolites, presence of macro- and mesopores and to a small degree, in evaluating the pore shape and size (Figure: 1B). TEM is also an established technique that provide a lot of information about mesoporosity in hierarchical zeolites. It explains the internal structures of a hierarchical zeolites. It also provides better imaging resolution and insight into the internal structure when compared to other characterization techniques as shown in figure I (A). Nitrogen adsorption is another analytical tool used to determine the surface area and pore size distribution of zeolite and other porous materials. The applicability of these materials is determined by the accessibility of the active site to probing molecules. The pore size, pore distribution and pore volume, is responsible for the control of transport phenomena and selectivity especially for catalyzed reactions as depicted in figure 2 (B). Hierarchy Factor exposes the extent of structural order in porous materials. It can be defined as the relative mesopore surface area ($S_{\text{meso}}/S_{\text{BET}}$) multiplied by the relative microporosity ($V_{\text{micro}}/V_{\text{meso}}$) and other parameters. HF can be derived from the N₂ adsorption-desorption analysis.

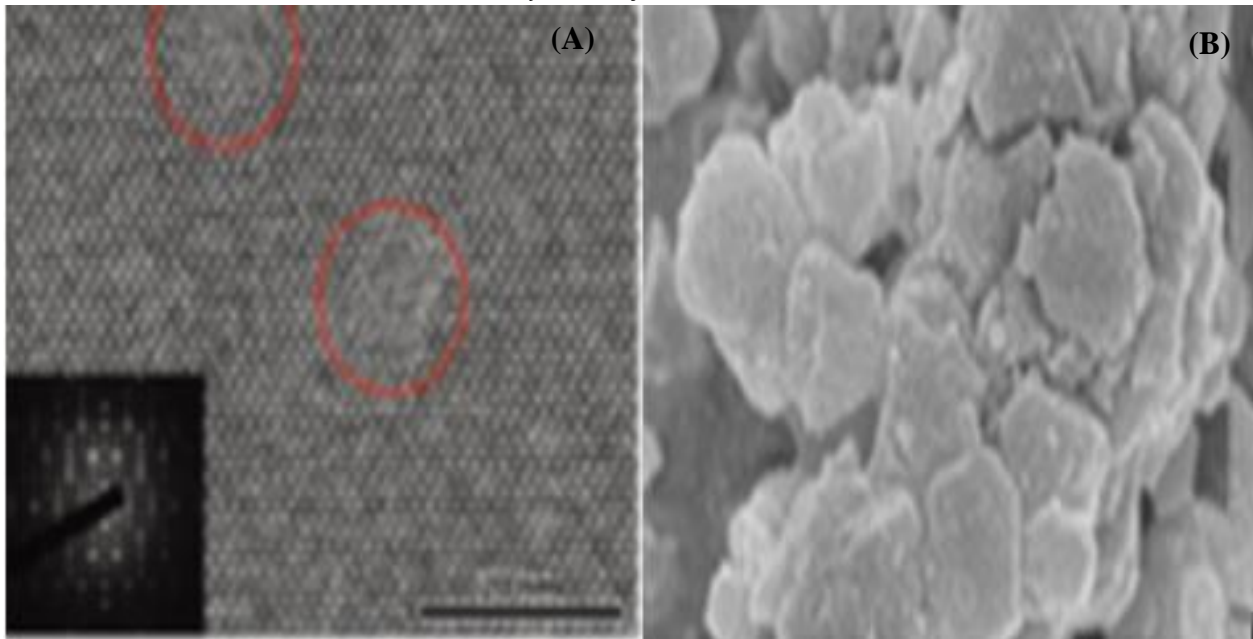


Figure: 1 (A) TEM image of Hierarchical Zeolite Y, (B) SEM image of Hierarchical zeolite Y.

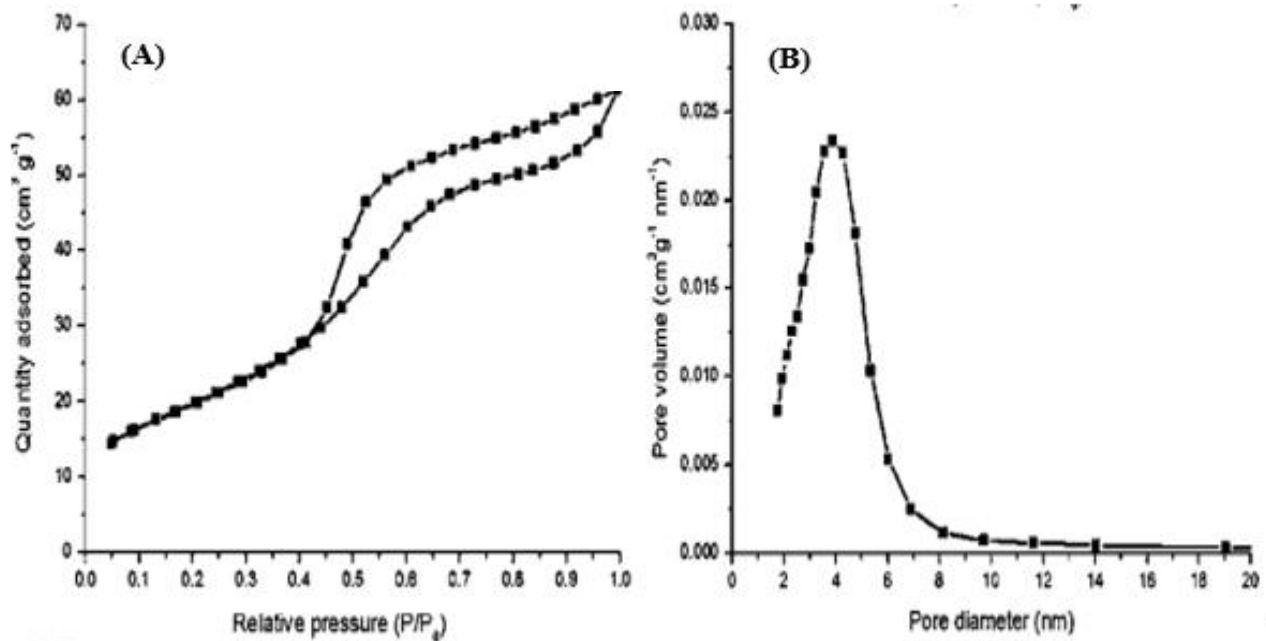


Figure: 2 Low temperature nitrogen adsorption measurements: adsorption-desorption isotherm (A) and the pore size distribution (B). (Seo *et al.*, 2018)

The isotherm (A) exhibit a hysteresis loop. The loop is made up of upper branch representation increasing addition of the adsorbent and progressive withdrawal. The hysteresis described the filling and removal of the mesopore by capillary condensation and B is the pore volume as it relates to pore diameter.

3 PREPARATION OF HIERARCHICAL ZEOLITE Y

Different workers have introduced interconnected mesoporous and microporous pore systems in zeolites (Dorien *et al.*, 2020; Reprich *et al.*, 2020). They described two approaches in hierarchical zeolite production, top-down and bottom-up, as depicted in Figure 2. Top-down methods are used when available, or commercial zeolites are treated to create additional

pores by etching part of it. This approach resulted in the destruction of the framework and reduction in the Si/Al ratio of the parent zeolites. The bottom-up approach is the creation of an additional pore in the zeolites during

the synthesis of the zeolites by incorporating a pore directing substances (Mesoporogen) in the precursor gel. Other methods are nanozeolites and their assembly.

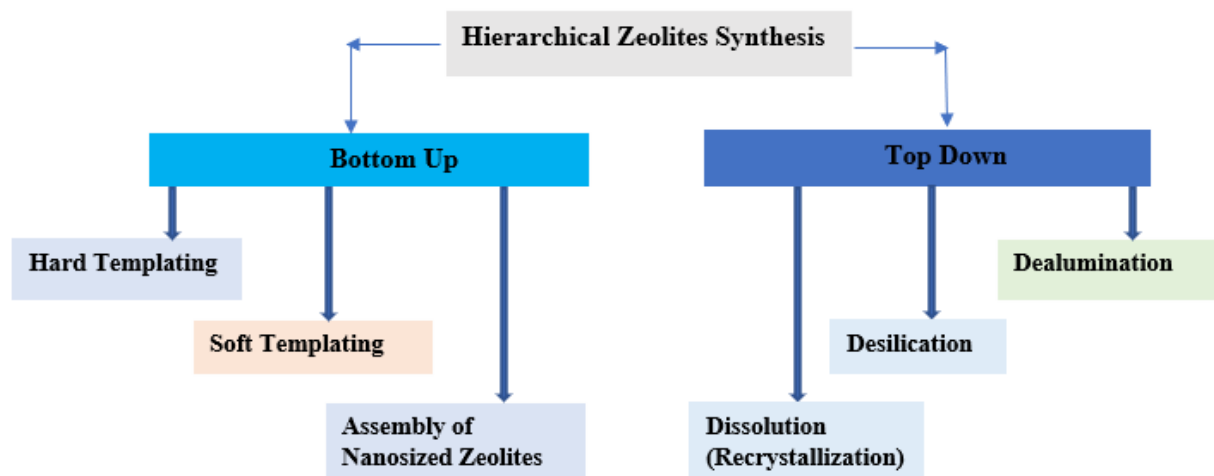


Figure 3: Synthesis Approaches of Hierarchical Zeolites

In a bottom-up approach, the zeolite synthesis is modified by adding templates to create different pore systems. One method is hard templating, where inert solid substances are added to the synthesis mixture and are embedded into the zeolite crystal during its crystallization. Another method is soft-templating, where surfactant molecules, which form surfactant arrays, are used to direct the formation of an additional mesopore system during the zeolite synthesis. The removal of the templates via, e.g., calcination or extraction results in the formation of the other pores.

3.1 Bottom-Up approach

In the bottom-up approach, hierarchical zeolite is directly synthesized from a silica-alumina gel by adding an extra-crystalline template (mesoporogen) to the original template used as the micropore template (templating approach) or by altering the reaction conditions (non-templating approach (Saepurahman, 2021)). The formation of zeolites is within the structure of the templates which is later removed by calcination of the synthesizes zeolite to create the needed mesoporosity.

3.1.1 Hard-templating method

Hard templates are used to be implanted in the zeolite crystals, and the hard templates were burnt out after calcination, and the zeolite will generate many

mesopores. The mesopores and micropores volume can be adjusted by varying the hard template. It is a method that uses solid materials with specific sizes and properties acting as mesopore templates, which can either be removed after synthesis by high-temperature calcination or form a composite with the resulting zeolite. They are mostly chemical inactive. Different types of solid materials, especially those with a carbonaceous origin, have been utilized as hard templates, and they have shown better characteristics such as ease of removal by calcination and chemical and thermal stability. By using various types of carbonaceous materials, e.g, nanoparticles (Bhupendra *et al.*, 2021), aerogels, carbon black, nanofibers and nanotubes (Samer *et al.*, 2021), carbon nanocrystals (Abdulridha *et al.*, 2020 and Bhupendra *et al.*, 2021) various hierarchical zeolites have been obtained (Xicheng *et al.*, 2021; Jia *et al.*, 2018). Carbon nanocrystals are ($550\text{m}^2\text{g}^{-1}$) and abundant surface hydroxyl groups made CNCs ideal template in a composite material.

The disadvantages of hard templates are that they are used in large quantities to adjust the texture properties, and much energy is required to burn it off. It has been reported that hard template zeolites Y are hydrothermally and mechanically less stable, and the mesopores' interconnectivity is low. The formation of

random mesopores structures can be out of control using hard templates.

Samer and co-researchers prepared mesoporous Y zeolites using hard templates. They compared hard templates like carbon nanotubes and nanocrystalline cellulose and concluded that nano-crystalline-cellulose is the more effective, economical and sustainable hard template than the carbon nanotubes for the formation of inter-crystal mesoporous Y zeolites (Samer *et al.*, 2021).

3.1.2 Soft templating

This route employs structural directing agent micropores formation and mesoporogen a relatively flexible material like polymers, surfactants, or organosilanes which acts as a templating agent for mesopores formation during crystallization processes. The utilization of micropore and mesopore templates earlier proved challenging to synthesize the needed hierarchical zeolites due to phase segregation and amorphous pore walls (Shiying *et al.*, 2022; Tranyi *et al.*, 2021; Zheng *et al.*, 2021). The templates form a scaffold around which the formation of mesopores takes place. The mesoporogen are chemically active and interact with the synthesized zeolites. The templates are removed by calcination, and the mesopores are formed where the templates are removed (Hanie *et al.*, 2021; Wu *et al.*, 2022). The advantages of soft templating include the

size of the pores can be controlled, a template can be utilized as a structural directing agent and mesoporogen, and a variety of them to choose from. Soft templates like surfactants (PDDA and CTAB) got a hydrophobic alkyl chain and hydrophilic quaternary ammonium group which is helpful in the formation of micropores and mesopores (Dorien *et al.*, 2020; Qing *et al.*, 2021; Jiayuan *et al.*, 2021; Qing *et al.*, 2022). Soft templating has its disadvantages. It goes from the high cost of templates to the emission of poisonous gases during calcination to remove the templates. Control of zeolite seed formation or multi-step synthesis was also challenging, but over-dependence on the synthesis condition and the time it takes remains a setback. These issues can be conquered by careful selection of novel soft templates, such as dual-function polyquaternary ammonium surfactants, dual-function polymers, silylane cationic polymers, silanized zeolitic seeds and organosilanes.

Soft templates were used extensively in the syntheses of hierarchical zeolite Y as depicted in the table 1

Table:1 Materials and Reagents used as Soft Templates for the Synthesis of Hierarchical Zeolites Y.

S/N	Soft Templates	Synthesis Conditions			References
1	Poly-dimethyl diallyl ammonium chloride.	48h ^a	650rpm ^b	60 °C ^c	48h ^d Alam <i>et al.</i> , 2018
2	Pluronic 127 (Blocked Copolymer)	24h	600rpm	110 °C	9h Dorien <i>et al.</i> , 2020
3	Poly ethylene glycol and CTAB	24h	600rpm	110 °C	9h Qing <i>et al.</i> , 2022
4	Organosilane Surfactant	24h	650rpm	100 °C	24h Panel <i>et al.</i> , 2016
5	Polydimethyl diallyl ammonium Chloride and NaOH.	24h	650rpm	110 °C	48h Aasif <i>et al.</i> , 2020
6	Polydimethyl diallyl ammonium Chloride and Graphene	12h	600rpm	110 °C	24h Aasif <i>et al.</i> , 2018
7	Tetramethyl ammonium hydroxide and CTAB	24h	650rpm	90 °C	24h Hamed <i>et al.</i> , 2019
8	Polydimethyl diallyl ammonium Chloride and NH ₄ OH solution	24h	650rpm	90 °C	24h Aihu <i>et al.</i> , 2020
9	CTAB and Pluronic 127	2h	600rpm	98 °C	16h Zhao <i>et al.</i> , 2021

Synthesis Condition: a(Aging time), b(stirring rate), c(Crystallization Temperature) and d(Crystallization Time)

All the synthesized zeolite-Y samples were characterized by XRD, FT-IR, SEM, EDAX, TEM, TGA, CO₂-TPD, and Nitrogen adsorption-desorption measurements. The characterization results showed that the zeolite-Y samples synthesized at optimized soft templates like PDDA/Al₂O₃ and NaOH/Al₂O₃ and others in table 1 exhibited higher crystallinity, higher BET surface area, and larger total pore volume than the sample synthesized in the absence of the template

3.1.3 Additive-Free Synthesis Route:

Traditional synthesis strategies of hierarchical zeolites via post-treatment or directing synthesis with mesoporous templates are often characterized by high energy consumption and substantial use of expensive and environmentally unfriendly organic templates. New green synthesis approach has been developed to effectively synthesize hierarchical zeolites that involve self-pillaring, steaming, seed assistance, and kinetic control of crystallization parameters (Risheng *et al.*, 2019). These additive free synthesis routes of hierarchical zeolite are one in which the morphology modifying agent (mesoporegen) is avoided (Jan-Paul *et al.*, 2021). The synthesis of additive-free zeolite has not been fully documented and cannot be applied in the industries; however, this template-free method may be employed in the large-scale production of industrially important zeolite catalysts for catalytic applications if adequately harnessed. The introduction of mesoporosity in zeolite Y is affected by the following factors: Reduction of crystallization temperature, the molar concentration of the precursor, and quantity of the solvent (water). The control of nucleation and crystal growth of precursor gel by varying the crystallization parameters form hierarchical zeolites without external templating agents (Jing-Quan *et al.*, 2016). The synthesized or commercial zeolites seeds are added to the precursor gel to improve the crystallinity (Rishabh *et al.*, 2021; Bastian *et al.*, 2022). The adjustment of crystallization parameters is also employed to control the nucleation and growth of the precursor. Synthesis of hierarchical zeolites Y was carried out by adjustment of Si/Al ratio from 1.1 to 1.9 through a hydrothermal process. The crystallization in the Teflon stainless steel autoclave at temperature of 100°C for 24 h. The synthesized zeolite y has a micropore of 0.74nm and mesopore of 10nm (Xiaoli *et al.*, 2018). Additive-free synthesis is the most cost-effective and environmentally friendly way of hierarchical zeolites Y synthesis.

Khaleel *et al.*, 2016 synthesized hierarchical zeolite Y with this molar concentration Al₂O₃: 4.9-12 Na₂O:3.6-14SiO₂:214-300 H₂O. The synthesis precursors were ice-bathed for 1h. aged at room temperature for 24h and crystallized at 60°C for 48h. Preparing the synthesis gel at 0°C using an ice bath is a promising way to synthesize sub-micron-sized zeolite Y particles.

Jia *et al.* (2018) synthesized additive-free hierarchical zeolite Y with a molar concentration of Al₂O₃: 13.6-36Na₂O: 3-8SiO₂: 545.5-1440H₂O. The precursor was aged at 0°C for 5h and crystallized at a temperature of 60°C for 24h. They used 60°C as their second temperature step and claimed that at 50 °C their reaction mixture stayed amorphous. The synthesized zeolite has a pore volume of 0.26 cm³/g and a surface area of 544m²/g.

Du *et al.* (2018) synthesized hierarchical zeolite Y with a molar concentration of Al₃O₂: 10-18.3Na₂O:10-22SiO₂ and 815H₂O. The synthesis gel was aged at room temperature for 2h, crystallized at 70°C for 24 h, and obtained hierarchical zeolite with a pore volume of 0.33m³/g. The optimum procedure for the template-free synthesis of HY was accessed to be the aging time of (0-8days), crystallization time of (24-72 h), the crystallization temperature of (90-100°C), and the molar ratio of 4.65-6.00. This crystallization parameter gave a pore volume of 0.303 cm³g⁻¹ and BET surface area of 624m²g⁻¹ and the synthesized HY has a strong affinity to linear alkylbenzene (Jahadideh *et al.*, 2021).

It is possible to say that the synthesis molar concentrations used for the additive free synthesis of hierarchical zeolites Y are mostly in the range of composition for the conventional zeolite Y with differences in aging and crystallization temperature. Water content in the synthesis gel is another most important parameter in the synthesis of hierarchical Zeolite Y. It directly affects the particle diameter and crystal thickness. An increase in the water content increases particle diameter and crystal thickness (Gaber *et al.*, 2019). Lower water content in the synthesis precursor leads to an increase in the EMT and a decrease in the particle diameter. In the same content, an increase in Na₂O content in the synthesis gel leads to smaller assemble and thinner crystals.

3.2 Top-Down Approach (Demetallation method)

For the top-down approach, synthesized zeolites are subjected to post-treatment to introduce mesoporosity.

A Review On Synthesis Of Hierarchical Zeolites Y

The easiest way to achieve this is by dealumination using the steaming and chemical treatments, such as acid leaching or reaction with EDTA or other chelating agents that can remove the resulting extra-framework alumina. Another way of demetallation is desilication which is the removal of silica from the different frameworks using a base like sodium hydroxide or organic base ammonium hydroxide (Imbachi- Gamba

and Villa, 2021). This approach was utilized in developing Ultra-Stable -Y zeolites used in many applications. Other methods that have been employed include recrystallization, demetallation, coating of zeolite crystals on macro-porous supports, delaminating and shaping can also be used. Demetallation methods can easily be adapted on an industrial scale (Dorien *et al.*, 2020).

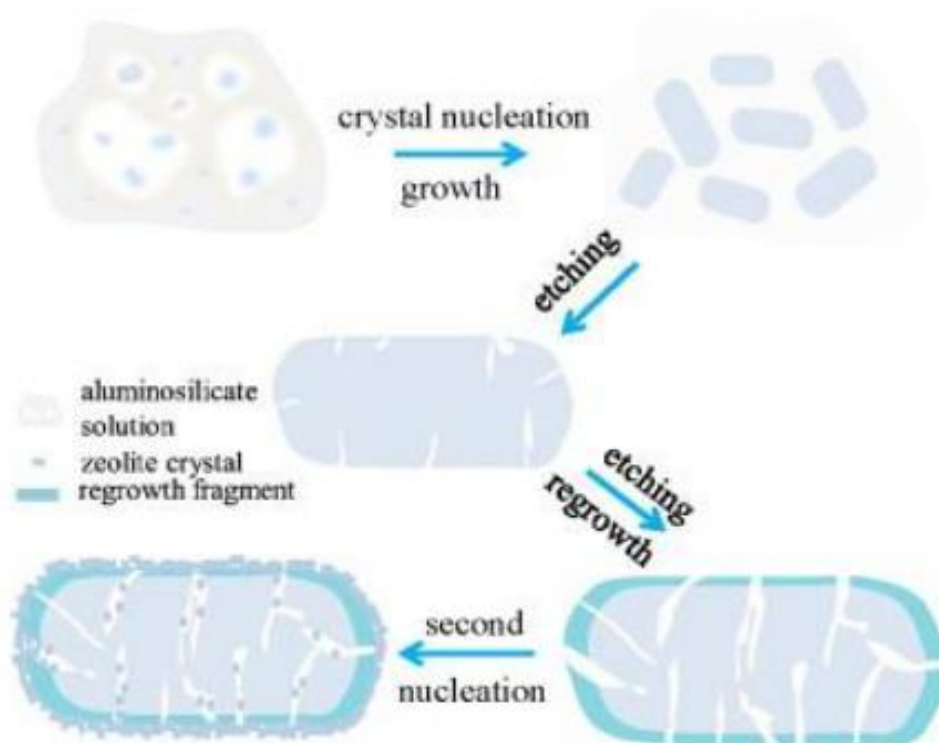


Figure 4: The mechanism for the formation of Hierarchical Zeolites (Hua *et al.*, 2015)

3.2.1 Dealumination

Dealumination is a method of introducing mesopores and macropores in a zeolite while maintaining the intrinsic microporosity of the parent zeolites. It involves using acid, steam, and heat to remove aluminium from the zeolite framework to create mesopores. The acidity and Si/Al ratio of the parent zeolite are altered. In the past, dealumination was first used to increase the Si/Al ratio in zeolites, but it was discovered that apart from increasing the acid concentration, the resulting zeolites also had better stability, and mesopores were generated (Nurudeen, 2015).

Steaming and acid leaching using hydrochloric and sulphuric acids as the leaching agents are the most straight forward and general methods of dealumination (Imbachi- Gamba and Villa, 2021). Steaming is a hydrothermal treatment usually carried out at elevated

temperatures higher than 500°C in the presence of steam (Shuhui *et al.*, 2021; Qi *et al.*, 2021 and Faisal *et al.*, 2021). With these conditions, the Si–O–Al bonds present in the

zeolite is broken, resulting in the removal of framework aluminium. The mobile and less stable silicon species could migrate to other sites and condense with silanols, filling some vacant sites and growing large voids emanating from mobile silicon species and removing aluminium (Imbachi- Gamba and Villa, 2021). The changes in zeolite structure as a result of steaming do not necessarily occur at the maximum temperature but at any temperature that permits water to penetrate the pores causing significant migration of Al^{3+} in the framework to extra-framework positions (Hamid *et al.*, 2022). The unstructured materials deposited on the external surface or on the mesoporous surface of the treated zeolite crystals might cause partial blockage of the micropores making a mild acid treatment with mineral acids needed

(Qi *et al.*, 2021). The formation of mesopore based on this mechanism depends on the stability of Al sites against hydrolysis and aluminium concentration, so zeolites possessing low Si/Al ratios are used for studies on steaming. Dealumination techniques have been used in the industries to introduce mesopore in a zeolite. Still, the disadvantages include partial amorphization of the zeolite causing a drop in crystallinity, disconnection in the formed cavities, and mesopores being detached or lying within the zeolite framework, which can inhibit the molecule transport in the crystal. Moreover, the pore size distribution of the formed mesopores is wide.

Imbachi and co-researcher dealuminated a Commercial zeolite USY (CBV500, Si/Al = 2.6) with oxalic acid and desilicated it with ammonium hydroxide in cetyltrimethylammonium bromide, and acid-washed with lactic acid for obtaining hierarchical zeolite. The treatment lowers the deactivation rate of the modified zeolite than the CBV500 (Imbachi-Gamba and Villa 2021).

The steam and acid treatment as a means of dealumination was demonstrated by the work of Hamid *et al.* (2022) used chemical and hydrothermal methods to create mesopores in zeolites Y. The combination of steam and chemical treatment resulted in the collapse of the structure of parent zeolites creating void spaces. The catalyst was impregnated with NiMo and utilized as NiMo/FAU+Al₂O₃ as support. The life and activity of the catalyst were enhanced (Hamid *et al.*, 2022). Nitric acid and steam were also used to dealuminate zeolite Y by Qi and co-researchers. They used it to inhibit the degradation of toluene in different humidity. The dealuminated zeolites Y was used after impregnation with manganese oxide (Qi *et al.*, 2021). Synthesis of zeolites composite Y/ZSM-5 through vapour phase transport method was done to check its affinity towards Toluene, Cyclohexane, and Butylacetate. The zeolite which was dealuminated by Steam and HCl has a wider pore, good regeneratory ability, and high thermal stability than the parent zeolite (Shuhui *et al.*, 2021)

Wenlin *et al.* (2017) prepared hierarchical zeolite Y through a facile SiCl₄ dealumination plus alkaline treatment process with the addition of surfactant dimethyloctadecyl[3(trimethoxysilyl)propyl] ammonium chlorides (TPOACl). The alkaline treatment in the presence of TPOACl leads to the protection of zeolite microporosity and hierarchical pore structures with increased mesoporosity and narrow distribution of

mesopores. The zeolite possesses a high percentage of mesopores with excellent catalytic performance.

The aluminium in the framework can also be removed by only acid leaching using concentrated acid solutions. Other than the mentioned methods, chemical treatment with silicon tetrachloride and calcination, ammonium hexafluorosilicate, and ethylene diamine tetra acetic acid have also been used as agents in dealumination for the synthesis of hierarchical zeolites (Dorien *et al.*, 2020). Shuhui *et al.* (2021) and De-Jong *et al.* (2010) did similar work on subjecting a commercial zeolite Y to steam and acid leaching. The zeolite of bulk Si/Al ratio of 28 was subjected to base leaching afterward. The N₂ physisorption results indicated that the dealuminated zeolite Y possesses a multi-modal porosity with micropores of size 1 nm, small mesopores close to 3 nm, and larger mesopores (~30 nm) (Shuhui *et al.*, 2021; De-Jong *et al.*, 2010).

Wenlin *et al.* (2017) deduce that hierarchical zeolite Y with high mesoporosity and integrated crystalline and hydrothermal stability is desired for heavy oil conversion. In his approach, steam, acid, and alkaline treatment are reported for fabricating hierarchical zeolite Y with high mesoporosity and extraordinarily high crystallinity. A zeolite precursor was prepared through an acid pre-treatment step by using fluorosilicic acid and hydrochloric acid, in which the zeolite crystal could be healed by the migration of Si into the skeleton. The hierarchical zeolite Y showed remarkable catalytic activities, the high selectivity of liquid products, and the low selectivity of bottom oil in heavy oil conversion.

The disadvantages of dealumination include a reduction in the active acid sites in the zeolite due to the removal of framework Al, which was originally an acid site, and the mesoporous zeolites synthesized contained many isolated cavities instead of interconnected mesopores providing little or no solution to the diffusional problem of microporous zeolites and its hierarchical structure is meant to solve. The fast dissolution kinetics and the relatively slow intra-crystalline diffusion of the OA-NH₄F etching solutions resulted in a different core-shell-like structure with a porous and Si-rich shell, preserving the unique advantages of single crystals with interconnected micro-and mesopores.

3.2.2 Desilication

Desilication is the removal of silica atoms from the zeolite framework to create mesopores by contacting them with an alkaline solution. Silicon in the precursor

A Review On Synthesis Of Hierarchical Zeolites Y

is dissolved by organic or inorganic base e.g., NaOH, NaHCO and TPAOH to make adequate mesoporosity (Zijian *et al.*, 2022). The process of desilication is initiated at the boundary of the zeolite's crystals or at the defeat site. The use of organic base involves a longer reaction time and elevated temperature due to its reactivity. Some factors affect the processes of desilication:

- The morphology of the parent zeolites
- The aluminium content
- The Si/Al ratio
- The parent zeolite morphology also plays a significant role in the dissolution process during desilication.

The framework aluminium is often referred to as the ‘‘pore-directing agent’’ (PDA) owing to its ability to control intra-crystalline mesopore formation. Aluminium accounts for the acidity of the zeolites. It also migrates from the reacting solution to form amorphous layers that block the micropore of treated zeolites, thereby forcing a mild acid wash to free the micropores after desilication. This method of creating mesopores in hierarchical zeolites is protonic. Additional ion exchange step is not required after calcination. The desilicated zeolites' micropores and the mesopores' interconnectivity after the process are mostly maintained.

Some researchers concluded that this post-treatment method can enhance the catalytic performance and catalytic lifetime (Shahid *et al.*, 2017; Ahmed *et al.*, 2017 and Zhang *et al.*, 2017). The zeolites showed a lower deactivation rate due to the high external surface area, mesopore volume, and pore mouth, which made hierarchical zeolites less sensitive to carbon deposition. The introduction of mesopores in a zeolite for hydrotreatment of guaiacol through desilication was performed with NaOH and TBAOH. There was an increase in the mass transfer of guaiacol and an improvement in the accessibility of the active sites, thereby enhancing the catalytic display of hydrodeoxygenation and hydro-dearomatization reaction (Lingyu *et al.*, 2022)

A commercial parent Y-zeolite (Si/Al = 2.48) was modified via desilication using NaOH. The treatment reduced Si/Al ratio from 5.36 to 2.57 with an enhanced specific area. The desilicated zeolite Y improved the total aromatic percentage and reduced the acidic group in co-pyrolysis oil (Tewodros *et al.*, 2021). Desilication of FAU was also examined with the sonochemical-

assisted procedure. A high silica extraction was noticed within 30 to 15min of exposure. The removal of silica was observed to occur at the bulk of the zeolites. The researchers concluded that sonochemical-assisted desilication is more effective than the traditional desilication procedures (Kuteranski *et al.*, 2022; Dorien *et al.*, 2020). The alkaline treatment of zeolites Y has shown tremendous mesopores formation as observed in the modification that led to Si-O-(OH)-Al bond. The silica extraction formed a framework structure creating more tetrahedral extra framework lewis acidic aluminium (Ping *et al.*, 2021). The effects of NaOH and NaOH/TPAOH in desilication of NaY were examined. The highest total surface areas and absorption capacity was observed in the zeolite treated with NaOH/TPAOH solution (Ghasem *et al.*, 2022)

Imbachi-Gamba and Aída (2019) synthesized hierarchical zeolites Y by two methods, following desilication procedures of commercial zeolites. Starting from USY zeolite (Zeolyst CBV720, Si/Al=15), the effect of the amount of CTAB in the desilication media and the hydrothermal treatment time on the synthesized materials were analyzed. The results showed that the surfactant amount significantly influences the material's relative crystallinity and textural properties than synthesis time.

High aluminum content was observed to have soothing effects on the surrounding silicon atoms preventing their dissolution, which leads to few mesopores, while for low aluminum content, a large number of the zeolites could be dissolved, resulting in low productivity and large pores. Owing to these drawbacks, a new method was developed to prepare the hierarchical zeolite post-treatment with different concentrations of sodium aluminum solution (NaAlO₂), basic solution of NaOH, and piperidine, respectively (Kalpana *et al.*, 2021). This process of desilication presents a more reasonable alkaline etching method than the NaOH etching method. Sodium aluminum solution (NaAlO₂) extracted Si species selectively protected the structure by simultaneously repairing the defects resulting from desilication with Al species. In contrast, a combination of basic solution of NaOH and piperidine prevented the excessive dissolution of Si species by NaOH, resulting in the controlled desilication within the crystals and maintaining the micropores simultaneously (Kalpana *et al.*, 2021). The newly formed mesopores enhanced the accessibility of acid sites in the micropores and shortened the diffusion path length, resulting in higher catalytic performance and a longer lifetime in

hydrocarbon cracking. NaOH etching method is widely used to prepare the hierarchical zeolite. Recent progress in the desilication method is by introducing organic additives such as tetrabutyl ammonium and tetrapropyl ammonium (Ghasem *et al.*, 2022) or inorganic additives (such as $\text{Ga}(\text{OH})_4$ and $\text{Al}(\text{OH})_4$, which act as external PDA to control the intracrystalline mesoporosity during the process of base leaching (Kuterasiński *et al.*, 2022). The affinity of the PDA to the zeolite surface plays a vital role in the pore formation process. One useful advantage of external PDA is that the organic additives prevent realumination during desilication, producing solids with Si/Al ratios close to the starting zeolite. It also expands the suitability of the desilication method for controlling mesopore formation in all silica zeolites. The criteria for selecting organic pore directing agents in

base leaching (using NaOH) were investigated over USY zeolites with Si/Al ratio ranging from 15 to 385, with the result indicating that efficient PDAs should possess organic matters in the range of ca. 10–20 carbon atoms and must be positively charged (Ghasem *et al.*, 2022).

Like dealumination, desilication alters the framework Si/Al ratios; but unlike dealumination, it decreases Si/Al ratios. Usually, some extra-framework aluminium species might remain after the base leaching due to realumination. Therefore, acid treatment or ion exchange is required as an additional step to take off these aluminium species for opening the mesopores (Dorien *et al.*, 2020)

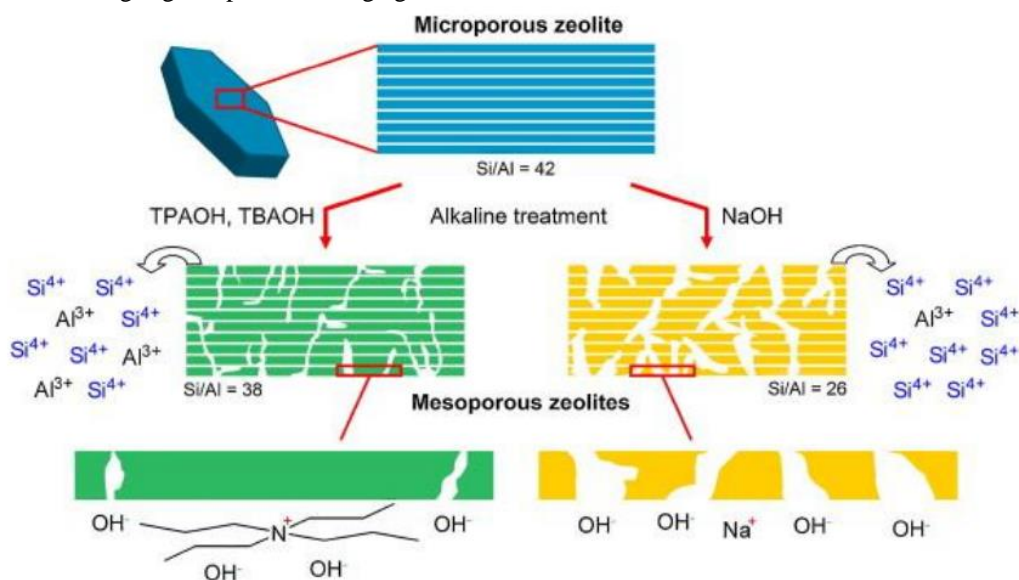


Figure 5: Mechanism for the formation of Hierarchical zeolites by desilication (Ge *et al.*, 2015)

4. MIXED METHODS OF HIERARCHICAL ZEOLITES SYNTHESIS

This method involves creating hierarchical structures in zeolites by combining two or more assemblies and demetallization approaches (Fig. 6). A typical method is zeolite recrystallization, in which base leaching of zeolites is performed in the presence of surfactants. It can produce ordered mesoporosity within the zeolite crystals by local rearrangement of its framework with an adequate selection of the treatment conditions; if not, zeolite mesoporous oxide composites might be prepared. To obtain mesopores between 2.5 to 4.5 nm, zeolite Y, Garcia-Martinez and coworkers 2012 reported that the surfactant chain length can vary. They successfully synthesized uniformly distributed mesoporous zeolite Y by hydrothermal treatment with dilute ammonium

hydroxide (NH_4OH) and CTAB as the surfactant at 150 °C for 10–20 h. treatment with dilute ammonium hydroxide (NH_4OH) and CTAB as the surfactant at 150 °C for 10–20 h.

Dekum *et al.*, 2017 developed mesostructured zeolite Y from NaY with low Si/Al by a one-step method based on a bifunctional surfactant. The surfactant ammonium salt (TPHAC) acted as a template and dealumination. The dealumination came from the coordination of $-\text{Si}-\text{OH}$, a product of hydrolysis of TPHAC with framework aluminium ions. Utilization of kaolin to synthesize NaY zeolite was also studied and the presence of crystalline NaY seeds is important in synthesizing NaY in the synthetic or natural precursor. The mesoporosity was introduced into zeolite crystal through the surfactant approach.

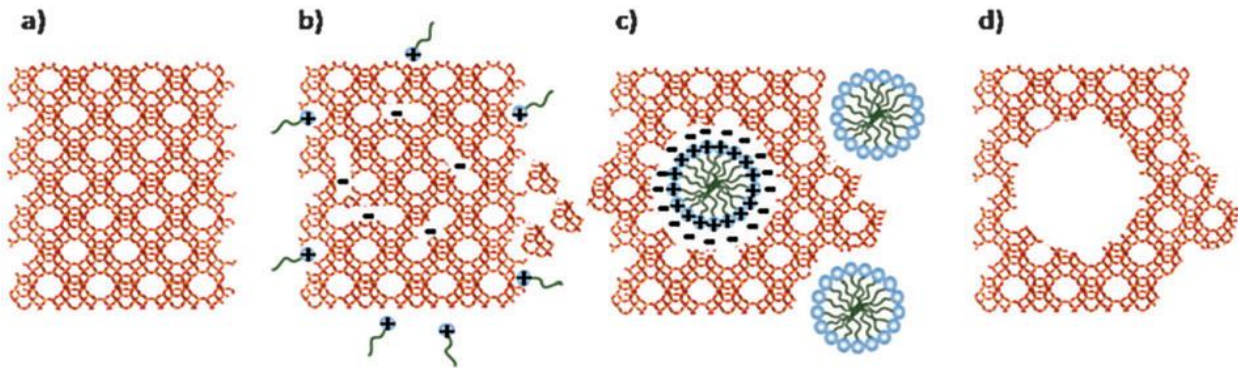


Figure 6: Schematic diagram of (a) zeolites Y (parent) (b) Si-O-Si bond breaking in alkaline media (c) rearrangement of crystal to admit surfactant (d) after template removal.

Various methods have been developed in the last decades to create hierarchical zeolites. In general, the limitations of these methods, namely, the top-down and the bottom-up approaches, are presented in Table 2.

Table 2: Various methods of synthesis of zeolite and their limitations

Method	Limitation	Reference
Top-down		
Dealumination	Occurrence of zeolite of an amorphization, leading to drop of crystallinity. The cavities and mesopores are not connected within the zeolite framework and surface.	Chen <i>et al.</i> , 2020
Desilication	Interconnected mesopores are formed, and large micropores zeolite is retained. Using a highly concentrated alkaline solution caused loss of zeolite and decreased microporosity.	Wang <i>et al.</i> , 2020
Dissolution-Recrystallization	It occurs in the presence of surfactants and involves high synthetic costs.	Zhai <i>et al.</i> , 2021
Bottom-up		
Soft templating	Amorphous mesoporous materials are formed instead of crystalline hierarchical zeolites. Defect sites and hydrothermal stability of zeolite are created during synthesis. Higher economic cost and release of toxic gases.	Jia <i>et al.</i> , 2019
Hard templating	Required high temperature, leading to loss of product. As a result of its hydrophobic nature, applications are limited. Hydrothermally and mechanically less stable and low interconnective mesoporosity.	Jia <i>et al.</i> 2019
Template free	The mechanistic synthesis is not fully documented.	Chen <i>et al.</i> 2020

5. CONCLUSION

Hierarchical zeolite Y has demonstrated a great advantage over the conventional micropores zeolites. Various synthesis strategies have been discussed in the brief review. The hard template requires high energy consumption but can form an ordered interconnected

controllable mesopore, and carbon nanocrystals were found to be the most effective hard template, but this approach cannot be applied at an industrial scale. The soft template has its own advantages of easy removal by calcination, but a flue gas that could be poisonous may be generated during calcination. The cationic

amphiphilic template is not easily synthesized as it involves sophisticated steps in the production and expenses and is environmentally benign. The morphology modifying agents and the calcination steps are the drawbacks of the synthesis. This synthesis route involves using a large amount of energy to remove the templates and generation of waste in the environment. Creating mesopore through dealumination and desilication is a promising industrial-scale production of zeolite Y as it does not require any templates but the distortion of the parent zeolites is not avoidable. In view of the above drawbacks, additive-free synthesis route is more advantageous than the abovementioned routes. It is basically the adjustment of crystallization parameters and some additional aging steps with no expensive templating agents. The calcination steps that are mostly accompanied with flue gases is avoided.

Outlook

The synthesis of hierarchical zeolites Y is an evolving area of research. The disadvantages of various synthesis approaches have been enumerated in this brief review. The additive free synthesis route should be properly harnessed and documented as it is the most viably synthesis route for industrial application.

REFERENCES

- Aasif A. D., Issam I., Balasubramanian V. V., Kyriaki P.G. S., Stephane M. and Yasser A W. (2020) Synthesis of hierarchical porous Zeolite-Y for enhanced CO₂ capture. *Microporous and mesoporous materials*, 303, 110261.
- Aasif A. D., Suresh K. R., Hemant M., Yasser Al W., Balasubramanian V.V., Georgios N.K., Gnana S., Stephane M., Mikael B. and Saeed M.A.(2021) Water vapor adsorption on metal-exchanged hierarchical porous zeolite-Y. *Microporous and Mesoporous Materials*, 326, 111380
- Abdulridha, S.; Jiang, J.; Xu, S.; Zhou, Z.; Liang, H.; Mao, B.; Zhou, Y.; Garforth, A.A.; Jiao, Y. and Fan, X. (2020). Cellulose nanocrystals (CNCs) as hard templates for preparing mesoporous zeolite Y assemblies with high catalytic activity. *Green Chem.*, 22, 5115–5122.
- Ahmed N., Shahid A., Saleh, T., Al-Thabaiti, S., Basahel, S., Schwieger, W. and Mokhtar, M. (2017) Solvent-Free Biginelli Reactions Catalyzed by Hierarchical Zeolite Utilizing a Ball Mill Technique: A Green Sustainable Process. *Catalysts* 7, 84.
- Alam T., Krisnandi Y. K., Wibowo W., Nurani D. A., Rahayu, D. U. C. and Haerudi H. (2018) *Synthesis and Characterization Hierarchical HY Zeolite Using Template and Non-Template Methods*. Department of Chemistry, Faculty of Mathematics and Natural Sciences (FMIPA), University Indonesia, Depok 16424, Indonesia.
- Bai, R., Song, Y., Bai, R. and Yu, J. (2021). Creation of Hierarchical Titanosilicate TS-1 Zeolites. *Advanced Materials Interfaces*, 8(4), 2001095.
- Bastian R., Karolina A. T., Kamila P., Gabriela G. and Kinga G. (2022) High-Silica Layer-like Zeolites Y from Seeding-Free Synthesis and Their Catalytic Performance in Low-Density Polyethylene Cracking. *Appl. Mater. Interfaces*. <https://doi.org/10.1021/acsami.1c21471>
- Bastian R., Tobias W., Wilhelm S. and Alexandra I. (2020) Layer-like FAU-type zeolites: A comparative view on different preparation routes. (Review) *Frontiers of Chemical Science and Engineering*, 14, 127–142
- Bhupendra K, S., Yongseok K., Seungdon K. and Kyungsu N. (2021) *Synthesis of Mesoporous Zeolites and Their Opportunities in Heterogeneous Catalysis*. Department of Chemistry, Chonnam National University, 77 Yongbong-ro, Buk-gu, Gwangju 61186, Korea *Catalysts* 11(12), 1541; <https://doi.org/10.3390/catal11121541>
- Bo M., Shenyong R., Zhi L., Suofu N., Xinyue Z., Weiyu S., Qiaoxia G. and Baojian S.(2021) A facile organic-free synthesis of high silica zeolite Y with small crystal in the presence of Co²⁺ *Microporous and Mesoporous Materials*, 323, 111248
- Chen, L. H., Sun, M. H., Wang, Z., Yang, W., Xie, Z. and Su, B. L. (2020). Hierarchically structured zeolites: from design to application. *Chemical Reviews*, 120(20), 11194-11294.
- Dabbawala, A.A., Ismail, I., Vaithilingam, B.V., Polychronopoulou, K., Singaravel, G., Morin, S., Berthod, M. and Al Wahedi, Y., (2020) Synthesis of hierarchical porous Zeolite-Y for enhanced CO₂ capture. *Microporous and Mesoporous Materials*, 303, 110261.
- De Jong K. P., Zečević J., Friedrich H., de Jongh P. E., Bulut M., VanDonk S., Kenmogne R., Finiels A., Hulea V. and Fajula F. (2010) Zeolite Y crystals with trimodal porosity as ideal

A Review On Synthesis Of Hierarchical Zeolites Y

- hydrocracking catalysts. *Angewandte Chemie*, 122(52): 1027210276
- Dekun J., Honghai L., Xiao W., Hongtao L., Xionghou G., Chunyan X. and Shuyao W.(2017). Mesostructured Y zeolite from NaY with low Si/Al by one-step method based on bifunctional surfactant. *Material Chemistry and Physics* 196, 284-287
- Dorien K., Brent S., Jonathan V. W., Qiang Z., Jihong Y., and Bert F. S. (2020) State of the Art and Perspectives of Hierarchical Zeolites: Practical Overview of Synthesis Methods and Use in Catalysis (Review) *Advanced Material* 2004690
- Du Y., Kong Q., Gao Z., Wang Z., Zheng J., Qin B., Pan M., Li W. and Li R. (2018) Flower-like hierarchical Y with dramatically increased external surface: A potential catalyst contributing to improving pre-cracking for bulky reactant molecules. *Industrial & Engineering Chemistry*
- Faisal M., Muhammad F. I. and Muhammad R. U. (2021) Synthesis methods and recent advances in hierarchical zeolites: A brief review. *Journal of the Iranian Chemical Society*, volume 18, 2215–2229.
- Gaber S., Gaber D., Ismail I., Alhassan S. M., and Khaleel M. (2019) Additive-free synthesis of house-of-card faujasite zeolite by utilizing aluminosilicate gel memory. *Crystal Engineering Communication*, 21(11): 1685–1690
- García-Martínez J., Johnson M., Valla J., Li K. and Ying J. Y. (2012) Mesostructured zeolite Y-high hydrothermal stability and superior FCC catalytic performance. *Catalysis Science & Technology*, 2(5): 987–994
- Ge T., Hua Z., He X., Zhu Y., Ren W., Chen L., Zhang L., Chen H., Lin C. and Yao, H.(2015) One-pot synthesis of hierarchically structured ZSM-5 zeolites using single micropore-template. *Chin. J. Catal.* 36, 866–873
- Ghasem D., Seyed R. S., Javad A. and Maryam N. (2022) Effect of desilication of NaY zeolite on sulfur content reduction of gasoline model in presence of toluene and cyclohexene. *Chemical Engineering Research and Design*, 178, 523-539
- Hamid K., Mohammad K., Saeed S. and Mehdi R.(2022) Influence of adding a modified zeolite-Y onto the NiMo/Al₂O₃ catalyst utilized to produce a diesel fuel with highly reduced sulfur content. *Microporous and Mesoporous Materials*, 332, 111704
- Hanie K., Jafar T., and Sahar A.(2021) Synthesis of hierarchical SAPO-34 zeolites with tuned mesopore structure for methanol to olefins (MTO) reaction using polyethylene glycol as a soft template. *Journal of Sol-Gel Science and Technology*, 100, 286–298
- Hua Z., Ge T., He X., Zhu Y., Ren W., Chen L., Zhang L., Chen H., Lin C. and Yao, H., (2015) One-pot synthesis of Hierarchically structured ZSM-5 zeolite using single micropore-templates. *Chin. J. catal.* 36, 866-873
- Imbachi-Gamba C. F. and Villa A. L. (2021)Statistical analysis of the influence of synthesis conditions on the properties of hierarchical zeolite Y. *Material today Chemistry*, 20, 100442
- Jahandideh J., Hafizi A. and Rahimpour M. R. (2021) Experimental Investigation of Facile and Template-Free Synthesis of Zeolite Y for the Alkylation of Benzene. *Topics in Catalysis*
- Jan-Paul G., Katharina K., Bastian R., Wilhelm S. and Alexandra I. (2021). Layer-Like Zeolite X as Catalyst in a Knoevenagel Condensation: The Effect of Different Preparation Pathways and Cation Exchange. Institute of Chemical Reaction Engineering, Friedrich-Alexander University Erlangen-Nürnberg, 91058 Erlangen, Germany *Catalysts*, 11(4), 474.
- Jia X.; Han L.; Ma Y. and Che S. (2018) Additive-free synthesis of mesoporous FAU-type zeolite with intergrown structure. *Science China Materials*, 61(8): 1095–1100
- Jia X., Khan W., Wu Z., Choi J. and Yip A. C.(2019). Modern synthesis strategies for hierarchical zeolites: Bottom-up versus top-down strategies. *Advanced Powder Technology*, 30(3), 467-484.
- Jiayuan W., Mingquan L., Yajie F., Cederick C. A., Yujia J., Ruiqin Y., Xu S., Chuang X. and Elton M.(2021) An ambient pressure method for synthesizing NaY zeolite. *Microporous and Mesoporous Materials*, 320, 111073
- Jing-Quan W., Ya-Xi H., Yuanming P. and Jin-Xiao M. (2016) New hydrothermal route for the synthesis of high purity nanoparticles of zeolite Y from kaolin and quartz. *Microporous and Mesoporous Materials*, 232, 77-85
- Kalpna C., Maheria A. L. and Gunjan S.(2021) Microalgae Oil Upgrading over Zeolite-Based Catalysts. *Catalytic and Noncatalytic Upgrading of Oils* Chapter 4pp 89-124ACS

- Symposium Series Vol. 1379 ISBN13: 9780841298422 ISBN: 9780841298415.
- Khaleel M., Xu W., Lesch D. A., and Tsapatsis M. (2016) Combining pre-and post-nucleation Trajectories for the synthesis of high FAU-content Faujasite nano-crystals from organic-free sols. *Chemistry of Materials*, 28(12): 4204–4213
- Kuterasiński L., Filek U., Zimowska M., Napruszewska B. D., Gackowski M. and Jodłowski P.J.(2022) Ultrasonically prepared mesoporous zeolites with faujasite type structure as catalysts for the production of diethyl ether and ethylene from ethanol. *Materials Research Bulletin*, 147, 111652
- Lingyu T., Roya H., Benedettade C., Martina D., Laura P., Marco S., Ramin K. and Paolo D. F. (2022) Guaiacol hydrotreating with in-situ generated hydrogen over ni/modified zeolite supports. *Renewable Energy*, 182, 647-658
- Maghfirah A., Imi M. M., Fajar A. T. N. and Kadja G. T. M. (2020). A review on the green synthesis of hierarchically porous zeolite. *Materials Today Chemistry*, 17, 100348.
- Nurudeen Salahudeen (2015). *Development of zeolite Y and ZSM -5 composite catalyst from Kankara kaolin*. Department of Chemical Engineering, Ahmadu Bello University Zaria, Nigeria,
- Panel B. L., Kaihong X., Su Cheun Y. F. and Hongxia (2016) Direct synthesis of hierarchical USY zeolite for retardation of catalyst deactivation. *Chemical Engineering Science*, vol, 153 page 374-381
- Ping Z., Sebastian M., Shunmugavel S. and Anders R.(2021)Modification of commercial Y zeolites by alkaline-treatment for improved performance in the isomerization of glucose to fructose. *Molecular Catalysis*, 510, 111686
- Qi S., Hao D., Jian Z., Bowen X., Yuhao W. and Chao L. (2021)Manganese supported on controlled dealumination Y-zeolite for ozone catalytic oxidation of low concentration toluene at low temperature. *Chemosphere*, 271,129604
- Qin Z., Cychosz K. A., Melinte G., El Siblani H., Gilson J P., Thommes M., Fernandez C., Mintova S., Ersen O. and Valtchev V. (2017) Opening the cages of faujasite-type zeolite. *Journal of the American Chemical Society*. Vol. 139(48): 17273–17276
- Qing Z., Yi Z., Fumin W., Xubin Z., Guojun L., Yongkui L., Mengyue L. and Mengyao L., (2022)One-step controllable strategy for synthesizing hierarchical Fe-MFI/MCM-41 composites using CTAB as a dual-functional template. *Microporous and Mesoporous Materials*, 329, 111515
- Rishabh J., Adam J. M. and Jeffrey D. R.(2021). Controlling Nucleation Pathways in Zeolite Crystallization: Seeding Conceptual Methodologies for Advanced Materials Design. *Journal of America Chemical Society*, 143, 51, 21446–21460
- Risheng B., Yue S., Yi L. and Jihong Y.(2019) Creating Hierarchical Pores in Zeolite Catalysts, (A review)*Trends in chemistry*, 1(6), 601-611
- Saepurahman Si(2021) A top-down approach to preparation of H-Y zeolite nanoparticles *Asia-Pacific journal of science and Technology*. Vol. 26 No. 02.
- Samer A., Yilai J., Shaojun X., Rongxin Z., Zhongyuan R., Arthur A. G. and Xiaolei F.(2021)A Comparative Study on Mesoporous Y Zeolites Prepared by Hard-Templating and Post-Synthetic Treatment Methods. *Applied Catalysis A: General* Vol. 612, 117986.
- Seo J. K., Heon L., Young K. P. Sun J. K.(2018) Assessing the electrochemical performance of a supercapacitor electrode made of copper oxide and activated carbon using liquid phase plasma. *Applied Surface Science* 446
- Shahid A., Lopez-Orozco S., Marthala V. R., Hartmann M. and Schwieger W. (2017). Direct oxidation of benzene to phenol over hierarchical ZSM-5 zeolites prepared by sequential post synthesis modification. *Microporous Mesoporous Mater.* 237, 151–159.
- Shiyong L., Huanhuan Y., Sen W., Mei D., Jianguo W. and Weibin F.(2022)Facile synthesis of hierarchical macro/microporous ZSM-5 zeolite with high catalytic stability in methanol to olefins. *Microporous and Mesoporous Materials*, 329, 111538
- Shuhui W., Yaquan W., Chao S., Taotao Z., Jingjing Z., Ziyang W., Wenrong L., Jiaxin L., Mingxue S., Aijuan Z., Lingzhen B.,Zhiqiang W.,Mengyao Y. and Yaqiong Z.(2021)Novel preparation of binder-free Y/ZSM-5 zeolite composites for VOCs adsorption. *Chemical Engineering Journal*, 417, 1291721.
- Tewodros K., Dada M A., Islam A. K. and Vuppaladadiyam E., A.(2021) Thermo-catalytic co-pyrolysis of ironbark sawdust and plastic

A Review On Synthesis Of Hierarchical Zeolites Y

- waste over strontium loaded hierarchical Y-zeolite. *Journal of Environmental Management*, 299, 113610
- Tianyi F., He D., Jingshuang Z., Peng B., Jiafei L. and Xianghai G. (2021) Direct synthesis of hierarchical zeolites through mesoporous 3D wormhole framework using single-head quaternary ammonium salt as structure-directing agent *Journal of Materials Science* volume 56, 6110–6123.
- Wang D., Sun H., Liu W., Shen Z. and Yang W. (2020). Hierarchical ZSM-5 zeolite with radial mesopores: preparation, formation mechanism and application for benzene alkylation. *Frontiers of Chemical Science and Engineering*, 14(2), 248-257.
- Wenlin L., Jinyu Z., Yibin L. and Chunyan T. (2017) Hierarchical Zeolite Y with Full Crystallinity: Formation Mechanism and Catalytic Cracking Performance. *Energy & Fuels* 31(4) ·
- Wu L., Linfeng L. and Xiaohui C. (2022) Fast synthesis of hierarchical nanosized pure Si-Beta zeolite with low organic template content via the solvent-free method. *Journal of Solid State Chemistry* Volume 308, 122899.
- Xiaoli J., Lu H., Yanhang M. and Shunai C., (2018) Additive-free synthesis of mesoporous FAU-type zeolite with intergrown structure *Science China Materials* volume 61, pages 1095–1100
- Xicheng J., Changbum J. and Alex C.K. Y. (2021) *Synthesis Strategies for Hierarchical Zeolites*. Book Editor(s): Wey Yang Teoh, *Fuel*, 313, 122669
- Atsushi Urakawa, Yun Hau Ng, Patrick Sith <https://doi.org/10.1002/9783527813599.ch7>
- Xing Z., Kunyue L., Changmin H. and Yinyong S. (2018) Preparation of Titanium-containing Hierarchical Zeolite Y and Its Catalytic Performance in Oxidative Desulfurization of Dibenzothiophene. *Current Catalysis*, Volume 7, Issue 2.
- Zhang J., Bai S., Chen Z., Wang Y., Dong L., Zheng H., Cai F. and Hong M. (2017) Core-shell zeolite Y with ant-nest like hollow interior constructed by amino acids and enhanced catalytic activity. *Journal of Materials Chemistry. Materials for Energy and Sustainability* 5(39):20757–20764 56.
- Zhao J., Yin Y., Li Y., Chen W., and Liu B. (2016) Synthesis and characterization of mesoporous zeolite Y by using block copolymers as templates. *Chemical Engineering Journal*, 284: 405–411.
- Zheng W., Baorong W., Jie S., Peixin R., Xianqing X., Weilin L. and Xingtian S. (2021) The silanization process for the hydrothermal synthesis of hierarchical titanium silicalite-1 *Microporous and Mesoporous Materials*, 327, 111407
- Zijian W., Rongxin Z., Jieguang W., Zhongwei Y., Yanjuan X., Lingjiang K., Hongquan L. and Aizeng M. (2022) Hierarchical zeolites obtained by alkaline treatment for enhanced n-pentane catalytic cracking

JOURNAL OF THE NIGERIAN SOCIETY OF CHEMICAL ENGINEERS
INSTRUCTION TO AUTHORS

1. TYPES OF PUBLICATION

The Journal of the Nigerian Society of Chemical Engineers will publish articles on the original research on the science and technology of Chemical Engineering. Preference will be given to articles on new processes or innovative adaptation of existing processes. Critical reviews on current topics of Chemical Engineering are encouraged and may be solicited by the Editorial Board. The following types of articles will be considered for publication:

- a. Full length **articles or review papers**.
- b. **Communication** – a preliminary report on research findings.
- c. **Note** – a short paper describing a research finding not sufficiently completed to warrant a full article.
- d. **Letter to the Editor** – comments or remarks by readers and/or authors on previously published materials.

The authors are entirely responsible for the accuracy of data and statements. It is also the responsibility of authors to seek ethical clearance and written permission from persons or agencies concerned, whenever copyrighted material is used.

For now the journal is published twice in a year, March/April and September/October.

2. MANUSCRIPT REQUIREMENTS

- a. The **Manuscript** should be written in clear and concise English and typed (single column) in Microsoft Word using double spacing on A4-size paper, Times New Romans font and 12 point. A full length article or review should not exceed 15 pages. Margin should be Normal (i.e. 2.54cm for Top, Bottom, Left & Right margins).
- b. The **Manuscript** should be prepared in the following format: Abstract, Introduction, Materials and Methods, Results, Discussion, Conclusion, Acknowledgements, and References..
- c. The **Manuscript** must contain the full names, address and emails of the authors. In the case of multiple authorship, the person to whom correspondence should be addressed must be indicated with functional email address. As an examples, authors' names should be in this format: **Momoh, S. O., Adisa, A. A. and Abubakar, A. S.** If the addresses of authors are different, use the following format:

***Momoh, S. O.¹, Adisa, A. A.² and Abubakar, A. S.³**

Use star * to indicate the corresponding author.

- d. **Symbols** should conform to America Standard Association. An abridged set of acceptable symbols is available in the fourth edition of Perry's Chemical Engineering Handbook. Greek letters, subscripts and superscripts should be carefully typed. A list of all symbols used in the paper should be included after the main text as **Nomenclature**.
- e. All **Units** must be in the SI units (kg, m, s, N, etc).
- f. The **Abstract** should be in English and should not be more than 200 words. The Abstract should state briefly the purpose of the research, methodology, results, major findings and major conclusions. Abstracts are not required for Communications, Notes or Letters.
- g. **Citation** must be in the Harvard Format i.e. (Author, Date). Examples are (Smith, 1990) or (Jones et al, 2011). (Kemp, 2000) demonstrated that; (Mbuk, 1985; Boma, 1999; Sani, 2000) if more than two authors. (Telma, 2001a), (Telma, 2001b); etc if the citation have the same author and year of publication.
For more information on Harvard Referencing: Guide visit <http://www.citethisforme.com/harvard-referencing>
- h. **References** must also be in the Harvard Format i.e. (Author, Date, Title, Publication Information). References are listed in alphabetical order. Examples are shown below:
Haghi, A. K. and Ghanadzadeh, H. (2005). A Study of Thermal Drying Process. *Indian Journal of Chemical Technology*, Vol. 12, November 2005, pp. 654-663
Kemp, I.C., Fyhr, C. B., Laurent, S., Roques, M. A., Groenewold, C. E., Tsotsas, E., Sereno, A. A., Bonazzi, C. B., Bimbernet, J. J. and Kind M.(2001). Methods for Processing Experimental Drying Kinetic Data. *Drying Technology*, 19: 15-34.
- i. **Tables** should contain a minimum of descriptive materials. Tables should be numbered serially throughout the manuscript in Arabic numerals (1, 2, 3, etc), and should be placed at the referenced point with captions (centralised) placed at the top of the table.
- j. **Figures**, charts, graphs and all illustrations should be placed at the referenced point, numbered serially throughout the manuscript in Arabic numerals (1, 2,

Instruction To Authors

3, etc) and incorporated in the text. Caption for Figures should be placed at the bottom of the Figure (centralised). Lettering set or symbols should be used for all labels on the figures, graphs, charts, photographs even when drawn in colours. (Note that figures drawn in colours may be unreadable if printed in black and white).

- k. **Equations** should be typed using MS Word Equation Editor and should be centred and numbered serially throughout the manuscript (in Arabic numeral) at the right margin.
- l. Wherever possible, **Fractions** should be shown using the oblique slash. E.g. x/y
- m. **Footnotes** should not be incorporated in the text.
- n. **Acknowledgements** should appear at the end of the paper, before the list of references.

3. SUBMISSION OF MANUSCRIPTS

Manuscripts should be submitted by sending a Microsoft Word document (taking into account the Manuscript Requirements described in section 2 above) to the following email address: nschejournal@yahoo.com and copy stevmomoh@yahoo.com.

All correspondences are directed to the Editor-in-Chief using the submission emails addresses: nschejournal@yahoo.com and copy stevmomoh@yahoo.com. Meanwhile the online submission of articles on the journal website will soon be ready.

Authors should note that:

- a. All authors listed in the manuscript have significantly contributed to the research.
- b. All authors are obliged to provide retractions or corrections of mistakes.
- c. All references cited are listed and financial support acknowledged.
- d. It is forbidden to publish same research in more than one journal.

The fee charged for paper review and publication will be borne by the authors as follows:

- a. Manuscript Review charges = N6,500 payable by both Members and Non-Member. Overseas is \$30.00.
- b. Publication Charges = N10,000 payable by Non-Members and Members who are not financially up-to-date. Overseas is \$40.00.
- c. Members would only get one (1) Journal free and buy the other if they so wish.
- d. Corresponding Author whose paper is published on a particular edition would get one (1) free copy on

behalf of all the co-authors. Other co-authors will buy if they so wish.

All fees are paid after the paper had been accepted for publication. These charges may be reviewed from time to time by the Governing Board of Directors of the Society.

4. ACCEPTED PAPERS

On acceptance, authors will be required to submit a copy of their manuscripts using Microsoft Word by emails to nschejournal@yahoo.com and copy stevmomoh@yahoo.com.

The following additional information should be observed for accepted papers: (i) Typed in Microsoft Word using 1.15 spacing on A4-size paper, Times New Romans font and 10 point; (ii) Margin should be 2.54cm for Top & Bottom; 2.20cm for Left & Right margins; (iii) The abstract should be one column document while the body of the manuscript should be double columns with 0.5cm gutter spacing except some tables and figures that may have to go in for one column document.

5. PUBLICATION

Full NSChE Journal edition in hard copy will be published twice annually – March/April Edition and September/October Edition.

6. REPRINT

Reprints are available on request at a moderate fee per page. Orders must be placed before the paper appears in Print.

7. READER'S INFORMATION

The papers are wholly the view of their author(s) and therefore the publisher and the editors bear no responsibility for such views.

8. SUBSCRIPTION INFORMATION

The subscription price per volume is as follows:

- | | | |
|-----------------------------------|---|-----------|
| a. Individual Reader | - | N3,000.00 |
| b. Institutions, Libraries, etc.- | - | N5,000.00 |
| c. Overseas Subscription | - | \$100.00 |

Request for information or subscription should be sent to the Editor-in-Chief through the following emails addresses: nschejournal@yahoo.com and copy stevmomoh@yahoo.com.

9. COPYRIGHT NOTICE

By submitting your manuscript to the Journal, you have agreed that the copyright of the published material belongs to the journal.

10. PRIVACY STATEMENT

The names and email addresses entered in this journal site will be used exclusively for the stated purposes of this journal and will not be made available for any other purpose or to any other party.